ULTRASONIC MEASUREMENT OF SOLID PROPELLANT BURNING RATES IN CLOSED BOMBS AND SUBSCALE MOTORS

A THESIS SUBMITTED TO
THE GRADUATE SCHOOL OF NATURALAND APPLIED SCIENCES
OF
MIDDLE EAST TECHNICAL UNIVERSITY

BY

ÖZEN ATAK

IN PARTIAL FULFILLMENT OF THE REQUIREMENTS
FOR
THE DEGREE OF DOCTOR OF PHILOSOPHY
IN
MECHANICAL ENGINEERING

JANUARY 2016

Approval of the Thesis:

ULTRASONIC MEASUREMENT OF SOLID PROPELLANT BURNING RATES IN CLOSED BOMBS AND SUBSCALE MOTORS

submitted by **ÖZEN ATAK** in partial fulfillment of the requirements for the degree of **Doctor of Philosophy in Mechanical Engineering Department, Middle East Technical University** by,

Prof. Dr. Gülbin Dural Ünver
Dean, Graduate School of Natural and Applied Sciences

Prof. Dr. Tuna Balkan
Head of Department, Mechanical Engineering

Assoc. Prof. Dr. Cemil Yamalı
Supervisor, Mechanical Engineering Dept., METU

Examining Committee Members:

Prof. Dr. Kahraman Albayrak
Mechanical Engineering Dept., METU

Assoc. Prof. Dr. Cemil Yamalı
Mechanical Engineering Dept., METU

Prof. Dr. Derek K. Baker
Mechanical Engineering Dept., METU

Prof. Dr. Nevzat Onur
Mechanical Engineering Dept., ÇANKAYA UNI.

Asst. Prof. Dr. Özgür Bayer
Mechanical Engineering Dept., METU

Date:

I hereby declare that all information in this document has been obtained and presented in accordance with academic rules and ethical conduct. I also declare that, as required by these rules and conduct, I have fully cited and referenced all material and results that are not original to this work.

Name, Last name : ÖZEN ATAK

Signature :

ABSTRACT

ULTRASONIC MEASUREMENT OF SOLID PROPELLANT BURNING RATES IN CLOSED BOMBS AND SUBSCALE MOTORS

Atak, Özen
Ph.D., Department of Mechanical Engineering
Supervisor: Assoc. Prof. Dr. Cemil Yamalı

January 2016, 153 pages

In the scope of this thesis, applications of ultrasonic measurement method on closed bombs and test motors were investigated with various aluminized and non-aluminized propellants with the main target of evaluation of burning rates. Detailed comparison between conventional methods for solid propellant burning rate measurements such as strand burner, firing of subscale test motors and ultrasonic measurement was performed. Burning rate evaluation of eight propellant batches were determined by thirty three closed bomb tests. For qualification of the ultrasonic measurement method, twelve tests that belong to HSTYPE5 propellant batch were investigated. The results showed good agreement with the results of firing of subscale test motors. Monte Carlo simulation was used for performing the uncertainty analysis related to closed bomb tests. Uncertainty for the closed bomb test set up used in Roketsan is between %2 and %10. Regarding to the test motor studies, a test motor was designed and manufactured for the purposes of the applications of ultrasonic measurement. Three successful tests were carried out with three different types of propellants. After qualification of the measurement method on closed bombs, studies of test motors were performed. The results obtained from the test motors were compared with the results of firing of subscale test motors for the same propellant composition. The results were comparable with each other.

Moreover a numerical analysis was conducted in order to determine thermal profile at motor case that belongs to subscale test motor 3. At first, a test case was chosen from the open literature and various turbulent models were considered to predict the pressure and velocity profiles related to experimental study. The results showed that K omega SST turbulence model was suitable for thermal analysis of subscale test motor. During the firing of subscale test motor, thermocouples were employed on motor case with the main target of measuring temperatures at stated locations. Results of the numerical study were compared with the results of the experimental study.

Keywords: Closed Bomb, Ultrasonic measurement method, Burning Rate, Subscale motors

ÖZ

ULTRASONİK ÖLÇÜM YÖNTEMİ KULLANILARAK KAPALI BOMBALARDA VE KÜÇÜK ÖLÇEKLİ TEST MOTORLARINDA YAKIT YANMA HIZININ BELİRLENMESİ

Atak, Özen
Doktora, Makine Mühendisliği Bölümü
Tez Yöneticisi: Doç. Dr. Cemil Yamalı

Ocak 2016, 153 sayfa

Bu tez kapsamında, aluminyum parçacıklı ve parçacıksız yakıtlar kullanılarak ultrasonik test yönteminin kapalı bombalarda ve test motorları üzerindeki uygulamaları araştırılmıştır. Yanma hızı belirleme metotları arasında detaylı bir karşılaştırma yapılmıştır. Sekiz yakıt kafilesine ait yanma hızı değerlendirmesi otuz üç adet kapalı bomba ateşlemesi ile gerçekleştirilmiştir. Ultrasonik yanma hızı yönteminin kalifiye edilmesi amacıyla gerçekleştirilen HSTYPE5 kafilesine ait on iki adet kapalı bomba ateşlemesi incelenmiştir. Kapalı bomba ateşlemelerinin belirsizliği Monte Carlo simulasyonu ile belirlenmiştir. Roketsan'da kullanılan kapalı bomba test düzeneğinin belirsizliği %2 ile %10 arasında değişmektedir. Ultrasonik test yönteminin test motorları üzerindeki uygulamaları için bir adet test motoru tasarlanmış ve imalatı yapılmıştır. Üç farklı yakıt çeşidi için üç farklı ateşleme gerçekleştirilmiştir. Ultrasonik test yönteminin kapalı bombalar ile kalifiye edilmesinden sonra test motoru çalışmalarına başlanılmıştır. Aynı yakıt kompozisyonuna sahip statik ateşlemeler ile ultrasonik test yöntemi kullanılarak ateşlenen test motorları karşılaştırılmıştır. Sonuçların yakın olduğu görülmüştür. Bunlardan başka, üçüncü ultrasonik motor ateşlemesinin motor duvarında sıcaklık tahmini yapabilmek amacıyla sayısal bir çalışma gerçekleştirilmiştir. İlk başta açık

literatürden bir adet deneysel çalışma seçilmiş ve çeşitli türbülans modelleri deneysel çalışmaya ait olan basınç ve hız profillerinin tahmini açısından incelenmiştir. Sonuçlar en uygun türbülans modelinin K omega SST türbülans modeli olduğunu göstermiştir. Ultrasonik motor ateşlenirken ısıl çiftler ile belirlenen noktalardan sıcaklık ölçümü alınmış ve sayısal çalışmanın sonucu test sonuçları ile karşılaştırılmıştır.

Anahtar Kelimeler: Kapalı Bomba, Ultrasonik Ölçüm Yöntemi, Yanma Hızı, Test Motorları

To My Son,

ACKNOWLEDGMENTS

I wish to express mine deepest gratitude to my supervisor Assoc. Prof. Dr. Cemil Yamalı for their guidance, advice, criticism, encouragements and insight throughout the research.

I would also like to thank to Prof. Dr. Nevzat Onur, Prof. Dr. Kahraman Albayrak, Prof. Dr. Darek Baker and Ass. Prof. Dr. Özgür Bayer for their suggestions and comments.

I would like to express my deepest thankfulness to Franck Cauty for sharing his precious experience with me and his precious comments about the tests.

I would like to express mine deepest appreciation to a number of people from various departments of Roketsan who have provided data & critical reviews and helpful discussions as this work progressed.

I would like to thank to Dr. Mine Yumuşak , for her crucial suggestions, sharing her experience and her great support.

I would like to express my deepest thankfulness to Dr. Bora Kalpaklı for his precious suggestions and answering all of my nonsense questions.

I would like to express my deepest appreciation to Uğur Arkun for his precious suggestions and his great support.

I wish to express my deepest gratitude to my colleagues Berkan Zıraman for helping me performing the tests and being my fellow traveler, Berkan Mumcu, Funda Kömbe, Onur Ozan Kalkan, Yusuf Ata, Ozan Kömbe, Nevzat Çakmak and İsa Tufan for their great supports.

I would like to thank to Mehmet Demirbaş and his team about performing the closed bomb tests and static firing tests.

I would like to thank to Neslin Önsoy and her team for preparing the propellant samples and their advices.

I specially would like to thank my husband Yusuf Atak and my son Demir Atak for being in my life. I am very grateful for their great love, constant encouragement and endless support during this difficult period of my life.

I would like to thank my wonderful family; İsmet Kurtul, Neziha Kurtul, Özgür Veli Kurtul and Ozan Kurtul who supported and encouraged me at every moment of my whole life.

I would like to express my gratefulness to GOD for my true love Demir Atak.

Lastly, I would like to gratefully acknowledge Roketsan Missiles Industries Corporation for the support in achieving this goal.

TABLE OF CONTENTS

ABSTRACT v
ÖZ vii
ACKNOWLEDGMENTS x
TABLE OF CONTENTS xii
LIST OF TABLES xvi
LIST OF FIGURES xvii
LIST OF SYMBOLS xxii
LIST OF ABBREVIATIONS xxiii
CHAPTERS
1. INTRODUCTION 1
1.1 Motivation 1
1.2 Research Objectives 2
1.3 Method of Investigation 4
1.4 Chapter Guide 4
2. LITERATURE REVIEW 7
2.1 Main Parts of Rocket Motor 7
2.2 Composite Propellant 8
2.3 Burning Rate 8
2.3.1 Parameters That Affect the Burning Rate 8
2.3.1.1 Effect of Pressure in Combustion Chamber 9
2.3.2 Effect of Temperature 10
2.4 Influence of Burning Rate on Performance 10
2.5 Burning Rate Measurement Methods 11
2.6 Burning Rate Evaluation Methods in Roketsan 12
2.6.1 Strand Burner 12
2.6.2 Sub Scale Motors 13
2.6.3 Closed Vessel 14
2.6.4 Laser Ignition Test Setup 15
2.7 Microwave Method 16

2.8 Plasma Capacitance Gages 16
2.9 X-Ray 17
2.10 Ultrasonic Pulse-Echo Method 17
3. ULTRASONIC PULSE ECHO TECHNIQUE 19
3.1 Ultrasonic Theory 19
3.2 Methods Performed for Propagation Time Determination 20
3.2.1 EDUM Method 21
3.2.2 Zero Crossing 21
3.2.3 Cross Correlation 22
3.2.4 Moving Gate 22
3.3 Wave Propagation 23
3.3.1 Pressure and Temperature Effect on Wave Propagation 25
3.4 Burning Rate Evaluation for Static Firing Tests and Closed Bombs 26
3.5 The Application of Ultrasonic Technique in Closed Bombs 27
3.5.1 The Application of Ultrasonic Technique in ONERA 32
3.6 The Application of Ultrasonic Technique on Motors 33
4. ULTRASONIC MEASUREMENT ON CLOSED BOMB TEST SETUP 41
4.1 Introduction 41
4.2 Closed Bomb 42
4.3 Data Acquisition System 43
4.4 Ultrasonic Transducer 44
4.5 Nitrogen Tanks 45
4.6 Pressure Relief Valve 45
4.7 Rupture Disc 45
4.8 Igniter 45
4.9 Coupling Material 46
4.10 Propellant 47
4.11 Experimental Procedure 48
4.11.1 Casting Process of Propellant 49
4.11.2 Casting Process of Coupling Material 50
4.11.3 Process of Inhibitor Covering 50
4.11.4 Determination of Wave Velocity of Propellant 51
4.12 Evaluation of Wave Velocity of Coupling Material 52
4.13 Bonding Operations 52

4.14 Leakage Test of Closed Bomb Test 54
4.15 Application of Closed Bomb Test 54
5. CLOSED BOMB TEST RESULTS 55
5.1 Closed Bomb Test Results 55
5.2 Results of OMTYPE1 56
5.3 Results of OMTYPE2 59
5.4 Results of HSTYPE1 62
5.5 Results of HSTYPE2 67
5.6 Results of HSTYPE3 70
5.7 Results of HSTYPE4 71
5.8 Results of BTYPE1 73
5.9 Results of HSTYPE5 74
5.10 Assessment of Burning Rate Measurement Methods Performed in Roketsan 82
5.11 Conclusion 84
6. ULTRASONIC MEASUREMENT ON TEST MOTORS 87
6.1 Introduction 87
6.2 Experimental 87
6.3 Test Preparation 88
6.4 Results and Discussions 90
6.4.1 Test 1 90
6.4.2 Test 2 93
6.4.3 Test 3 96
6.5 Conclusion 98
7. NUMERICAL STUDIES 99
7.1 Introduction 99
7.1.1 Test Case 99
7.1.2 Determining Turbulence Model 99
7.1.3 Results 101
7.1.4 Conclusion 104
7.2 Thermal Analysis of Subscale Test Motor 104
8. UNCERTAINTY ANALYSIS 109
8.1 Introduction 109
8.2 Related Literature Survey 110

9. CONCLUSIONS AND RECOMMENDATIONS 113
9.1 Conclusions 113
9.2 Recommendations... 114
APPENDICES 121
A STUDIES FOR RESEARCH OF ERROR SOURCES 121
A.1 The Research of Error Source Calculating of Burning Rate 121
A.1.1 Test Case 1 122
A.1.2 Test Case 2 124
A.1.3 Test Case 3 125
A.1.4 Test Case 4 126
B PRESSURE EFFECT ON WAVE PROPOGATION....................................... 129
C STANDARD OPERATING PROCEDURE... 133
C.1 Configuration of ACL-8112 DG/HG.. 133
C.2 Settings of Screen.. 134
C.3 Ut Settings... 134
C.4 Starting the Test 137
C.5 Replay 138
D ASCAN FILE OF CLOSED TEST BOMB... 141
E BURNING RATE CALCULATION CODE 143
F UNCERTAINTY DETERMINATION OF CLOSED BOMBS 147
F.1 Uncertainty in Initial Thickness of the Propellant................................. 147
F.2 Uncertainty in Pressure 148
F.3 Uncertainty in Propagation Time 149
G CALIBRATION OF PRESSURE SENSOR 151
CIRRICULUM VITAE.. 153

LIST OF TABLES

TABLES

Table 1 Facilities which have Ultrasonic measurement method and Their Application Areas [7] 27
Table 2 Coupling Material Preparation [31] 50
Table 3 Ingredient of Inhibitor 51
Table 4 Details of Closed Bomb Tests 56
Table 5 Combustion data of Test 1 57
Table 6 Combustion Data of Test 2 and Test 3 61
Table 7 Combustion Data of Tests 65
Table 8 Burning Rates of HSTYPE1 67
Table 9 Combustion Data’s of Test 10,11,12 68
Table 10 Combustion Data’s of Test HSTYPE3 71
Table 11 Combustion Data belong to HSTYPE4 73
Table 12 Combustion Data belong to BTYPE1 74
Table 13 Burning Rates at 10.34 MPa 81
Table 14 Burning Rates at 13.79 MPa 81
Table 15 Pressure Exponents of HSTYPE5 82
Table 16 Test Motors Used in Application 87
Table 17 Results of the Methods 93
Table 18 Results of the Methods 96
Table 19 Results of the Methods 98
Table 20 Geometry of Duct [36] 100
Table 21 Experimental Conditions [36] 100
Table 22 Mesh Structure and Number 105
Table 23 Boundary Conditions 105
Table 24 The Details of Tests 122
Table 25 The Steps for Running a Test 139
Table 26 Calibration Table 151

LIST OF FIGURES

FIGURES

Figure 1 Basic representation of a rocket motor [12] 8
Figure 2 Example of evaluation of pressure exponent... 9
Figure 3 Variability in Reference Burning Rate and Exponent Effect on Performance [4] 11
Figure 4 Parameters which affect the pressure deviation [4] 11
Figure 5 Static firing tests carried by Roketsan 13
Figure 6 a) Pressure and b) Thrust curves gathered by a static firing test in Roketsan 14
Figure 7 Closed Bomb that is used in Roketsan 15
Figure 8 Laser Ignition Test Setup used in Roketsan 16
Figure 9 Schematic representation of ultrasonic measurement and example of a waveform.. 20
Figure 10 Zero Crossing Method [35] 22
Figure 11 Moving gate method modified from [35] 23
Figure 12 Ultrasonic echoes for various material temperatures belong to homogeneous propellant[14]... 24
Figure 13 Ultrasonic wave velocities belong to AP/HTPB composite propellant with respect to temperatures [14] 25
Figure 14 Ultrasonic demonstration for round trip method [23] 30
Figure 15 A sketch of combustion chamber and principle of the 30
Figure 16 Two-dimensional setup that was used in [1] 34
Figure 17 Axisymmetric motor without nozzle that was used in [1] 34
Figure 18 Test results for the axisymmetric motor test [1] 34
Figure 19 Test results for the two-dimensional test setup [1] 35
Figure 20 Propellant Sample Used in Closed Bomb Tests [15] 35
Figure 21 Test motor for burning rate evaluation [15] 36
Figure 22 Voltage output and chamber pressure of the test motor [15]................... 36

Figure 23 Test results obtained from burning rate evaluation motor [15] 37
Figure 24 Ultrasound wave which reflects from insulation degradation surface [30]38
Figure 25 Measured surface temperature and Degraded thickness with respect to time [30] 38
Figure 26 Web thickness and burning rate with respect to time [30] 39
Figure 27 Layout of the Test Setup 42
Figure 28 Schematic figure of the test setup components modified from [27]........ 42
Figure 29 Photo of Closed Bomb 43
Figure 30 Ultrasonic sensor and BNC connector with coupling material................ 44
Figure 31 Nitrogen tank and regulator 45
Figure 32 Propellant sample holder and igniter 46
Figure 33 (a) a whole coupling material used for non-aluminized propellants (b) a whole coupling material used for aluminized propellants 47
Figure 34 (a) Schematic view of the coupling material placed in propellant sample holder... 47
Figure 35 Propellant samples which have (a) different lengths b) same lengths..... 48
Figure 36 Molds that are used for casting process of propellant samples................ 49
Figure 37 Propellant sample holder 51
Figure 38 Propellant samples which have various lengths 52
Figure 39 Coupling Materials used for determination of wave velocities 52
Figure 40 Propellant sample and propellant holder with coupling material 53
Figure 41 Final photo of propellant sample holder 53
Figure 42 Ultrasound echo settings 54
Figure 43 a) Measured pressure and time of flight (TOF) versus time b) Peak data versus time... 57
Figure 44 Burning rate versus pressure for Test 1 58
Figure 45 a) Measured pressure and time of flight versus time for Test 2 b) Peak data versus time for Test 2 59
Figure 46 a) Measured pressure and time of flight versus time for Test 3 b) Peak data versus time for Test 3 60
Figure 47 a) Measured pressure and time of flight versus time for Test 4 b) Peak data versus time for Test 4 60
Figure 48 Burning Rates versus pressure belong to OMTYPE2 62

Figure 49 a) Measured pressure and time of flight versus time for Test 5 b) Peak data versus time for Test 5 63
Figure 50 a) Measured pressure and time of flight versus time for Test 6 b) Peak data versus time for Test 6 63
Figure 51 a) Measured pressure and time of flight versus time for Test 7 b) Peak data versus time for Test 7 64
Figure 52 a) Measured pressure and time of flight versus time for Test 8 b) Peak data versus time for Test 8 64
Figure 53 a) Measured pressure and time of flight versus time for Test 9 65
Figure 54 Burning Rate Value for HSTYPE1 propellant versus pressure 66
Figure 55 Measured pressure and time of flight versus time for a) Test 10 b) Test 11 68
Figure 56 Burning Rate Value versus pressure for Test 11 and Test 12 69
Figure 57 Measured pressure and time of flight versus time for a) test 13 b) test14 and c) test 15 70
Figure 58 Burning Rate Value versus pressure that belongs to HSTYPE3 71
Figure 59 Measured pressure and time of flight versus time for 72
Figure 60 Burning Rate Value versus pressure belong to HSTYPE4 72
Figure 61 Measured pressure and time of flight versus time for a) Test 31 b) Test 32 c) Test 33 73
Figure 62 Burning rate versus pressure that belongs to BTYPE1 74
Figure 63 Measured pressure and time of flight versus time for 75
Figure 64 Measured pressure and time of flight for 76
Figure 65 Measured pressure and time of flight versus time for 77
Figure 66 Measured pressure and time of flight versus time for 78
Figure 67 Effect of Npoint on burning rate evaluation 79
Figure 68 Burning Rate versus pressure of HSTYPE5 80
Figure 69 Burning Rate Evaluation Cost versus Methods 83
Figure 70 Burning Rate Evaluation Time versus Methods 83
Figure 71 Amount of Wasted Propellant versus Methods 84
Figure 72 Components of the test motor a) front flap b) main body c) back flap ... 88
Figure 73 Technical Drawing of Test Motor 88
Figure 74 Coupling Material used in test motor firing tests 89
Figure 75 Assembly process of the test motor 89

Figure 76 Test Motor Firings that belong to a) Test 1 b) Test 2 c) Test 3 placed at ground test platform 90
Figure 77 Pressure and Time of Flight data with respect to time for test 1 91
Figure 78 Pressure data collected by two types of sensor for test 1 91
Figure 79 Burning rate and web thickness with respect to time for test 1 92
Figure 80 Burning rate and pressure with respect to time for test 1 92
Figure 81 Pressure and Time of Flight data with respect to time for test 2 94
Figure 82 Burning rate and web thickness with respect to time for test 2 95
Figure 83 Burning rate and pressure with respect to time for test 2 95
Figure 84 Pressure and Time of Flight data with respect to time for test 3 96
Figure 85 Burning rate and web thickness with respect to time for test 3 97
Figure 86 Burning rate and pressure with respect to time for test 3 97
Figure 87 Experimental setup used for test case [36] 100
Figure 88 Geometry of the test case 101
Figure 89 a) Detailed view of Mesh b) View of Mesh 101
Figure 90 Axial pressure distribution 102
Figure 91 Velocity profile at location 0.401 m 103
Figure 92 Velocity profile at location 0.461 m 103
Figure 93 Subscale Test Motor 104
Figure 94 Mesh view of subscale test motor 105
Figure 95 Static pressure distribution in test motor 106
Figure 96 Test results obtained from test 3 106
Figure 97 Termocouples places belong to test 3 107
Figure 98 Temperature distibution on test motor obtained by thermocouples 107
Figure 99 Temperature (Kelvin) distibution on test motor obtained from numerical analysis 108
Figure 100 Alumina particles distribution in test motor 108
Figure 101 Direct Monte Carlo Simulation Diagram used in uncertainty Measurement [33] 110
Figure 102 Uncertainty of Closed Bomb Tests versus Pressure 112
Figure 103 Burning rate results of test case 1 122
Figure 104 Derivative of Pressure with Respect to Time 123
Figure 105 Burning rate results of test case 2 124
Figure 106 Derivative of Pressure with Respect to Time 124

Figure 107 Burning rate results of test case 3 125
Figure 108 Derivative of Pressure with Respect to Time 125
Figure 109 Burning rate results of test case 4 126
Figure 110 Derivative of Pressure with Respect to Time 126
Figure 111 Wave velocity variation with pressure for propellant.......................... 130
Figure 112 Wave velocity variation with pressure for coupling material............. 130
Figure 113 Card configuration screen.. 133
Figure 114 Welcome screen of the software.. 134
Figure 115 UT setting 135
Figure 116 The place of G1 135
Figure 117 Pulser& Process.. 136
Figure 118 Test configuration... 136
Figure 119 WaveForm&Peak 137
Figure 120 Starting the test screen 138
Figure 121 Non-perpendicularity of the propellant sample 148
Figure 122 Calibration curve of pressure sensor.. 152

LIST OF SYMBOLS

SYMBOLS

C : mechanical wave velocity, m/s

dP/dt : pressure gradient, MPa/s

kp : wave velocity variation coefficient with respect to pressure for propellant, MPa^{-1}

lp : wave velocity variation coefficient with respect to pressure for coupling material, MPa^{-1}

P : pressure, MPa

r_b : burning rate, mm/s

T : temperature, K

α : coefficient of thermal expansion

t : time, s

t_b : burning time, s

τ : propagation time, µs

A_b : burning area, m^2

ρ_b : density of propellant, kg/m^3

U : uncertainty

p : propellant

c : coupling material

ref : reference

ini : initial

x : thickness, mm

i : first

f : last

W_b : web thickness, mm

LIST OF ABBREVIATIONS

EDUM	: Electronic Device for Ultrasonic Measurement
ONERA	: Office National d'Etudes et de Recherches Aerospatiales
AP	: Ammonium Perchlorate
HTPB	: Hydroxyly Terminated Polybutadiene
SNPE	: Societe Nationale des Poudres et Explosifs
USA	: United States of America
TOF	: Time of flight

CHAPTER 1

INTRODUCTION

1.1 Motivation

Determining burning rate of solid propellants is of critical importance for rocket industry as it directly affects performance of rocket motors. In industrial area ultrasonic measurement method has been used for determining burning rates of aluminized and non-aluminized propellants, however the results are distinctive for those stated propellant types and the formulations are under secret. For this reason, other rocket companies cannot drawn the formulations and conduct their studies from the determined results. From this point of view, gaining the ability of determining burning rates of propellants by using ultrasonic measurement method is a challenge.

Notwithstanding impressive progress on rocket area, burning rates with sufficient accuracy are still determined by experiments. Thereby various conventional methods for measurement of burning rates such as firing of subscale test motors and strand burner tests are in use by many facilities. The basic of these conventional methods is to determine burning rate by monitoring the burn time of an initially known thickness of the propellant. Therefore these methods provide the average burning rates of the solid propellants over the web at an average test pressure and burning rates over a pressure range of the propellants are not determined. That is why several tests have to carry out to determine burning rates of one propellant type. One of the objectives of this thesis is to contribute the burning rate evaluation process in the company by applying the ultrasonic measurement method on closed bombs. Gaining the ability of ultrasonic measurement method support to decrease the number of static firing tests completed during the development phase of solid rocket motors in Roketsan. The knowledge of the propellant burning rate is a must parameter in order to predict ballistic motor performance and process control during the propellant manufacturing. Hence at least four test motors are fired with the main target of burning rate evaluation for only one batch of propellant. If one can examine the process of burning rate evaluation in the company, it can be easily seen that more than thousand static firing tests are carried out in one year. In Roketsan, approximately 3000 subscale test motors are fired and many strand burner tests are carried out in one year. By firing a set of subscale test motors, burning rates of one propellant type is considered. For the rest of other propellant types, the same procedure is performed again. One subscale test motor firing test approximately costs 4.000 TL for the company. So in one year the company is ready to spend 1.2 million Euros for only burning rate evaluation. By gaining the ability of usage of ultrasonic measurement method, the company will not only save the money but also gains the technology of a non-destructive measurement method.

Another important topic for the Roketsan is erosive burning phenomenon that belongs to long rockets and degradation of internal thermal insulators of motors. Until now, these topics have not been considered by tests. By implementation ultrasonic measurement method on test motors, a future work opportunity related to erosive burning and degradation of internal thermal insulators by using ultrasonic measurement method is occurred.

1.2 Research Objectives

One of the objectives of this study is to apply a less costly way for determining burning rates of propellants instead of firing of subscale test motors and gaining the ability for using the method on motors for burning rate evaluation, degradation of thermal insulators and erosive burning phenomenon. The method has been used on these topics all over the world but the propellant composition for all companies are under secret. That is why the literature results of the various propellants could not be used during the development phase of the new propellants in Roketsan.

Ultrasonic measurement method has been used all over the word for many years. The method has advantages departed from other measurements systems such as money and time consuming. So the system is preferred by many companies such as SNPE and universities such as ALABAMA University.

Especially for burning rate evaluation, the ultrasonic measurement method would be less costly and easier to implement than firing of subscale test motors. Besides, evaluation of degradation of internal insulation in motors, instability, erosive burning phenomenon in large motors and burning rate evaluation in real motors can be considered by this method.

In this study, the first goal was to consider the method and gained the ability of usage of ultrasonic measurement method on closed bombs for the burning rate evaluation instead of firing of subscale test motors. The method was used with a closed bomb with various types of new propellants reformed by Roketsan. The results obtained from closed bomb tests were compared with the results of firing of subscale test motors and results of strand burner tests.

The system was used with a test motor called ultrasonic motor. A test motor was designed and manufactured for this purpose. Several static firing tests were performed with this test motor with the propellant type ANTYPE1, CRTYPE1 and BTYPE2. All results obtained from ultrasonic motors and firings of subscale test motors were considered.

A numerical study was performed. First of all a test case from literature survey was chosen for the purpose of qualification of the turbulence model and commercial code called ANSYS 16.0. The test case was an experimental study performed by [36]. K-omega SST turbulence model was chosen for the thermal analysis in ultrasonic test motor. The flow in test motor and thermal stresses in the parts of the test motor was considered. The temperatures obtained from the numerical study were compared with the real static firing test performed by ultrasonic motor.

1.3 Method of Investigation

Ultrasonic Measurement Method is a non-intrusive method that is used for burning rate determination of propellants, degradation of internal insulators, erosive burning applications and determination of instabilities of combustion. In this thesis for the experimental part, this method is performed with the aim of burning rate determination of composite propellants. Matlab R2012a is a tool for numerical computation and visulation. In this thesis for computation part Matlab R2012a is used. ANYSY 16.0 which is a computational fluid dynamics packet program is utilized to perform numerical studies.

1.4 Chapter Guide

In Chapter 1, section 1.1 outlines a general description and the necessity and the origin of this thesis. Section 1.2 explains general and specific objectives of the thesis.

Chapter 2 provides a survey of the literature regarding the topics covered in this thesis. Parts of the rocket motor are reviewed first, followed by a definition of burning rate and factors that affect the burning rate of composite propellants. Burning rate evaluation methods used in literature are summarized and principles of them are explained.

Chapter 3 explains the theory of ultrasonic measurement method following by explanations of methods performed for propagation time determination. Wave propagation is explained and the parameters that affect wave propagation are considered. Related literature survey is the last part of this chapter.

In Chapter 4, closed bomb test setup and parts of it used during the tests are explained briefly. Test results that belong to the closed bomb are given in Chapter 5.

Chapter 6 is dedicated to studies on subscale test motors. Preparation of the test motors and results of the tests were discussed briefly.

Chapter 7 is dedicated to studies on numerical studies which were performed to investigate thermal change in motor case. At the beginning, results of the test case are investigated. A suitable turbulence model was chosen as a result of this test case study. After that, study on test motor was explained. The temperatures on motor case are compared with the experiment results.

Chapter 8 is dedicated to study on uncertainty determination of closed bombs. A literature survey was given at the beginning of this chapter. Result of the uncertainty analysis was given at the end.

Chapter 9 concludes on the studies performed by ultrasonic measurement method and recommendations to other researchers about further studies.

CHAPTER 2

LITERATURE REVIEW

This chapter will discuss key inert components of a solid rocket motor, a brief definition of composite propellants and burning rate, factors that affect burning rate and a review of burning rate evaluation methods.

2.1 Main Parts of Rocket Motor

Figure 1 represents a schematic view of a rocket motor which has solid propellant grain. The main parts of a simple rocket motor are propellant grain, nozzle and motor case. Motor case is the main part of a solid rocket motor. It does not only contain the propellant in it but also serves as a highly pressurized vessel. Design of a motor case is based on combination of vehicle requirements and manufacturing limits. The thermal energy is converted to kinetic energy by expanding the combustion gases in the diverging part of the nozzle in order to generate the desired thrust. The propellant is burned by the igniter. Propellant grain of a rocket motor can be in various shapes such as star, cylindrical vs. in order to obtain desired burning surface hence thrust. Insulation is implemented to avoid motor case to high temperatures of combustion gases.

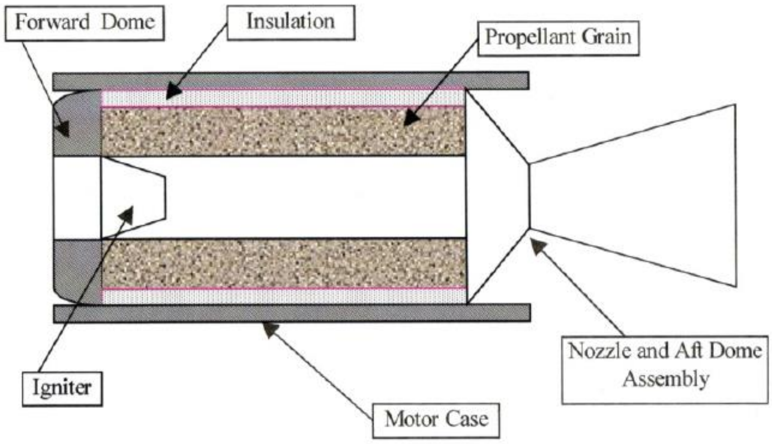

Figure 1 Basic representation of a rocket motor [12]

2.2 Composite Propellant

The composite solid propellant is a mixture that includes an oxidizer, such as ammonium perchlorate (AP), a binder such as cured hydroxyly terminated polybutadiene (HTPB), a metallic powder as a fuel and some other additives. The basic feature which influences the ballistic property of composite solid propellant is the burning rate. Burning rate plays an important role among other properties which control the performance of a rocket motor [2].

2.3 Burning Rate

Burning rate is a characteristic property belongs to propellant that affects the performance of a rocket motor directly. It influences the thrust of the motor hence the range of the rocket. While burning process of the propellant, the burning surface of the propellant recedes in the direction normal to the burning surface in an ideal case. The rate of regression of the propellant is called the burning rate, r_b.

2.3.1 Parameters That Affect the Burning Rate

The parameters that affect the burning rate of composite propellants are pressure in combustion chamber, initial temperature of the propellant grain, the composition of the propellant, the particle size of the oxidizer and erosive burning [2].

2.3.1.1 Effect of Pressure in Combustion Chamber

The burning rate is represented as a function of the chamber pressure and is defined as,

$$r_b = aP^n \tag{1}$$

Equation (1) is an empirical equation. In Equation (1), r_b is the burning rate usually centimeters per second or inches per second, P is chamber pressure usually MPa or psi, n is the pressure exponent and a is temperature coefficient which is not dimensionless [3]. This formula can be applied to double base, composite or composite double base propellants [3]. Temperature coefficient and pressure exponent should be calculated for each propellant formulation. Among the conventional burning rate evaluation methods such as firing of subscale test motors and strand burner tests, evaluation of burning rate of the propellant is performed by several tests. Several tests are performed at various pressures and a pressure exponent is found from the slope of the Log (r_b)-Log (P) curve shown in Figure 2.

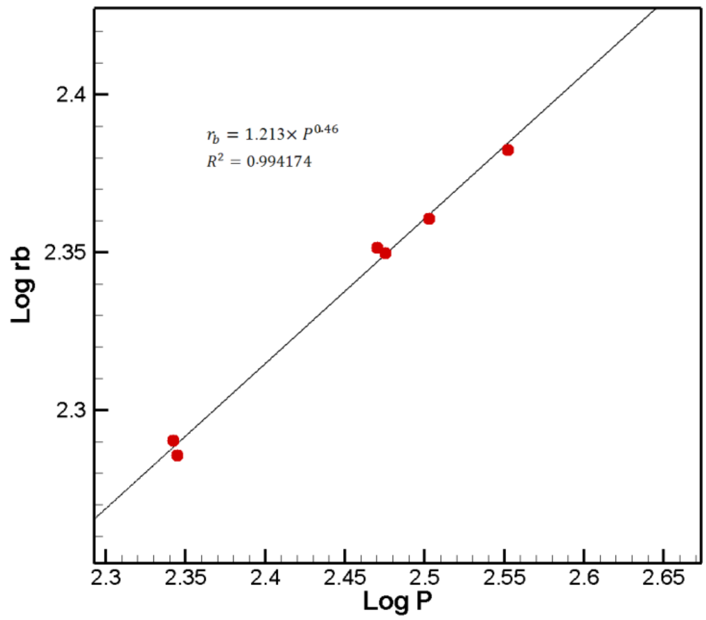

Figure 2 Example of evaluation of pressure exponent

As seen from the figure, for this propellant type, n is 0.46 and a is 1.213.

2.3.2 Effect of Temperature

Temperature affects the chemical reaction rates so initial temperature of the grain influences the burning rate [2]. Generally, temperature effect on burning rate is showed as,

$$\sigma_p = \left.\frac{\partial r_b}{\partial T}\right|_P \approx \left.\frac{lnr_{b2} - lnr_{b1}}{T_2 - T_1}\right|_P \tag{2}$$

In this equation, σ_p is known as temperature sensitivity of burning rate [3]. In other words, temperature sensitivity is the change of burning rate with respect to propellant initial temperature for a constant pressure.

2.4 Influence of Burning Rate on Performance

Performance of the solid rocket motors mainly depends on burning rates of the propellants used in motors. According to report published by Applied Vehicle Technology Panel [4], 1% variation of burning rate causes large variations in performance of 2% to nearly 7%. This variation is represented as a graphic shown in Figure 3. Variability of performance is illustrated by a formula included combustor chamber pressure (P), pressure exponent (n), variability of reference burning rate and variability of pressure exponent shown in equation (3).

$$\frac{\delta p}{p} \leq \frac{1}{|1-n|}\sqrt{\left(\frac{\delta r_{ref}}{r_{ref}}\right)^2 + \left(ln\left(\frac{P}{P_{ref}}\right)\delta n\right)^2} \tag{3}$$

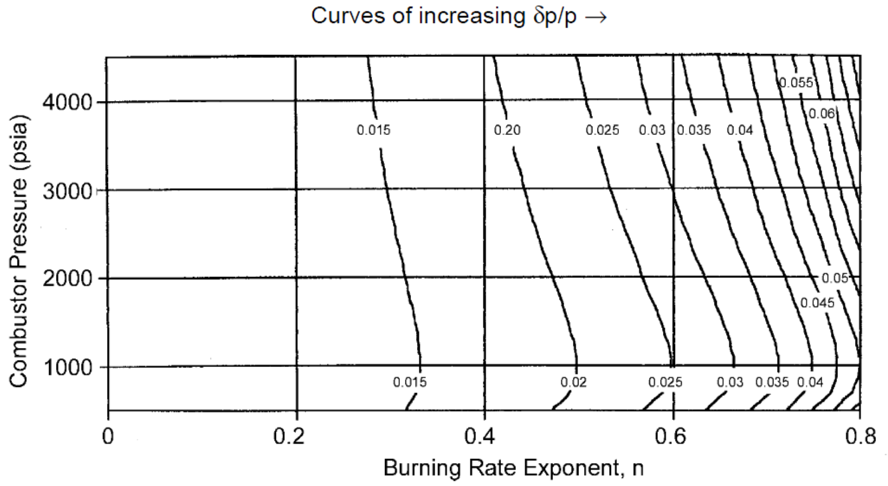

Figure 3 Variability in Reference Burning Rate and Exponent Effect on Performance [4]

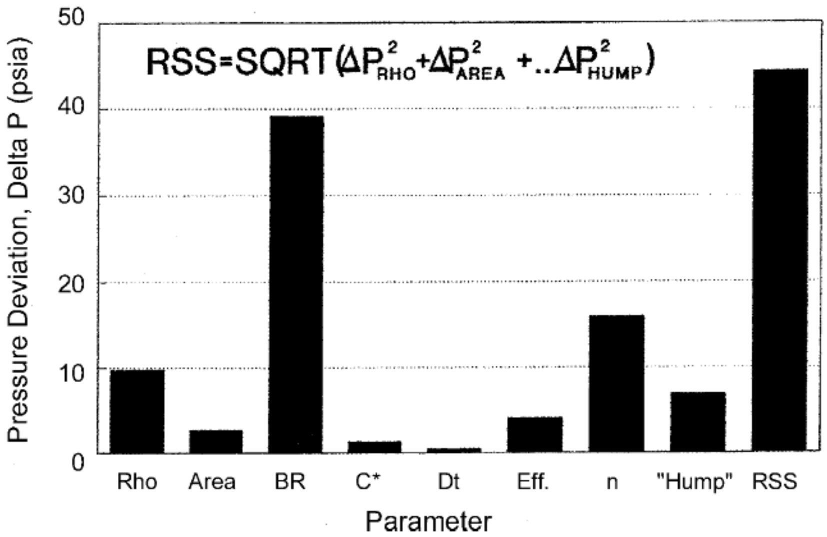

Figure 4 Parameters which affect the pressure deviation [4]

In Figure 4, the parameters which affect the pressure deviation in a combustor chamber is shown. Effect of burning rate is shown as BR is the most effective factor among other factors in the figure.

2.5 Burning Rate Measurement Methods

Generally evaluations of burning rates of propellants are performed by various burning rate measurement methods such as strand burners, firing of subscale test motors, closed vessels, etc. Although using the same sample in the tests, different results can be obtained. These differences come from various effects such as casting process of the propellant, distribution of the AP particles in samples, nature of the methods and uncertainties of measurement devices. In general, subscale test motors are preferred for burning rate evaluation of actual motors while strand burners are used in the first place for quick evaluation of propellants [4].

Various burning rate measurement methods are used for industrial purposes. Especially strand burner and firing of subscale test motors are used widely around the world. An alternative method, ultrasonic measurement method, also has been started to be used instead of other conventional methods. The advantages, disadvantages and usages of the methods will be explained in briefly. The burning rate evaluation methods that are used in Roketsan are explained in a different section.

2.6 Burning Rate Evaluation Methods in Roketsan

In Roketsan, there are various set ups which can be used for burning rate evaluation of energetic materials. Especially strand burners and firing of subscale test motors are preferred during the manufacturing process of various propellants. Except ultrasonic measurement method, the remained test set ups are not specialized for this purpose.

2.6.1 Strand Burner

Linear burning rate of a propellant can be measured by a strand burner under constant pressure and temperature. The strand burner used in Roketsan ignites the propellant in water and it has ignition unit, combustion chamber, temperature conditioning unit, pressurization unit, acoustic sensors and control/data collecting system. The propellant sample as stick form is placed into combustion chamber which is pressurized up to 300 bars and surrounded by temperature conditioning jackets. The propellant sample is ignited and the burning rate is measured by acoustic sensors. The major disadvantage of this method, combustion is occurred in a medium which cannot simulate the combustion chambers of the rocket motors. For this reason burning rates of propellants determined from this method are often smaller than the burning rates of propellants determined from static firing tests.

Strand burner is especially used with the purpose of consider the burning rates of propellant batch in a quick manner.

2.6.2 Sub Scale Motors

Lots of companies prefer this method for the purpose of determining the burning rates of various propellants batches. Test motors are designed and manufactured in small scales. The principle of this method is similar with the strand burner method with a difference of medium. The propellant is burned in a chamber and more propellant is used for combustion process. Web thickness of the propellant is known and burning rate of the propellant is found by mass balance at average chamber pressure. This method is known as more trustable than strand burner method, because it also simulates the conditions of chamber of a real rocket motor. Although it is more money consuming than strand burner method, it is more preferable. Figure 5 shows the static firing tests that carried by Roketsan. Pressure and thrust data belong to static firing tests are gathered during the firing tests and shown in Figure 6.

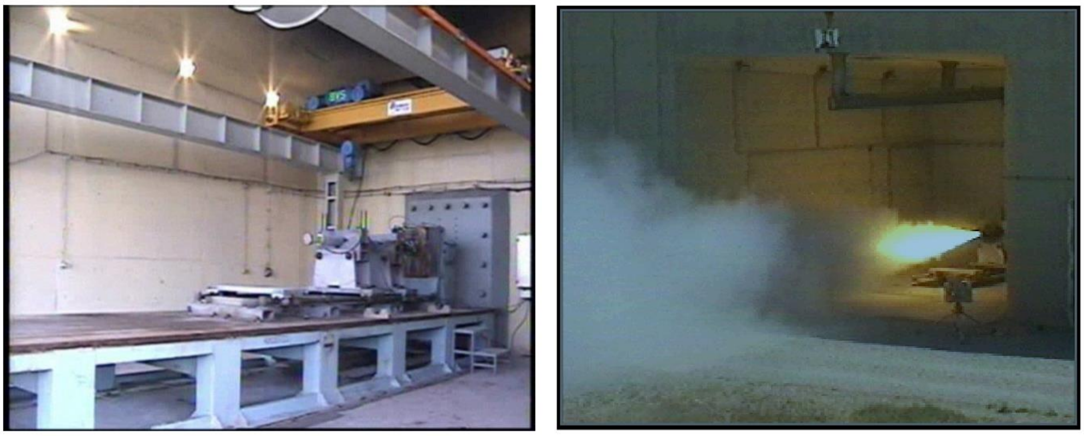

Figure 5 Static firing tests carried by Roketsan

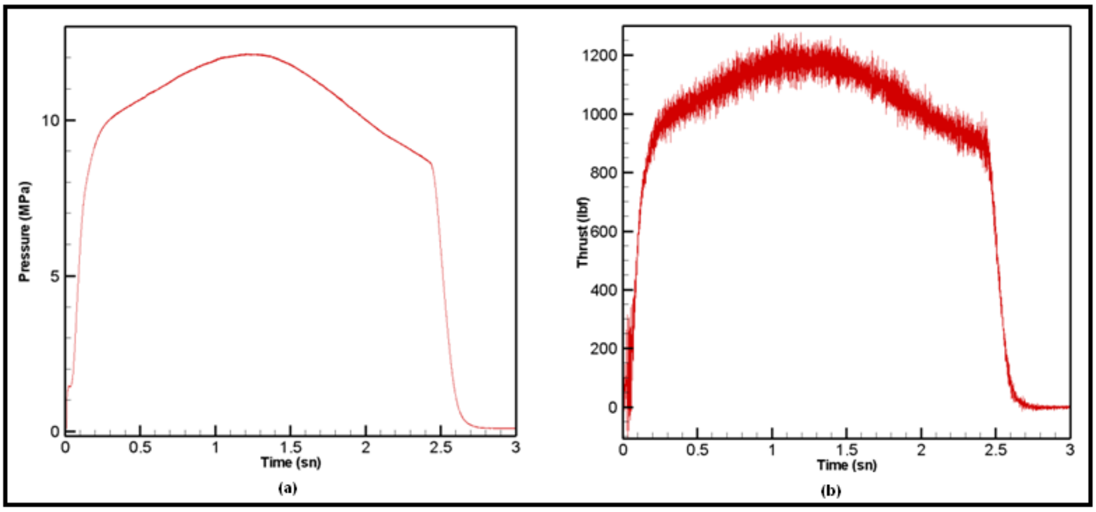

Figure 6 a) Pressure and b) Thrust curves gathered by a static firing test in Roketsan

With the main target of measuring the burning rates of various batches of propellants, more than thousand static firing tests are carried out in Roketsan every year.

2.6.3 Closed Vessel

The closed vessel setup that is used in Roketsan is shown in Figure 7. It includes a vessel which has 200 cc volume, one relief valve, two pressure transducers, and ignition squib. During the test, pressure with respect to time is collected by pressure transducers. After the test, geometric information and amount of sample are used for burning rate evaluation. This setup is basically used for burning rate evaluation of pyrotechnique materials that have high burning rates. The other main target of using this system in Roketsan is to measure time of ignition and ignition energies of propellant samples.

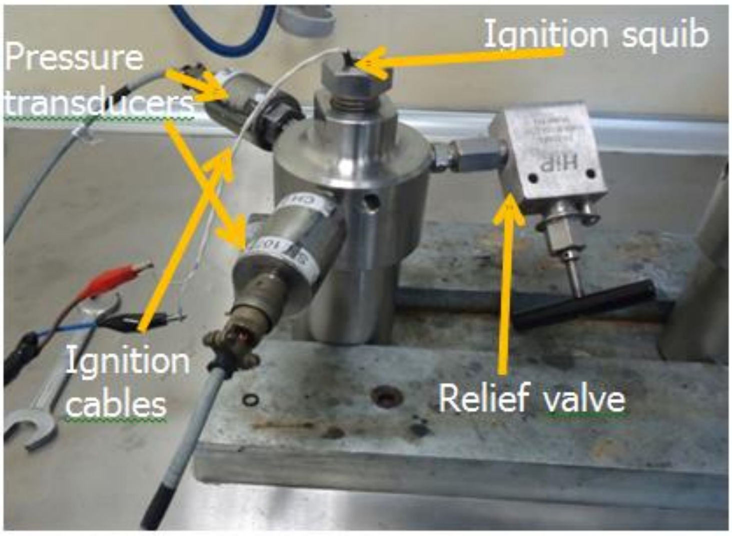

Figure 7 Closed Bomb that is used in Roketsan

2.6.4 Laser Ignition Test Setup

The system is made of laser ignition unit, combustion chamber unit, conditioning and pressurizing system, control and data acquisition system. The combustion chamber is pressurized to desired pressure with Nitrogen and conditioned the desired temperature. The temperature and pressure in combustion chamber are measured. When the desired temperature and pressure are obtained, CO_2 laser ignition is used and energy is transferred to sample surface. The propellant sample is started to burn and the process is monitored by high speed camera. The length of propellant sample is measured before the test. The time is determined by monitoring the combustion process by high speed camera.

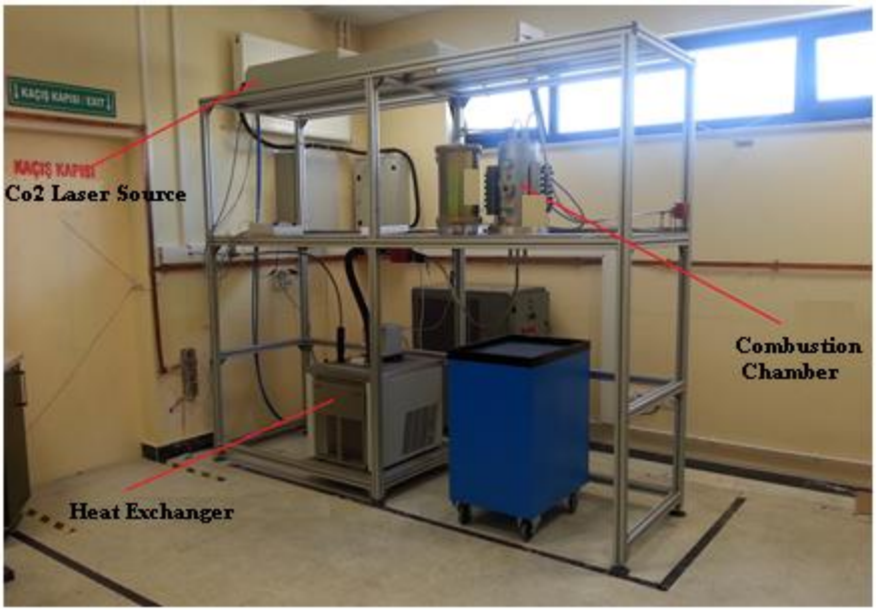

Figure 8 Laser Ignition Test Setup used in Roketsan

2.7 Microwave Method

Microwave method is based on propagation of electromagnetic waves through the propellant and reflection from the burning surface due to the huge difference of the electrical impedance between the propellant and the combustion gases. This method is similar with the ultrasonic measurement method. But a coupling material is not used between the microwave source and the measured material so undesirable waves can be occurred which are reflected from the surface [4].

Method is commonly used for unsteady combustion applications rather than steady state burning rate determination. This technique is expensive and finding a qualified person work on this topic is not easy [5].

2.8 Plasma Capacitance Gages

Plasma capacitance gages technique is based on determining variation of electrical capacities with time which is directly influenced by thickness of the material. This technique is especially used to determine degradation of insulation materials in France and USA. For solid propellant applications, it seems less expensive than ultrasonic measurement method [4]. Ability of this method which other methods are encountered some problems while measuring is performing measurement through the materials [5].

2.9 X-Ray

The basic configuration of X-Ray method consists of radiation source (flash or linear accelerator), the test article, energy converter (converting transmitted x-rays to visible light), and a recording device (film or video). By sending x-ray waves through the material, a portion of radiation energy is reflected without transmitted to the material. This method is much more expensive than other burning rate measurement methods [4].

2.10 Ultrasonic Pulse-Echo Method

The basic of this method is to send acoustic wave through the propellant by an ultrasonic sensor and receive the signal that is reflected from the burning surface due to acoustic difference between the combustion gases and the propellant. For burning rate measurement, small amount of propellant samples are sufficient to be tested. At the end of the test, web thickness of the propellant sample with respect to time is determined with time increments. Derivative of the web thickness of propellant with respect to time is the burning rate [4]. Details of the method are presented in Chapter 3.

CHAPTER 3

ULTRASONIC PULSE ECHO TECHNIQUE

3.1 Ultrasonic Theory

Ultrasonic theory principles and its applications areas used in propellant studies are found in several sources [6-9].

The ultrasonic pulse-echo technique is based on propagation of ultrasonic waves which reflect from the region of changing density (i.e., the propellant sample surface). Part of the wave is absorbed by the medium while remained part is reflected and received by the transducer [13]. The ultrasonic travel time through the propellant is calculated according to

$$t = \frac{c * \tau}{2} \tag{4}$$

Where τ is the propagation time, c is the speed of sound in the solid propellant, and t is the thickness of propellant [10]. In this equation the propagation time has to be divided by two because ultrasonic signal is reflected from the burning surface and the path that it takes is twice the distance.

An ultrasonic transducer transmits ultrasonic signals to the propellant and signals are reflected from the burning surface of the propellant because of distinctness between the densities. In this study, ultrasonic transducers are used as transmitter/receiver. An ultrasonic transducer introduces mechanical waves into the propellant. The unburned propellant is determined by measuring the elapsed time between transmission and reception of the wave. The burning rate is determined by derivation of the web thickness with respect to time of the propellant.

A coupling material is used between the transducer and propellant sample with the main target of avoiding hot gases from the transducer. Right hand surface of the propellant sample is the burning surface which burns through the transducer. Side surfaces of the propellant are covered with the inhibitor to obtain a burning process normal to the burning surface.

The waveform represents the signals which are occurred burning process of the propellant surface. First waveform represents the transducer pulsing. Second signal represents the transducer back signal. Third signal represents the signal that is occurred between the coupling material and the propellant surface occurred by density change. And the last signal shows the waveform that is reflected from the burning surface of the propellant which is occurred by density difference. While burning of the propellant sample, the return time of the burning surface echo occurs at shorter and shorter interval with respect to transducer signal[11].

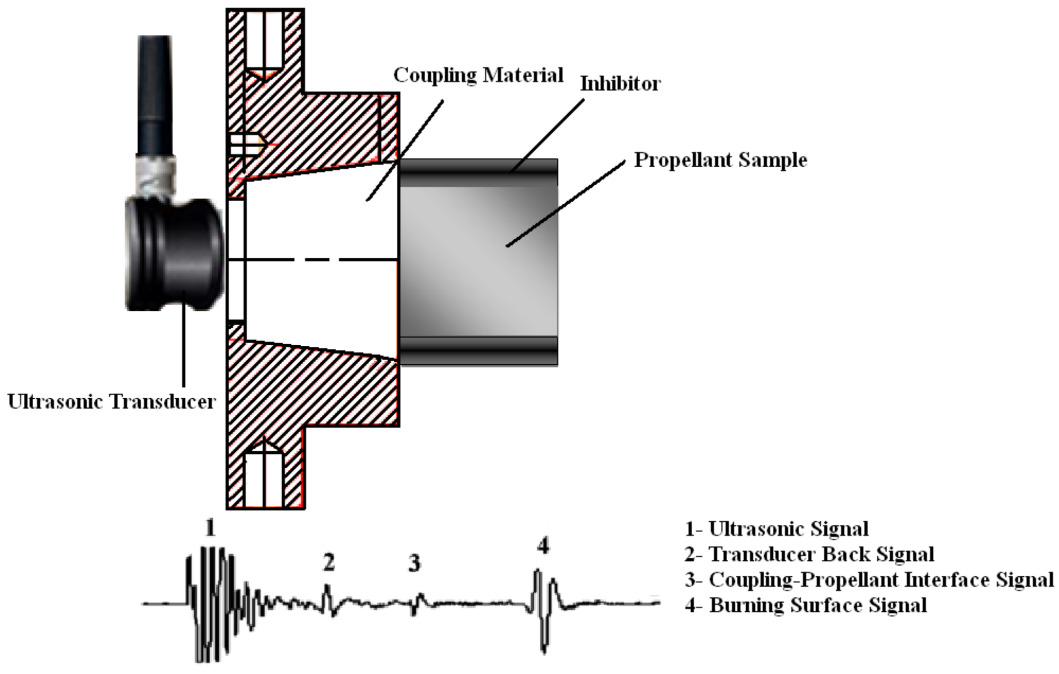

Figure 9 Schematic representation of ultrasonic measurement and example of a waveform

3.2 Methods Performed for Propagation Time Determination

Propagation time which is represented by time difference between signal reflected from burning surface of propellant and signal reflected from coupling material is determined by various methods such as EDUM, the Cross Correlation, the Zero Crossing method and Moving Gate. EDUM is an analog method whereas others are digital methods [12].

3.2.1 EDUM Method

EDUM method is used for detecting the propagation time through the propellant. This analog method generates a waveform, a propagation voltage, two masks and a propagation time gate. The calibration of the EDUM is performed by an oscilloscope by displaying all of these outputs. The first mask is used for hiding the peak which is reflected from back of the transducer shown in Figure 9. The second mask is used for covering the peak which is reflected from the interface of propellant and coupling material. So the EDUM does not detect wrong peaks whereas only peak of burning surface is considered. The propagation gate detects the correct peak and is shown on oscilloscope so the user can see the waveform. EDUM generates a propagation voltage which is proportional with time and these outputs are used for calibration [12].

3.2.2 Zero Crossing

Digital Zero Crossing method is based on the theory which is the same as EDUM method. The algorithm of the Zero Crossing method is based on two inputs; a mask and a threshold. The mask is used for determining the start point and ignoring all the data while threshold is used for ignoring all zero crossings. The first zero crossing point at x axis is the surface of the propellant [12]. An example of waveform belongs to Zero Crossing method is shown in Figure 10. This is a conventional method which most of researchers prefer to apply [35].

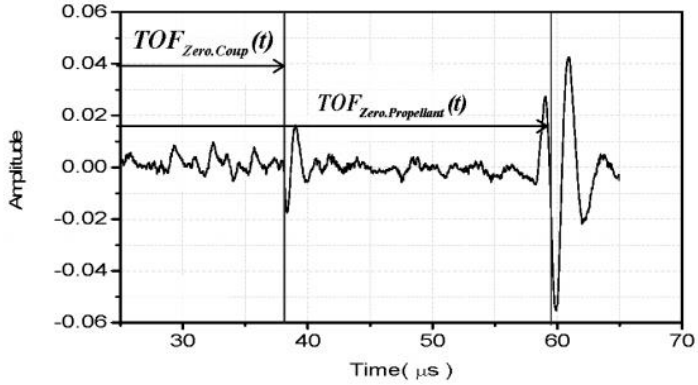

Figure 10 Zero Crossing Method [35]

3.2.3 Cross Correlation

This digital method is based on comparing combined area under two waveforms. This method assumes that area under two combined areas will be the greatest when the two waveforms are aligned. Two waveforms areas are compared first when they are at initial positions. Then with an increment, first waveform goes to left and the combined areas of waveforms are compared again. When the shifting of the waveforms is completed, the algorithm determines where the combined area of the two waveforms is at maximum. All waveforms are shifted and compared with the initial waveform. The recorded shift values are converted to time values and subtracted from initial propagation time with the aim of determining propagation time of burning surface [12].

3.2.4 Moving Gate

In this thesis moving gate method is used for determining propagation time. During the burning process of solid propellant, surface echo comes closer to interface echo and both of them move forward and backward during the test. Also noises are occurred. As a result of these, peak values of surface and interface echo cannot be determined easily. In this method before the start of burning process, virtual gates are placed at peak values of surface and interface echoes. So gates follow moving echoes [35]. The propagation time of burning surface is determined from the difference between the surface echo and interface echo.

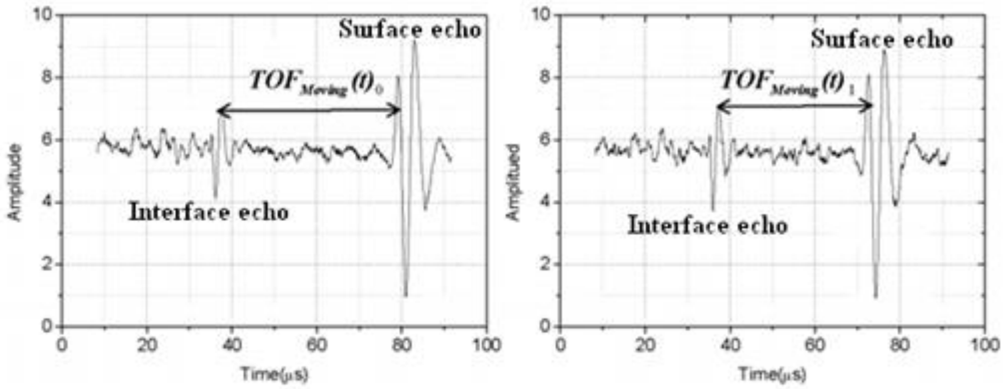

Figure 11 Moving gate method modified from [35]

3.3 Wave Propagation

Wave velocity or in other words speed of sound is affected by many factors such as material type, additives, direction, frequency of the wave and mainly temperature and pressure.

Accurate measurement of wave velocity is required for proper determination of burning rates. In literature there are various ways for determining wave velocity of propellants. Jeenu [9] summarizes the equations used for wave velocity determination. In this thesis, wave velocities of both coupling material and propellant sample are calculated from the equation (5) but modified by checking the equivalence between final web burn thickness and initial thickness of the sample [13].

$$C_{ref} = \frac{2 \times (x_2 - x_1)}{(TOF_2 - TOF_1)} \tag{5}$$

In this equation x_2 is the thickness that belongs to sample 2 and x_1 is the thickness that belongs to sample 1. The echo reflected from the surface of sample 2 is represented by TOF_2 and TOF_1 represents the echo reflected from the surface of sample 1.

In the work presented by Cauty [14], wave velocity variation with respect to temperature is clarified. Wave velocity can be measured easily when the echoes that reflect from the materials surfaces have sufficient amplitudes. Amplitudes show variance with respect to materials temperatures. At low temperatures, some echoes appear that cannot be recognized easily and interfered with the signals occurred from the transducer backside hence the measurement cannot be performed. The propellant surface echoes cannot be split up from those echoes. At high temperatures ($T \geq 50^0C$), exactly the opposite case is occurred. Propellant surface echo becomes smaller that cannot be measured [14].

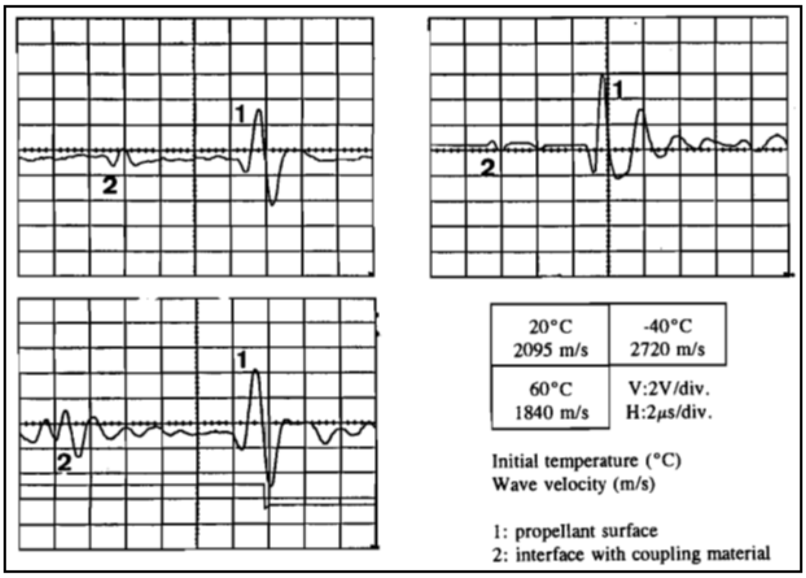

Figure 12 Ultrasonic echoes for various material temperatures belong to homogeneous propellant[14]

Figure 12 represents the ultrasonic echoes obtained from the experiments that are performed by [14]. Experiments were performed by a homogeneous propellant at different temperatures. One is performed at ambient temperature while others were performed at hot and cold temperatures. If it is considered, that will be seen that echoes at low temperatures are bigger than the ambient and hot temperatures because of damping factor.

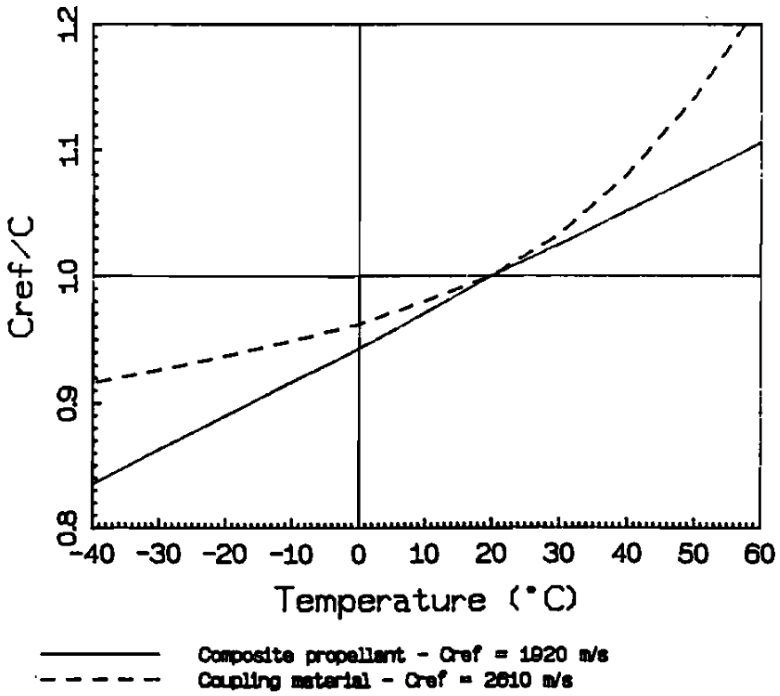

Figure 13 Ultrasonic wave velocities belong to AP/HTPB composite propellant with respect to temperatures [14]

Variation of ultrasonic velocities belongs to coupling material and propellant with respect to temperature is shown in Figure 13.

3.3.1 Pressure and Temperature Effect on Wave Propagation

Wave propagations or in other words speed of sound of materials is affected by temperature and pressure. In this study temperature effect on speed of sound is not taken into account because in the open literature, studies show that temperature can be neglected for composite propellants [6]. For insulation materials and energetic materials that have low burning rates, thermal profile is significant as pressure effect [6]. The pressure effect on speed of sound called wave velocity sensitivity coefficient with respect to pressure (k_p) is measured by pressurizing the closed bomb by an inert gas (Nitrogen) before the combustion tests. An example of k_p measurement is given in Appendix B.

Especially tests that are performed in closed bombs which have high dP/dt variation during the tests, k_p and l_p values become important [16]. That is why, Cauty [16] mentions the importance of pressure sensitivity of coefficient of wave velocity and summarizes the methods of measurement of various wave velocity sensitivity coefficient in the literature. In this paper methods of calculating pressure sensitivity of wave velocity by various researchers are discussed. The wave propagation relationship with pressure and temperature is shown in Equation (6). In this equation wave velocity sensitivity coefficient with respect to pressure is shown as $k_{p.}$

$$\frac{C_{ref}}{C} = \left[1 - k_p\left(P - P_{ref}\right)\right]\left[1 + k_T\left(T - T_{ref}\right)\right] \tag{6}$$

3.4 Burning Rate Evaluation for Static Firing Tests and Closed Bombs

Burning rate evaluation methods are summarized in Chapter 2. In this part especially burning rate evaluation of static firing tests and closed bomb tests which are used with ultrasonic measurement method is discussed.

Static firing tests are performed with subscale test motors which are designed to provide approximately constant pressure during the burning process. For this reason, burning rates obtained from static firing tests are average values at average pressures. Equation (1) is used for determining burning rates of static firing tests.

Burning rates obtained from closed bombs which are performed with ultrasonic measurement method are time dependent and changing over a pressure range. In this thesis, web thickness (W_b) which is defined as the length of burned propellant and burning rate (r_b) obtained by using ultrasonic measurement method are calculated from Equation (7) and Equation (8).

$$W_b(t) = \frac{C_{p,ref}}{2\left(1-k_p\left(P-P_{ref}\right)\right)}\left\{\frac{2W_{ini}}{C_{p,ref}} + \frac{2W_c l_p\left(P-P_{ref}\right)}{C_{c,ref}} - \Delta\tau(t)\right\} - \frac{k_T\left(T_s-T_{ref}\right)}{R_b} \tag{7}$$

$$r_b(t) = \frac{C_{p,ref}}{2\left(1-k_p\left(P-P_{ref}\right)\right)}\left\{\frac{d\Delta\tau}{dt} - \left(k_p\left[\frac{\frac{2W_{p,ini}}{C_{pref}} - \Delta\tau(t) + \frac{2W_{c}l_p\left(P-P_{ref}\right)}{C_{cref}}}{1-k_p\left(P-P_{ref}\right)}\right] + \frac{2W_c l_p}{C_{c,ref}}\right)\frac{dP}{dt}\right\} \tag{8}$$

In this equations, wave velocity in the propellant is represented as $(C_{p,ref})$, chamber pressure (P_c), time of flight (τ), coefficient of variation of the wave velocity for solid propellant (k_p), initial thickness of the propellant $(W_{p,ini})$, thickness of coupling material (W_c), reference mechanical wave velocity in the coupling material $(C_{c,ref})$, burning surface temperature (T_s), reference temperature (T_{ref}), thermal diffusivity (a) and coupling material wave velocity pressure variation coefficient (l_p) are given.

Derivation of these formulas in details is given in [18].

3.5 The Application of Ultrasonic Technique in Closed Bombs

Ultrasonic measurement method is first used by Osborn and Ho in Purdue University. After a while, it is been used by many universities and facilities all over world. In Table 1 facilities that are used by whom and where is summarized.

Table 1 Facilities which have Ultrasonic measurement method and Their Application Areas [7]

Country	Agency	Pub. Dates	Applications
France	ONERA *then* SME Roxel CAEPE	1979 to Present	. Propellant burning rate . Temperature sensitivity . Propellant response function . Uncured propellant burning rate . Erosive burning Small hybrid regression rate . Motor ballistics . Motor insulator erosion
Netherlands	TNO/ Delft University	1985 to present	. Laboratory hybrid rocket regression rate . Laboratory ramjet regression rate . Oxidizer burning rate
Italy	University of Napoli	1998 to present	. Small hybrid motor regression rate
United States	Purdue U. and Virg. PI	1965-67	. Propellant burning rate
	AEDC	1990's	. Motor ballistics, insulator erosion
	PSU	1995 to present	. Propellant burning rate . Laboratory hybrid regression rate . Propellant acoustic admittance
	UAH	1995 to present	. Propellant steady/transient burning rate . Propellant temperature sensitivity . Propellant response function
	UIUC	1995 to present	. Propellant steady/transient burning rate . Propellant response function
	ATK	2003 to present	. RSRM erosive burning
	Aerojet (ARC)	2003 to present	. Propellant burning rate
	Lockheed Martin	1996-2000	. Hybrid booster regression rate
India	Vikaram SSC	1990's to present	. Small motors burning rate

Industrial application of ultrasonic measurement method is studied by Jeenu et al. [9] using closed bomb test set up. In this paper especially test set up and preparation phases of the tests are considered. New techniques for preparation of specimen and test procedure are considered briefly. Approximately 300 batches of aluminized ammonium perchlorate/hydroxyl-terminated polybutadiene composite propellant of three different compositions are studied. This study is different from other studies by means of details of the procedure of preparation of the tests and is a good example for the industrial usage of the ultrasonic measurement method.

In the research of Marcus et al. [17] burning rates and temperature sensitivities of various composite propellants are considered by using ultrasonic measurement method. Closed bomb tests are performed at 145^0F (62.78^0C) and 75^0F (23.89^0C). Approximately ranging from 0.4% to 0.6% standard deviation is obtained for the burning rate evaluation. Also the test results are compared with the strand burner and subscale test motors. As Cauty et al. [14], in this study the burning rate values obtained from closed bomb test results are closer to strand burn test results.

In the research of Mumcu [18], ultrasonic measurement method is used for the purpose of determining burning rates of non-aluminized propellants in the closed bomb test set-up. This thesis includes eight closed bomb tests which are performed at ambient temperature in Roketsan. Also an uncertainty analysis is performed for test motor firing tests and closed bomb tests. After this study, some refinements have been performed to the burning rate determination in closed bomb test set up in Roketsan.

Also, the burning rate determination technique by means of code has been improved by some researchers as Linn [19] does. While calculating the burning rate, a modified cross correlation code is used in this study and compared with the old methods. Some differences are found among the burning rate evaluation codes.

Ultrasonic measurement method is also used with closed bombs with the target of determining temperature sensitivity of solid propellant [20]. In this study, tests are planned to perform at -40^{0}C to +60^{0}C temperature range with two groups of propellants. However, the tests below 0^{0}C could not be done because ultrasonic transducers could not work properly.

A review of ultrasonic measurement applications that are performed by various researchers are summarized in the paper of Frederick [21]. In this paper the main topics are about ultrasonic applications on closed bombs and subscale test motors.

In the study of Hyun Taek et all [22], two types of propellant are investigated with the purpose of considering burning rate scattering. One type is composite propellant while the other is double base propellant. It is concluded that especially variation in the material properties of the propellants such as sound velocity variation and attenuations induce scattering in the burning rates. They also compare the closed bomb test results with the strand burner test results. They conclude that ultrasonic measurement method of theirs cannot be used instead of strand burners since accuracy of the results are not enough to be used.

Hasegawa et al [23] develops a new ultrasonic method called Doppler which analyze each echoes without using a coupling material inserted between the ultrasonic transducer and propellant. This method is specialized at unsteady burning rates evaluation where round trip method cannot handle easily. They show that wavelet method is more accurate then round trip method. Also tests were performed without coupling materials. Schematic illustration of ultrasonic measurements in the round-trip method is shown in Figure 14 .

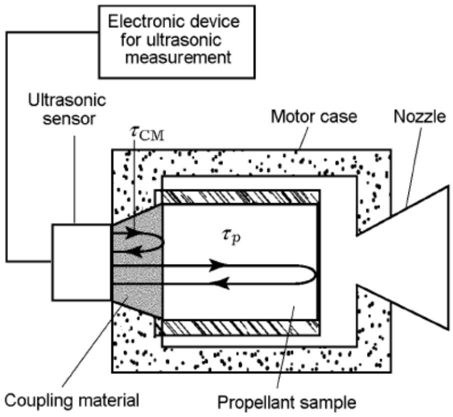

Figure 14 Ultrasonic demonstration for round trip method [23]

In the ultrasonic measurements performed by round trip method, a coupling material is used for protecting the ultrasonic probe in case of high temperature. In their study, K. Hasegawa and K. Hori mentioned about round trip disadvantages. They used an oscillation deadener circuit for eliminating the noise. The combustion chamber used in experiments is shown in Figure 15.

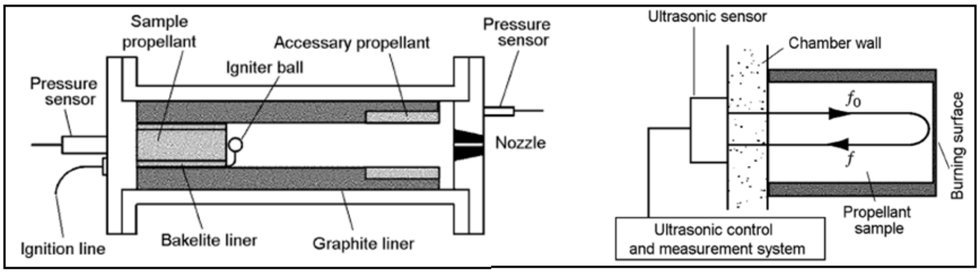

Figure 15 A sketch of combustion chamber and principle of the Doppler method [23]

In this setup coupling material is not used. Instead of using coupling material an oscillation deadener circuit is used. An end burning propellant with an outer diameter of 30 mm is used. Instead of Fourier transform method for analyzing frequency, wavelet method is used.

Kohga et al. [24] studies the speed of sound of uncured and cured propellants with the help of ultrasonic measurement method. They measure the variation of speed of sounds with respect to pressure and length of the samples.

Ultrasonic measurement method is performed with the object of measuring the response functions of propellants in an unsteady manner in the study of Salvo et al. [25]. Instead of using T-burner, a closed vessel is used and pressure oscillations are generated by injection of Nitrogen at low frequencies.

Korean researchers [26] consider ultrasonic measurement method with the aim of obtaining more accuracy results on closed bombs with two types of propellants. They compare the results with strand burner test results. The test results performed with a propellant type which has high burning rates are different according to strand burner test results. The second type of propellant which has low burning rate is comparable with the strand burner test results. The cause of disparity in results is not found.

Same Korean group [27] develop a data acquisition system which collects the ultrasonic signals at a rate of 2000 Hz and measure the burning rates with respect to pressure. Also the results are compared with the strand burner test results. Again closed bomb test results which performed with propellants that have low burning rates are not comparable with the strand burner test results. They decided to investigate attenuation of ultrasonic waves of propellants in order to find this disparity between the results in further studies.

An experimental study in Alabama University [28] is performed in order to investigate effects of steps, holes, roughness, and melt layers on propellants according to wave propagation. Instead of propellants, polyvinylchloride (PVC) materials and inert propellant specimens are used.

Ultrasonic technique is improved by the research center (ONERA) in France. Many investigations on this technique are performed. The studies that were performed in ONERA will be summarized in this part of the thesis.

3.5.1 The Application of Ultrasonic Technique in ONERA

This study [14] is performed with the main target of determining temperature sensitivities of the propellants which directly influence the burning rate hence performance of the rocket motors. A temperature range -40^{o}C to +60^{0}C is researched with ultrasonic measurement method with three types of propellants. Also the results are compared with the conventional methods such as strand burners and small scale test motors. But strand burner test results are better than the static firing test results. The main objective of this study was not to compare the burning rate results by other conventional methods. The main objective was to determine the reproducibility and feasibility that belong to tests performed with ultrasonic measurement method. In this study temperature sensitivity of the propellants are determined. In this thesis, all tests are performed with ambient temperature. But as a future work it is planning to perform closed bomb tests at various temperatures. For this reason this study is a guide for this purpose.

Cauty [5] summarizes the applications of non-intrusive measurement methods applied on energetic materials. Various non-intrusive measurement method applications such as erosive burning determination, ablation of thermal insulators, and determination of regression of energetic materials are searched.

Cauty and Erades [8] present the results of ultrasonic measurement applications and the factors that affect the measurement accuracy in this paper. After a while Cauty and Erades[6] also mention the effect of volume of closed bomb to the accuracy of burning rate determination in this paper. They consider the noise, errors and sensitivity of the ultrasonic measurement method rather than the burning rate evaluation. Especially initial thicknesses of the propellants, the volume of the closed bomb and noise of electronic devices have huge effect on the accuracy of the measurement method. They consider the advantages and limits of the ultrasonic measurement method for the further researchers who will deal with this method.

Cauty et al. [13] publishes a paper which is about automation of the solid propellant burning rate determination by using ultrasonic measurement method. They consider the program that was done for the industrial purposes. Also they consider the parameters that affect wave velocity of propellants and how they reflect this to industrial code. Detailed information of the usage of the program is exhibited in this study.

In ONERA also burning rate determination of uncured propellants are studied with the target of process control for Ariane5 solid propellant booster [29]. The basic challenge of this topic is to obtain a homogeneous paste without bubbles and to be sure of the thickness determined from the paste weight. Different procedures of test methods are performed with the main target of obtaining suitable signals reflected from the burning surface of the paste sample. Eventually, vibrating the paste sample in the sample holder (kept at 50˚C) and pressurizing the closed bomb between 1 to 7 MPa are the main procedures to obtain accurate burning rates.

3.6 The Application of Ultrasonic Technique on Motors

In the earliest studies Jean Claude Traineau and Paul Kuentzmann [1] study on ultrasonic applications on subscale rocket motors without nozzles. This study is performed for demonstrating integral-rocket ramjet missile systems. In this experimental study, they use two experimental set-ups. One of experimental set-up is a two dimensional setup and the other one is an axisymmetric motor without nozzle. In their studies they measure the time of flight as a result of these measurements, and the instantaneous burning rates are calculated. Burning rate is calculated by translating instantaneous web distance burned. While translating instantaneous web distance burned to burning rate, ordinate regularization method is used. In Figure 16 and Figure 17, the setups that are used in this study are shown.

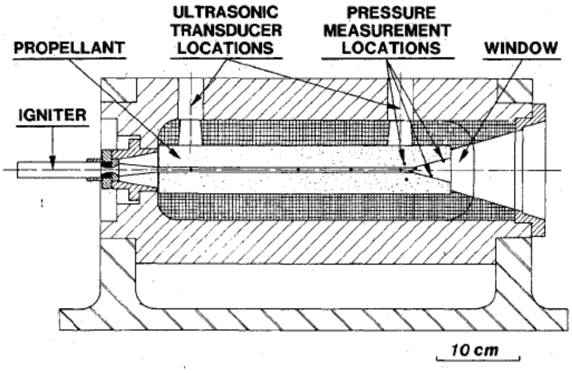

Figure 16 Two-dimensional setup that was used in [1]

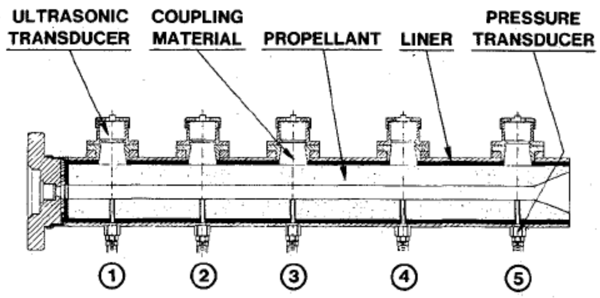

Figure 17 Axisymmetric motor without nozzle that was used in [1]

The results that were obtained from the experiments are shown in Figure 18 and Figure 19. Figure 18 shows the burning rate values obtained from axisymmetric motor test. In Figure 19, the burning rate at 675 mm from the head end of the motor is much more than the burning rate at 70 and 200 mm. This distinction occurs from erosive burning phenomenon.

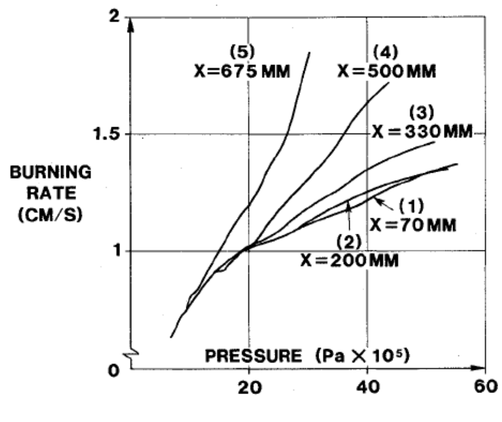

Figure 18 Test results for the axisymmetric motor test [1]

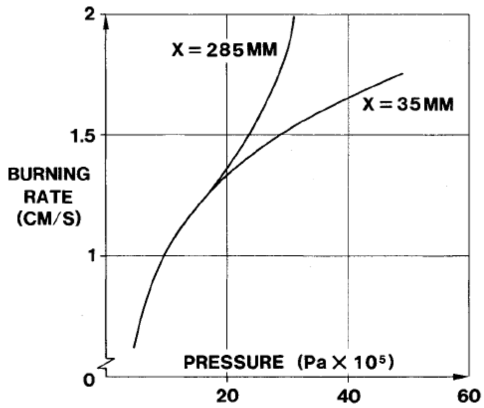

Figure 19 Test results for the two-dimensional test setup [1]

In the experimental study [15], Deepak et al. consider the pressure dependence of burning rate in a ballistic evaluation motor over a range of pressure from 2.5 to 4.5 MPa. In their study an aluminized composite solid propellant is used. In this study, before using the ultrasonic technique for the burning rate measurement in motors, it is first applied on end-burning propellant specimens. In Figure 20, the propellant specimen that is used in the experimental study is shown. Polymethyl methacrylate (PMMA) is used for the coupling material which reduces near field effects and protects the ultrasonic sensor from the combustion gases.

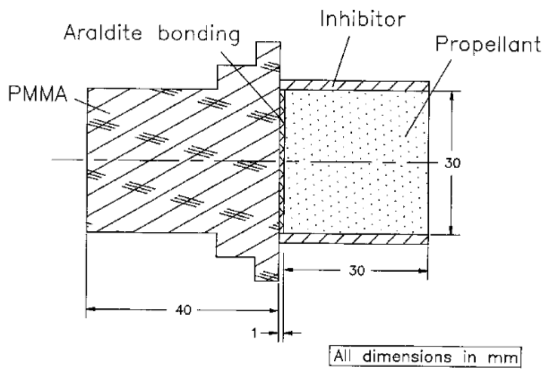

Figure 20 Propellant Sample Used in Closed Bomb Tests [15]

Before the application of ultrasonic technique used on ballistic evaluation motors, they show that the burning rate values are calculated by their systems within ±1 %. Also the ballistic evaluation motor that was used in experimental study is shown in Figure 21

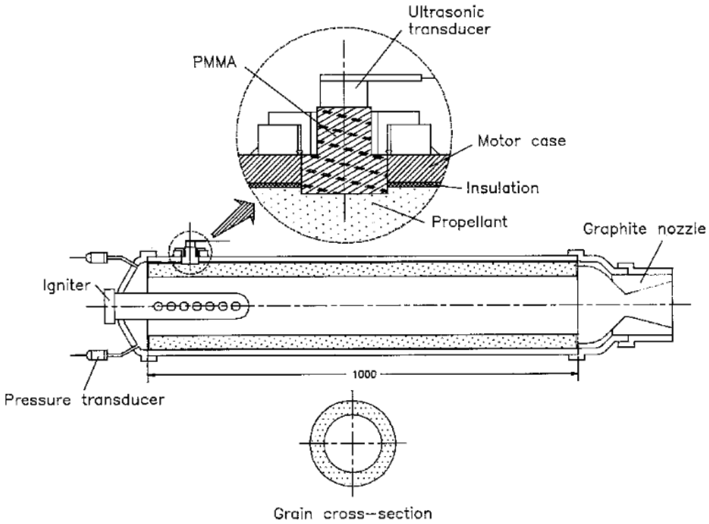

Figure 21 Test motor for burning rate evaluation [15]

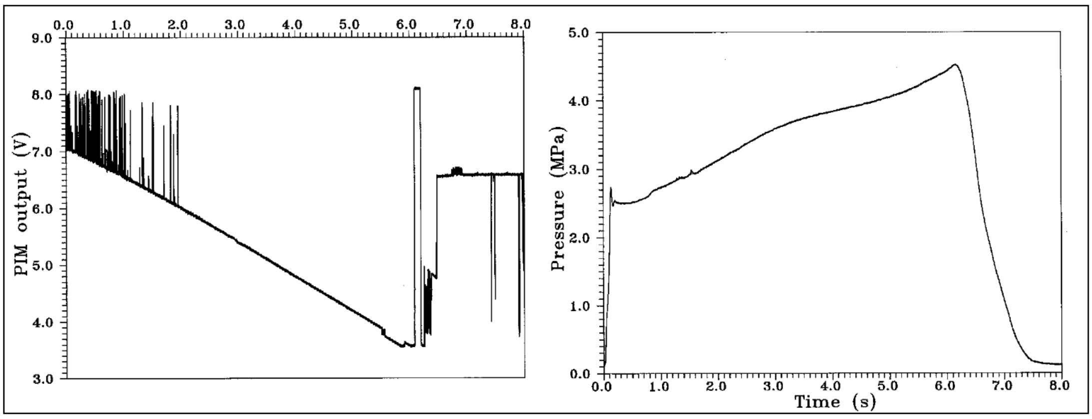

Figure 22 Voltage output and chamber pressure of the test motor [15]

In Figure 22, PIM output and motor pressure from a static test of the ballistic evaluation motor are shown. The output of PIM (voltage) was converted into time lapse by using the calibration constant of the equipment.

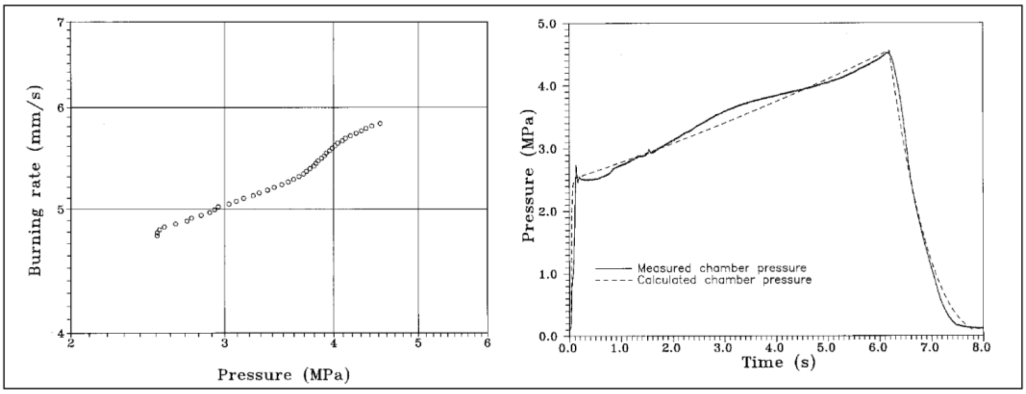

Figure 23 Test results obtained from burning rate evaluation motor [15]

The instantaneous web thickness of propellant with time is obtained and the instantaneous burning rate is evaluated from the slope of web thickness versus time. The instantaneous burning rate is shown in Figure 23. In this study, the accuracy of measured burning rates is checked by comparing the pressure history calculated using the derived burning rate law, with the measured pressure trace. The comparison of the pressure versus time curves is shown in Figure 23.

Ultrasonic measurement method can be applied on full scale rocket motors with the main target of determining insulation degradation and considering the combustion phenomena in the motor. This is the most difficult application field but also it is the most useful. Determining of insulation degradation is the way of checking the safety margins of the insulator. Attenuation, acoustic energy and transducer choice become a little more critical hence measuring the propagation time through the solid case is challenging [30].

Cauty [30] studies on full scale solid rocket motors by using ultrasonic method. He considers the internal insulator degradation and solid propellant combustion. Actually ultrasonic measurement method is used for verifying the thermo ablative computing code. The heat profile inside the material is computed by thermo ablative code. Time of flight which reflects from the internal insulation is measured and compared with the theoretical one that is determined from thermo ablative code. Knowledge of thermal properties of the insulator and its degradation process become more of an issue. Figure 24 represents a typical wave propagation that reflects from the burning surface.

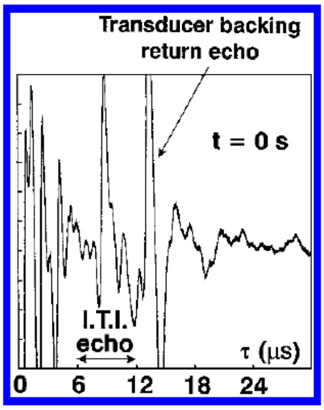

Figure 24 Ultrasound wave which reflects from insulation degradation surface [30]

During the test, ultrasonic waves are recorded in order to digitalize after the test. This procedure is performed for surveying the ultrasonic echoes that reflect from the degradation surface of insulator. The echoes coming from insulation surface are mixed with the baseline echoes. In Figure 24, ultrasound wave that reflects from insulation degradation surface is seen.

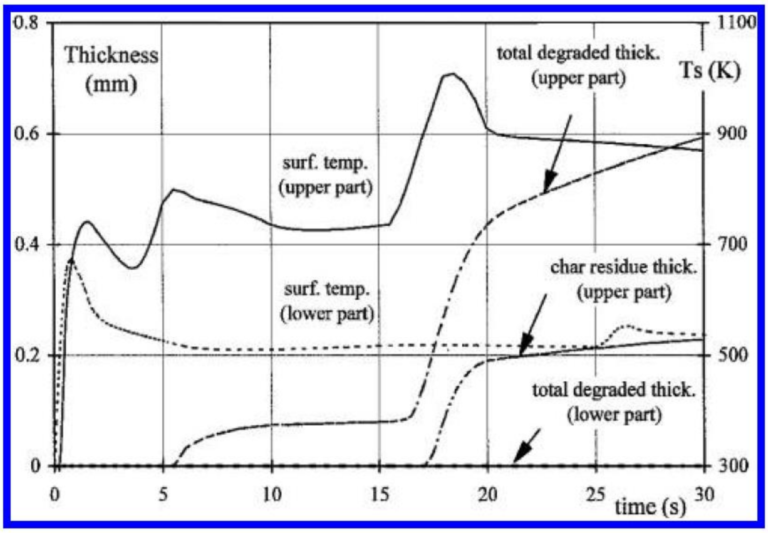

Figure 25 Measured surface temperature and Degraded thickness with respect to time [30]

In Figure 25 surface temperature distribution of upper part of flap zone and lower part of flap zone are shown. Upper part surface temperature is more than lower part, so total degraded thickness of insulation is also. In Figure 26 regression rates of the propellant during the static firing were obtained from the derivation of burned web thickness with respect to time are shown.

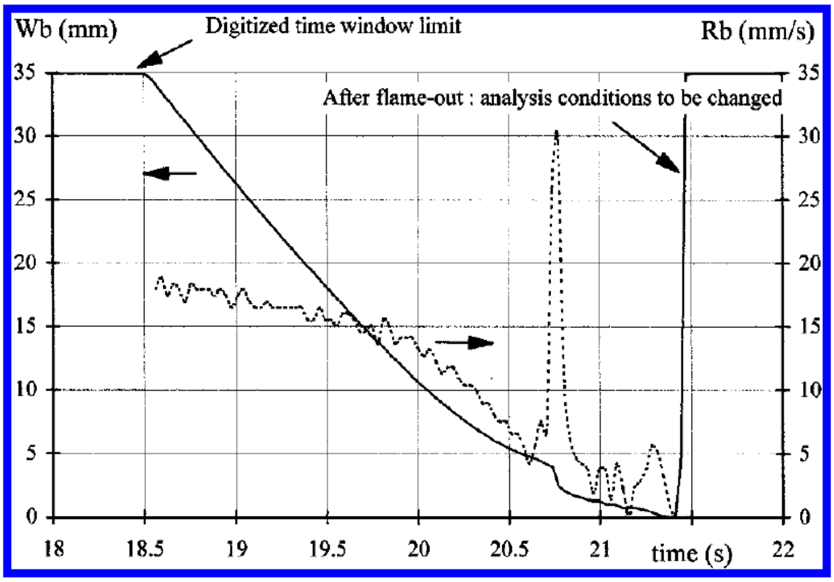

Figure 26 Web thickness and burning rate with respect to time [30]

CHAPTER 4

ULTRASONIC MEASUREMENT ON CLOSED BOMB TEST SETUP

4.1 Introduction

In this study a closed test setup is used for the purpose of evaluating burning rates of propellants. The purpose pursued in this work is to determine burning rates of different propellants used for rockets.

Ultrasonic measurement method has been used for many years at various areas such as burning rate determination of propellants, degradation of insulation materials and erosive burning applications. Especially at ONERA, research center in France, ultrasonic measurement method has been studied since mid-1970s. Cauty [7] summarizes the application areas of ultrasonic measurement technique. In this paper the setups that people used for burning rate determination, characterization of new energetic materials and erosive burning applications are introduced to people who deal with this topic.

The following section describes the software equipment, hardware equipment and test setup that used for burning rate determination. The parts of experimental setup are introduced briefly in the lower part. Also test set-up components can be seen in Figure 28.

The closed bomb is placed in a room with reinforced steel concrete walls. The layout of the test set up is seen in Figure 27.

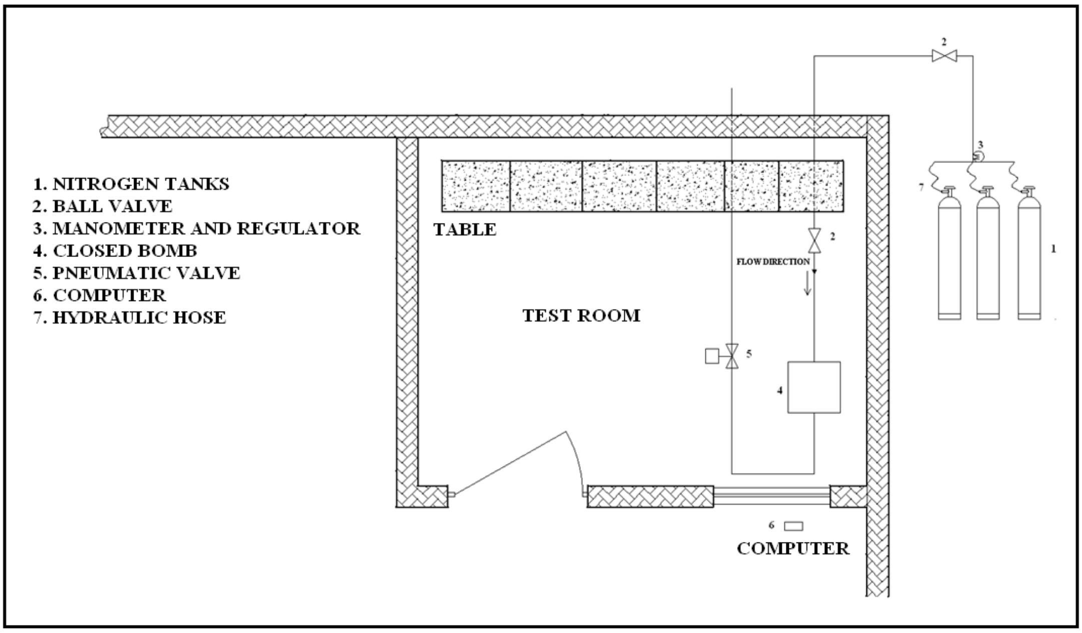

Figure 27 Layout of the Test Setup

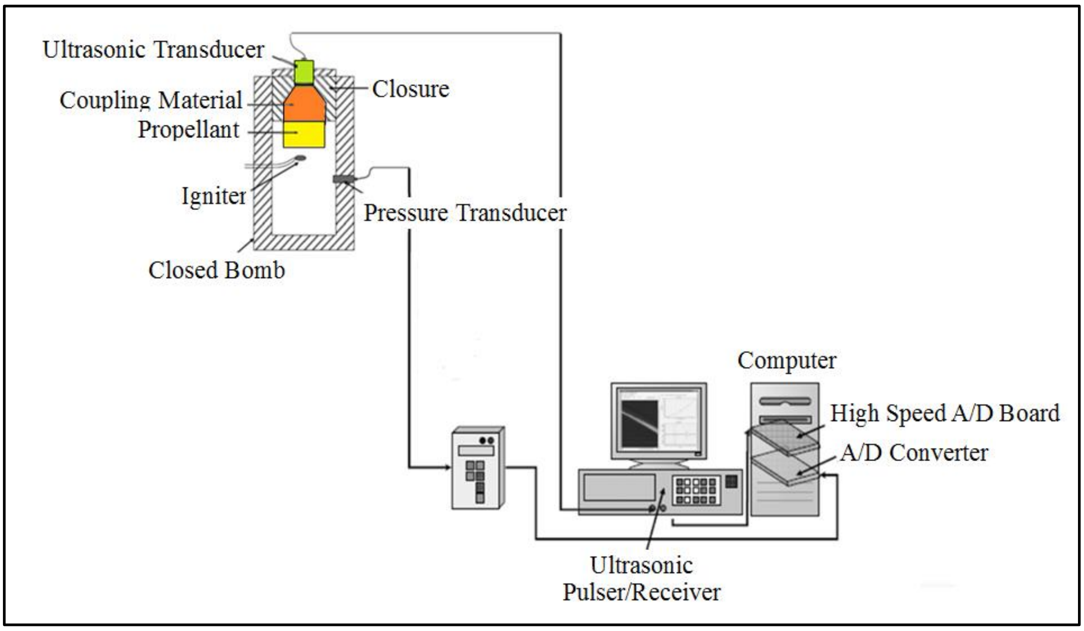

Figure 28 Schematic figure of the test setup components modified from [27]

4.2 Closed Bomb

The main part of the experimental setup is the closed bomb. A photo of closed bomb can be seen in Figure 29.

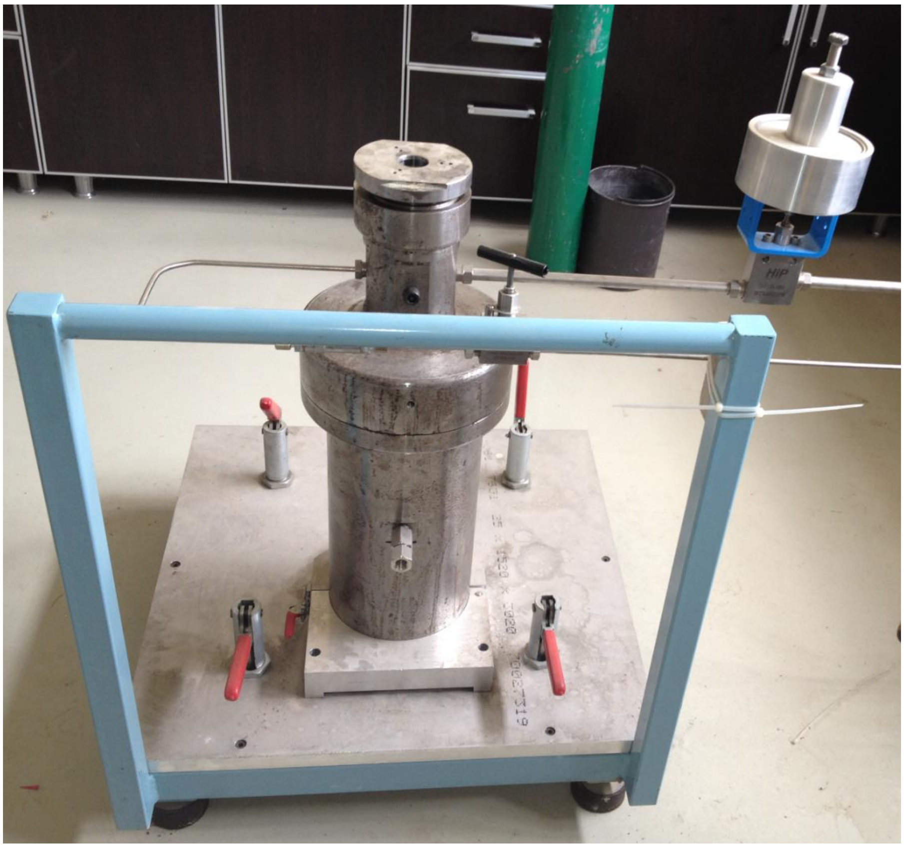

Figure 29 Photo of Closed Bomb

The closed bomb is located in a test room. It is made of 4140 steel. One port is located on the top of the closed bomb and is used for pressure transducer. Kistler 6215 model pressure transducer was used for pressure measurements for 18 tests. One port located on the closed bomb is used to pressurize the bomb with nitrogen during the pretests and the posttests. The propellant sample, coupling material, ultrasonic transducer and igniter are the base components of the closed bomb. The details of the components are discussed later. The pressure in closed bomb is increased hence burning rate while burning process in the closed bomb. The instantaneous web thickness of the propellant with respect to time is measured by ultrasonic measurement method. The safety test of this closed bomb is performed up to 5000 Psi. So the closed bomb tests were performed up to 5000 Psi.

4.3 Data Acquisition System

Data Acquisition System used in the experiments have one general timer card and one analog to digital card. Analog to digital card is 12 bits and has minimum 8 channels. The data acquisition system includes 5 ultrasonic data collection cards. SFT4001 HPCI type ultrasonic card is used in the data acquisition system. The data acquisition system is provided from Sofratest S.A. Every card has 2 ultrasonic channels. There are two independent channels which work on two modes, either single or twin pulser-receiver. Each analog to digital card has a frequency of 60 MHz on 8 bits. For one channel, maximum real time processing is 5000 pulses per second.

4.4 Ultrasonic Transducer

With the multi-channel high speed ultrasonic system, ultrasonic transducers are provided from Sofratest S.A. Ultrasonic transducers are used to measure time of flight data of the signals reflected from the propellant surface and coupling material. In this setup WC-100 type ultrasonic transducers which have 1 MHz frequency and 1 inch diameter are used. Connection between data acquisition system and transducer are provided by BNC connector. The signals are received and sent by the same ultrasonic transducers many times in seconds. The ultrasonic sensor that is used in the closed bomb tests is seen in
Figure 30.

Figure 30 Ultrasonic sensor and BNC connector with coupling material

4.5 Nitrogen Tanks

Nitrogen tanks are used for obtaining required pressure in order to start the burning process. A regulator is used for controlling the pressure supplied from the nitrogen tanks. The nitrogen tanks that were used are seen in Figure 31.

Figure 31 Nitrogen tank and regulator

4.6 Pressure Relief Valve

A normally closed selenoid relief valve is used to remote automatic on/off operation of valves. At the end of the test, pressure relief valve is opened and the combustion gases are relieved from the system.

4.7 Rupture Disc

A rupture disc is used to control pressure overload inside the pressure in closed bomb. If pressure increases to stated limit in closed bomb, rupture disc is ruptured and it provides the security.

4.8 Igniter

During the experiments two experimental ways are applied for ignition process. For the first eighteen tests igniter bag type igniter was used. It was glued to propellant surface with an adhesive in order to ignite with a trigger by giving 100 mA current. The propellant sample holder and igniter which were glued on propellant surface are shown in Figure 32. Later a double based propellant is used in order to ignite the propellant. This method change is performed for ignition delay. Bag type igniter was not strong enough so ignition delay was occurred.

Figure 32 Propellant sample holder and igniter

4.9 Coupling Material

The ultrasonic transducer which is used to send a mechanical wave travels through the tested materials is rarely mounted in direct contact with the propellant. A specific material called coupling material is used between propellant and transducer. It should have nearly the same acoustic impedance as the propellant. Coupling material created a delay line which avoids measurement from zero thickness. It is used to protect ultrasonic transducer from the severe conditions of temperature and pressure inside the closed bomb. Casting of the coupling materials used for tests are shown in Figure 33. In this study, two types of coupling materials are used; one for aluminized propellant and the other one is for non-aluminized propellants. Preparation of the coupling materials will be explained briefly. Also schematic view of the coupling material placed in closed bomb lid is shown in Figure 34. The propellant sample is glued to lower surface of the coupling material and ultrasonic transducer is placed on top of the coupling material.

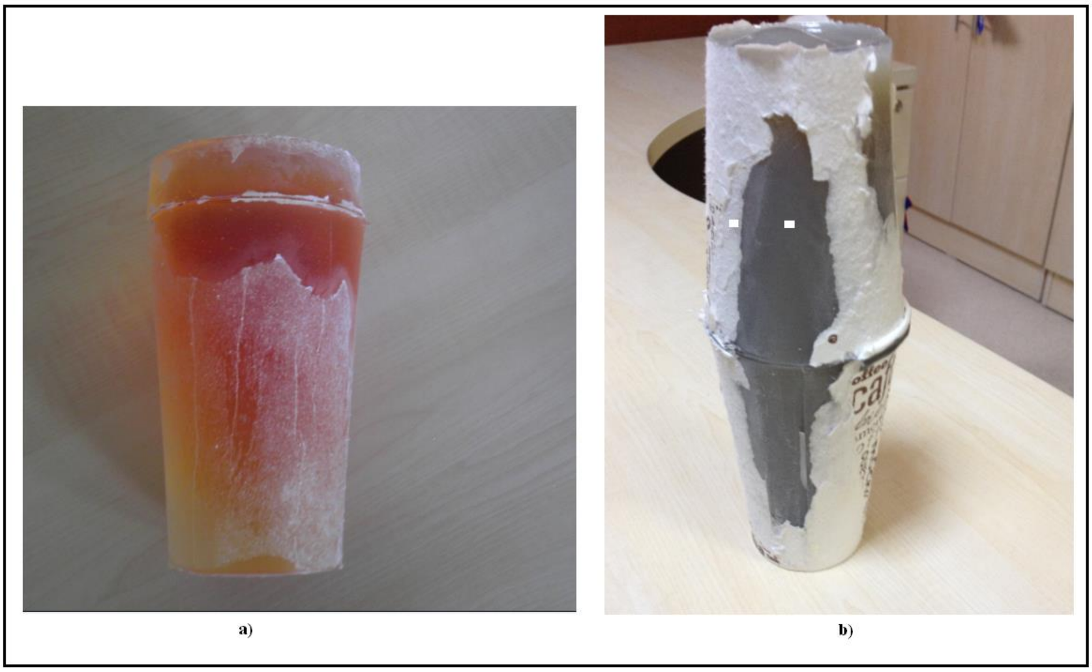

Figure 33 (a) a whole coupling material used for non-aluminized propellants (b) a whole coupling material used for aluminized propellants

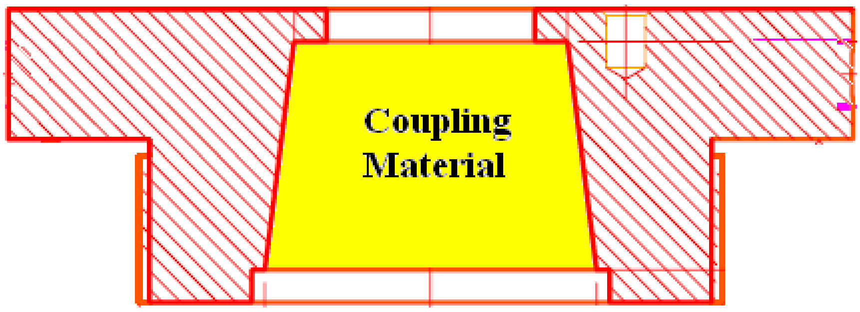

Figure 34 (a) Schematic view of the coupling material placed in propellant sample holder

4.10 Propellant

In this study, composite propellants which include a certain amount of AP (ammonium perchlorate), HTPB (hydroxyl terminated polybutadiene) and for some batches metal powder as aluminum are used. The main object of this study is to determine burning rates of solid propellants that is why the compositions of propellant and their batch numbers are very important. During the casting process of propellants, prepared mixing of propellant is poured in a mixer and named as AB-

XX called batch number as an example. In other words, batch number is the identification of the propellant mixing and is unique for this propellant composition. Burning rate versus pressure curves of same batch and same propellant is expected to be close to each other. If there is a difference between them, one should search for it. In Figure 35, examples of propellant samples are seen.

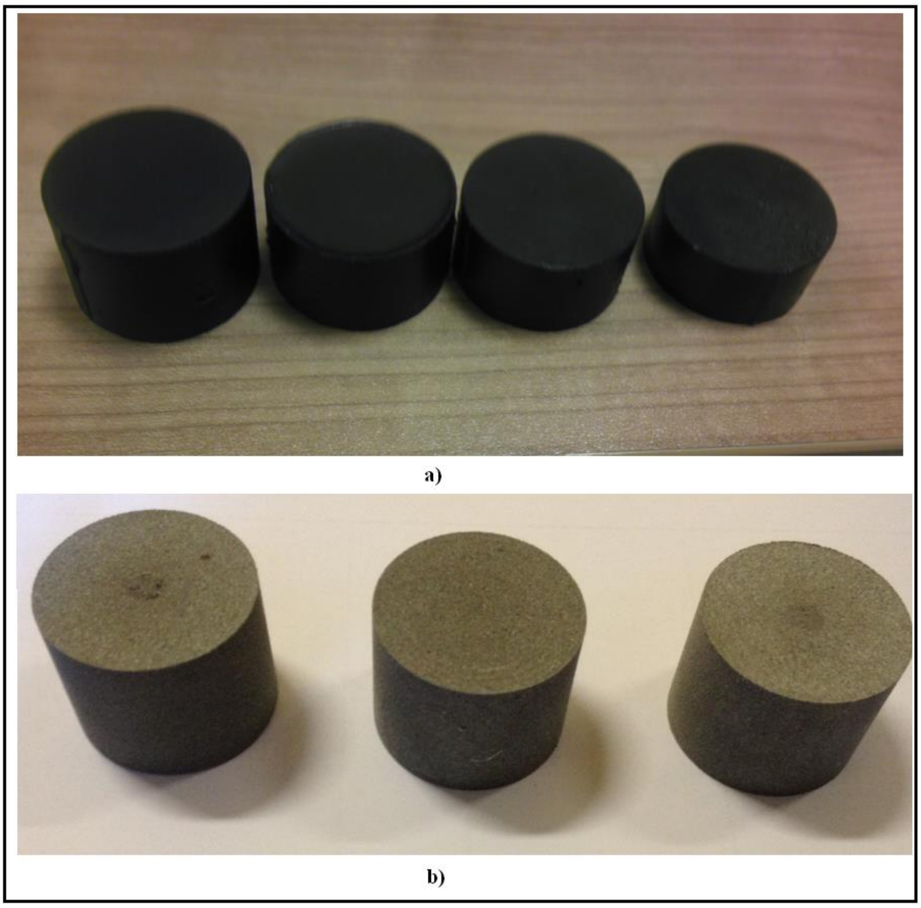

Figure 35 Propellant samples which have (a) different lengths b) same lengths

4.11 Experimental Procedure

Closed bomb tests with ultrasonic measurement method were performed with the aim of determination of burning rates of composite propellants. Test preparation studies and test procedure will be discussed briefly in this section. Also procedure which is applied during the tests is given in Appendix C. In this section, the preparation that should be performed before the closed bomb tests, the procedure during the tests and posttest processes are explained. The procedure includes three sections. These sections are; pretest, the processes during the test and gathering the data after the test. Before performing the tests, measurement of speed of sound of coupling material and propellant samples and control of bonding surface between propellant and coupling material were performed. In the last part, analyzing of the collected data should be performed.

Pre-tests steps are summarized below;

4.11.1 Casting Process of Propellant

Propellant samples are prepared by various ways during the study. One way is pouring the propellant mixture into molds that shown in Figure 36. The diameter of molds is 40 mm. The lengths of the propellant samples removed from the molds are respectively 19-20-21-22-23-24-25 mm. First eighteen propellant samples are prepared by this way. After these tests, method of preparation of propellant samples is changed due to avoid bubbles that can be occurred while pouring the mixture into molds. Preferred method is machining the propellant samples from a whole block.

Figure 36 Molds that are used for casting process of propellant samples

4.11.2 Casting Process of Coupling Material

In this part, the casting process of coupling material which is the interface between the propellant and ultrasonic transducer is explained briefly. There are two different preparation processes for coupling materials. One is for usage with aluminum composite propellant, and the other is for usage of non-aluminum composite propellant. The ingredients of the coupling materials are given in Table 2.

Table 2 Coupling Material Preparation [31]

The composite propellant with no aluminum		The composite propellants with aluminum	
Material	Quantity	Material	Quantity
ARALDITE DBF/CY230	70 g	ARALDITE DBF/CY230	60 g
HARDENER HY951	6.3 g	HARDENER HY951	5.4 g
-	-	Intensive silicon(SiO_2) (powder)	9.5 g (*)
-	-	Low density silicon (SiO_2) (wool)	1.2 g (*)

(*) For the propellant includes % 20 aluminum, %18 intensive silicon (powder), % 2 low density silicon (wool) are used.

After pouring the mixture into mold, the air in the mixture is removed by vacuum unit. This process lasts approximately 15-20 minutes. The mixture is cured at 27 ^{0}C for minimum 24 minutes. After curing process, the coupling material is removed from molds and is sent to lathe for final form. The control process for final form of coupling material is done by ultrasonic transducers. If there are bubbles in coupling materials, additional signals are occurred. For this reason, controlling the coupling material is very important.

4.11.3 Process of Inhibitor Covering

Lateral surface of propellant sample is covered with inhibitor with the aim of conducting the burning process in normal direction with respect to propellant surface. In Figure 37, plastic pipe is seen for pouring the inhibitor around the propellant. This plastic pipe has 50 mm inner diameter and length as same as propellant.

Table 3 Ingredient of Inhibitor

Materials	Quantity
ARALDITE CY208	40 g
HY951 (Hardener)	3.2 g

The upper surface of propellant should be covered with a plaster to prevent from inhibitor.

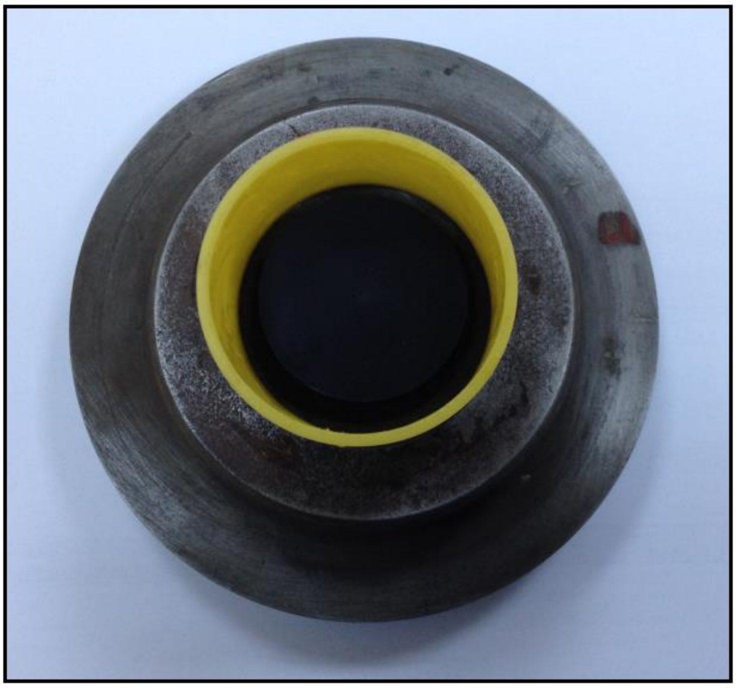

Figure 37 Propellant sample holder

4.11.4 Determination of Wave Velocity of Propellant

With the main target of determining the speed of sound (wave velocity) for one batch of propellant, various propellants are prepared with different lengths. Time of flight values of propellant samples that have different lengths are measured by ultrasonic transducers and equation (5) is used for evaluation.

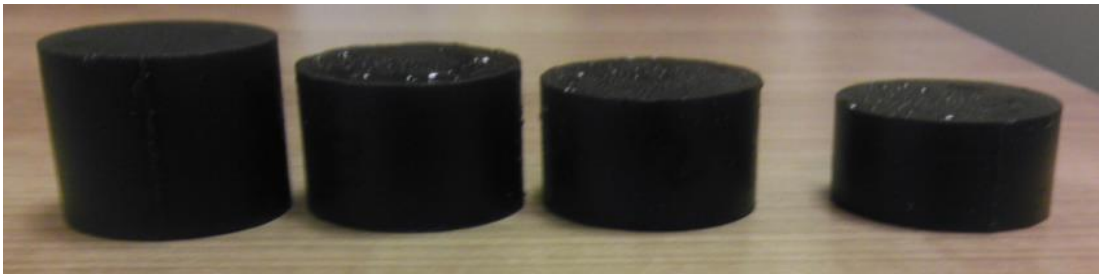

Figure 38 Propellant samples which have various lengths

4.12 Evaluation of Wave Velocity of Coupling Material

For the purpose of determining wave velocity that belongs to coupling material, different lengths of coupling material samples that are shown in Figure 39 are manufactured and return echoes of them are measured by ultrasonic transducers.

Figure 39 Coupling Materials used for determination of wave velocities

4.13 Bonding Operations

After casting processes, propellant and coupling materials are bonded to propellant sample holder of closed bomb. First of all, coupling material is glued in the sample holder. After that, propellant is glued on surface of coupling material. Especially bonding of coupling material in the propellant sample holder is critical for success of the test. Sometimes it is not glued properly in propellant sample holder and causes leakage. This situation is not desirable.

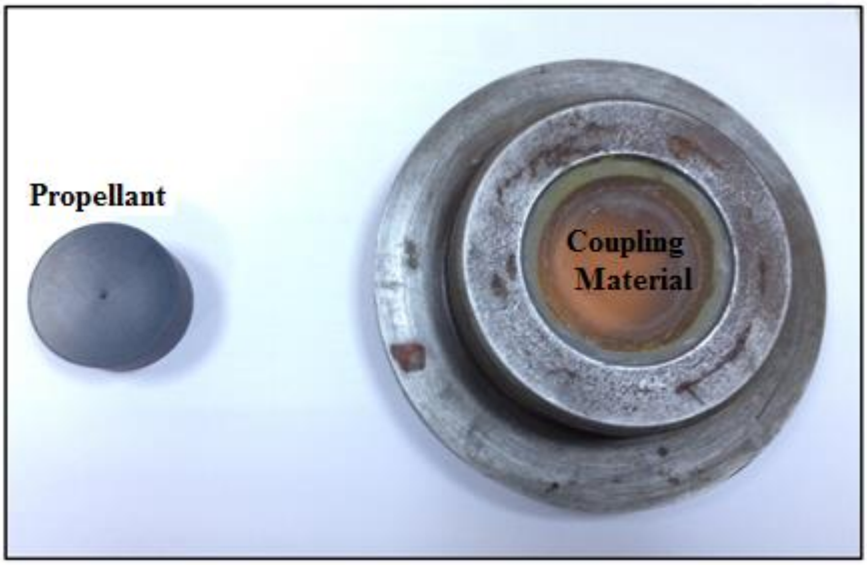

Figure 40 Propellant sample and propellant holder with coupling material

The final photo of the sample holder is ready to test is seen in
Figure 41. Preparations of sample holders of closed bomb tests are performed by Chemical Materials Production Laboratory of Roketsan.

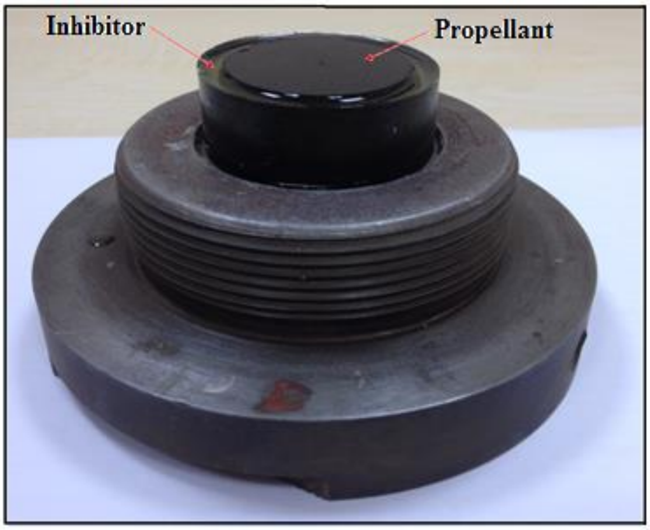

Figure 41 Final photo of propellant sample holder

4.14 Leakage Test of Closed Bomb Test

As a pre-test, closed bomb is pressurized with Nitrogen and leakage control of the setup is performed for all of the closed bomb tests.

4.15 Application of Closed Bomb Test

After preparations are completed, adjustment of the software is done for starting the tests. The acquisition process begins by setting the ultrasonic echoes shown in Figure 42. There are two gates. One is adjustable in position and the other is adjustable in width. Gate 1 selects the echo peak from which reflects from the burning surface of the propellant. This gate moves by the regression of the burning surface. Gate 2 gives the position of the second echo that reflects from the coupling material surface in other words interface between the propellant and the coupling material. The details of test procedure are presented in Appendix C.

Figure 42 Ultrasound echo settings

Closed bomb tests were conducted by the help of Static and Flight Tests Department of Roketsan.

CHAPTER 5

CLOSED BOMB TEST RESULTS

5.1 Closed Bomb Test Results

In this chapter closed bomb tests that were performed with ultrasonic measurement method are considered in details. Detailed comparison between closed bomb tests performed with ultrasonic method, static firing tests performed with subscale test motors and strand burner results is performed. In Table 4, the details of tests that were come true in the scope of this thesis are shown. In Roketsan, various propellant compositions are developed for solid rocket motors. Composition of propellants and quantities of the composition used are varied from a solid rocket motor to another. Every propellant composition has a propellant name. This propellant name differs from composition ingredients and the date which the propellant mixing is performed.

The propellant samples are produced by Chemical Materials Production Department of Roketsan.

Table 4 Details of Closed Bomb Tests

TEST NUMBER	PROPELLANT NAME	CONDITIONING TEMPERATURE (^0C)	COMPOSITION OF PROPELLANT
F001	OMTYPE1	21	(%84.6 AP, %9.5 HTPB)
F002	OMTYPE2	21	(%84.6 AP, %9.5 HTPB)
F003	OMTYPE2	21	(%84.6 AP, %9.5 HTPB)
F004	OMTYPE2	21	(%84.6 AP, %9.5 HTPB)
F005	HSTYPE1	21	(%82.3 AP, %9.5HTPB)
F006	HSTYPE1	21	(%82.3 AP, %9.5HTPB)
F007	HSTYPE1	21	(%82.3 AP, %9.5HTPB)
F008	HSTYPE1	21	(%82.3 AP, %9.5HTPB)
F009	HSTYPE1	21	(%82.3 AP, %9.5HTPB)
F0010	HSTYPE2	21	(%83 AP, %9.5 HTPB)
F0011	HSTYPE2	21	(%83 AP, %9.5 HTPB)
F0012	HSTYPE2	21	(%83 AP, %9.5 HTPB)
F0013	HSTYPE3	21	(%83 AP, %9.5 HTPB)
F0014	HSTYPE3	21	(%83 AP, %9.5 HTPB)
F0015	HSTYPE3	21	(%83 AP, %9.5 HTPB)
F0016	HSTYPE4	21	(%83 AP, %9.5 HTPB)
F0017	HSTYPE4	21	(%83 AP, %9.5 HTPB)
F0018	HSTYPE4	21	(%83 AP, %9.5 HTPB)
F0019	HSTYPE5	21	(%82 AP, %9.5 HTPB)
F0020	HSTYPE5	21	(%82 AP, %9.5 HTPB)
F0021	HSTYPE5	21	(%82 AP, %9.5 HTPB)
F0022	HSTYPE5	21	(%82 AP, %9.5 HTPB)
F0023	HSTYPE5	21	(%82 AP, %9.5 HTPB)
F0024	HSTYPE5	21	(%82 AP, %9.5 HTPB)
F0025	HSTYPE5	21	(%82 AP, %9.5 HTPB)
F0026	HSTYPE5	21	(%82 AP, %9.5 HTPB)
F0027	HSTYPE5	21	(%82 AP, %9.5 HTPB)
F0028	HSTYPE5	21	(%82 AP, %9.5 HTPB)
F0029	HSTYPE5	21	(%82 AP, %9.5 HTPB)
F0030	HSTYPE5	21	(%82 AP, %9.5 HTPB)
F0031	BTYPE1	21	(%72 AP, %9 HTPB, %19 Al)
F0032	BTYPE1	21	(%72 AP, %9 HTPB, %19 Al)
F0033	BTYPE1	21	(%72 AP, %9 HTPB, %19 Al)

5.2 Results of OMTYPE1

During the closed bomb test, the signal peak, time of flight and pressure are measured. Outputs of the test 1 are shown in Figure 43.

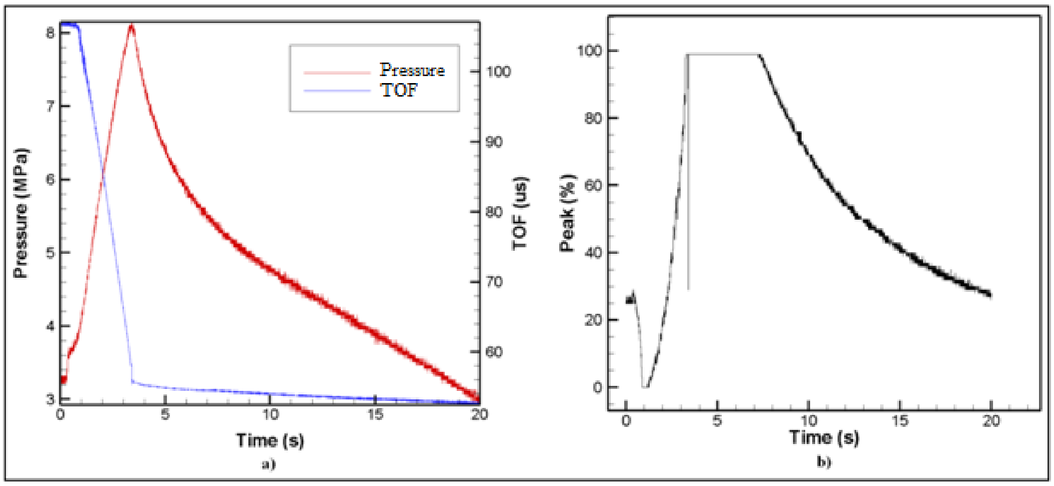

Figure 43 a) Measured pressure and time of flight (TOF) versus time b) Peak data versus time

If the Figure 43 is evaluated in details, it can be easily seen that peak data that is measured during the test exceeds the top range at approximately 3.5 second. This time coincides approximately at the end of burning time. During the combustion, the data that were measured are given in Table 5.

Table 5 Combustion data of Test 1

First Pressure (MPa)	Maximum Pressure (MPa)	Start of combustion (s)	Finish of Combustion(s)	Time (s)
3.27	8.15	0.6	3.386	2.786

The test lasts approximately 3 seconds but the data are collected during 20 seconds. This is done for collecting all measured data completely. The characteristics of combustion process are seen in Figure 43. Time of flight data stays constant until the burning process time is started. After the ignition of propellant, propellant is started to burn and the distance between the signal reflected from burning surface and signal reflected from interface hence time of flight is started to decrease. The time that belongs to start of decreasing time of flight is assumed the start of burning.

The pressure data shown in Figure 43 shows the pressure inside the closed bomb. Before the ignition of propellant, closed bomb is filled with nitrogen gas. The ignition pressure is called first pressure. With the starting of burning process the pressure rises up to a maximum pressure. The maximum pressure is the end of the burning process.

The peak data shown in Figure 43 is very important for test verification. The peak data shows us the amplitude of the signals. When the peak value is zero, it shows that the signal could not been handled. At that time the results may be wrong. For this reason the peak value has to be checked by the user.

By using the burning rate equation, the burning rate of the propellant batch was calculated and compared with the static firing test as shown in Figure 44. The closed bomb test does not include the pressures that were performed with subscale test motors. For this reason the comparison between the results is not performed with specific pressures.

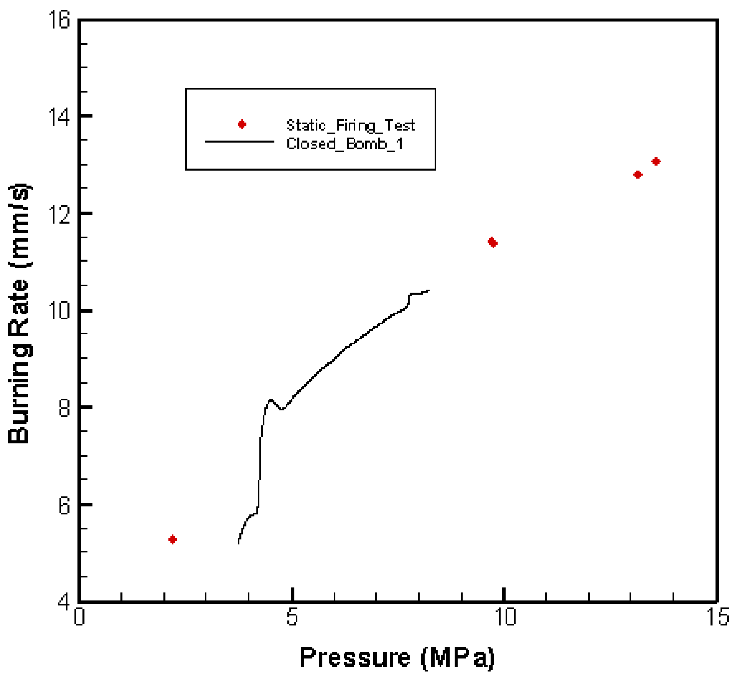

Figure 44 Burning rate versus pressure for Test 1

At the end of the test, analyzing of the measured data is very important for determining accurate burning rates. For accurate results, some operations must be performed as smoothing and filtration to the raw data which are measured during the test. Number of average data that has been used for smoothing and sensibility of numerical differentiation is very important for determining the burning rate. While smoothing the different number of raw data, different burning rate calculations can be occurred. While smoothing the data, least square method is used by using MATLAB.

According to Figure 44, the static test firing test results are compatible with closed bomb test results. Static firing tests were performed at each individual pressure while closed bomb test is performed for a pressure range.

5.3 Results of OMTYPE2

Three tests were carried out by OMTYPE2 propellant. The measured time of flight, pressure and peak values related to OMTYPE2 are shown in Figure 45, Figure 46 and Figure 47.

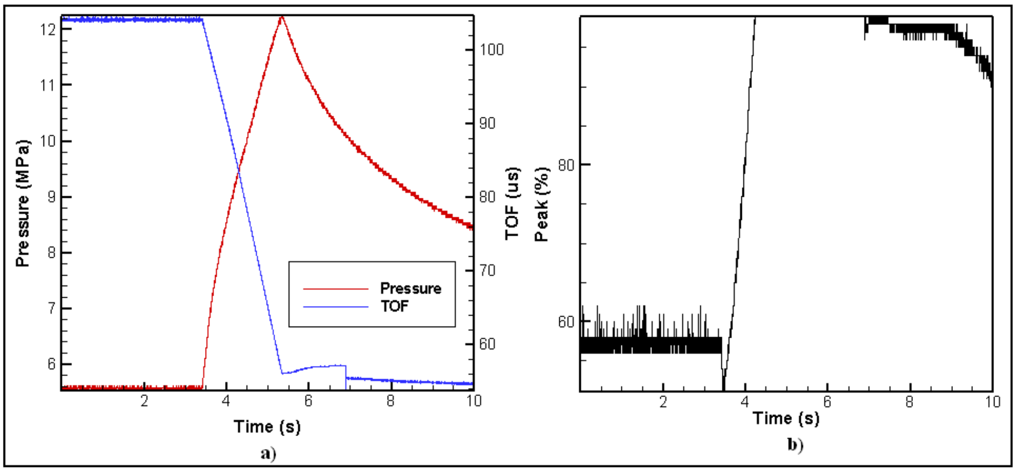

Figure 45 a) Measured pressure and time of flight versus time for Test 2 b) Peak data versus time for Test 2

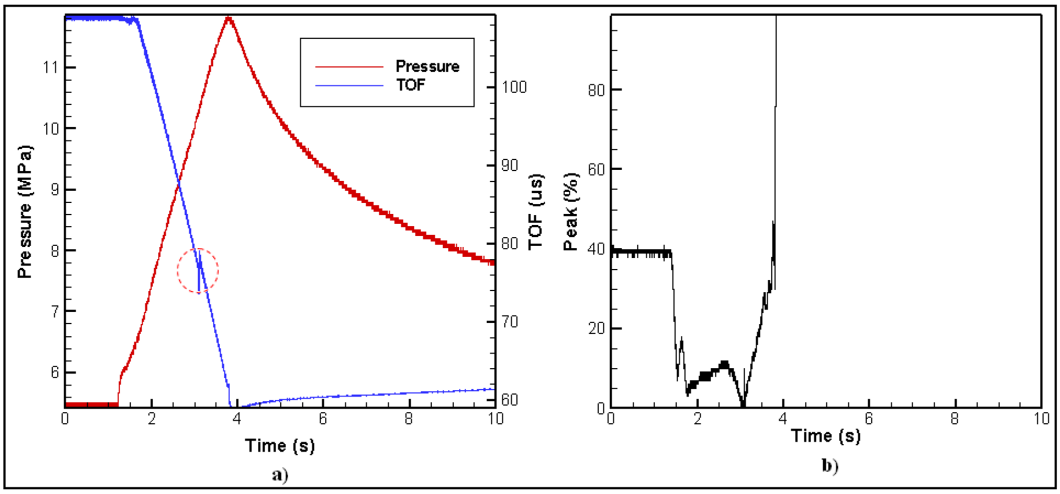

Figure 46 a) Measured pressure and time of flight versus time for Test 3 b) Peak data versus time for Test 3

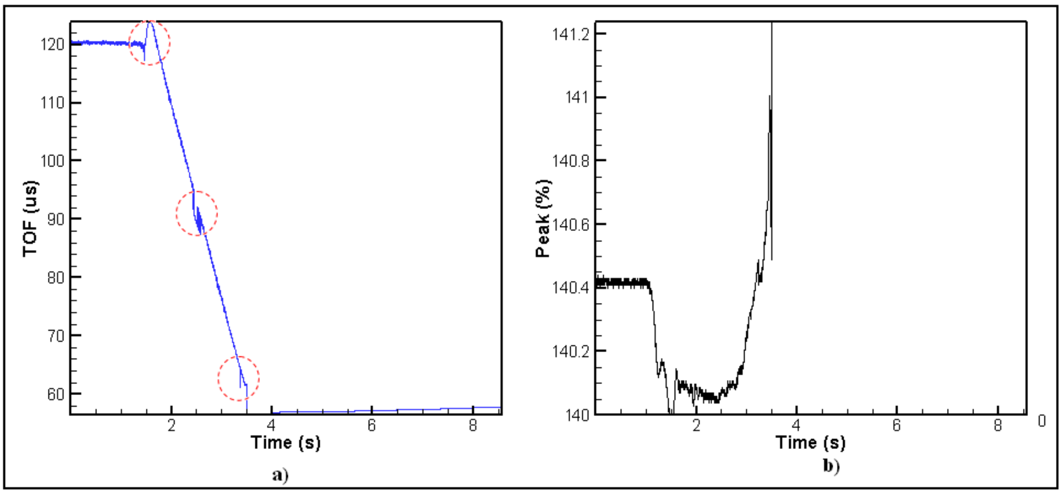

Figure 47 a) Measured pressure and time of flight versus time for Test 4 b) Peak data versus time for Test 4

If the peak values shown in Figure 45 are considered in details, it can easily be seen that the amplitude of the signal reached 100% value before the end of burning process which is approximately in 5.35 seconds. In this situation the gates that were used for tracking the signal reflected from the burning surface of propellant follow the wrong signals. At that situation, the acoustic signal that is sent from the ultrasonic sensor can be reflected from the burning surface of propellant with different peak values and the gates could track the wrong signal.

If the data shown in Figure 46 is considered, it can be easily seen that tracking process of the signals is faced of some problems. The pressure data is smooth but time of flight data has a fluctuation as shown in Figure 46. For determining the cause of this fluctuating the peak value that shown in Figure 46 has to be considered. Peak value at the time when fluctuation is occurred reaches its minimum value. In other words the gate tracks a wrong signal at that time.

At test 4, the pressure data of the test was not collected by ultrasonic measurement method. It was collected by another data collection system named as Kistler. Time of flight data of Test 4 is shown in Figure 47. Pressure was not tracked by the system. For this reason, Test 4 cannot be analyzed properly.

Table 6 Combustion Data of Test 2 and Test 3

Test Number	First Pressure (MPa)	Maximum Pressure (MPa)	Start of combustion (s)	Finish of Combustion (s)	Time (s)
2	5.57	12.26	3.4	5.35	1.95
3	5.47	11.87	-	3.775	-

In Figure 48, the results of static firing test and closed bomb test results are compared with each other.

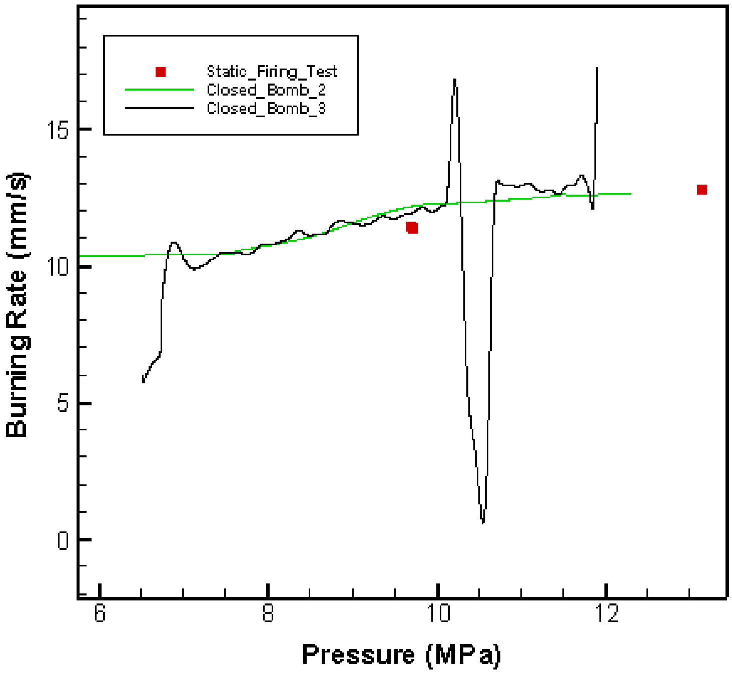

Figure 48 Burning Rates versus pressure belong to OMTYPE2

According to Figure 48, the results that obtained from static firing tests are not far from the results that obtained from the closed bomb tests. Also two closed bomb burning rates are closer to each other. The burning rate results obtained from test 3 show nonphysical results between 10 and 11 MPa due to fluctuation at time of flight data.

5.4 Results of HSTYPE1

Time of flight, peak and pressure data with respect to time related to HSTYPE1 propellant are shown in Figure 49 and Figure 50.

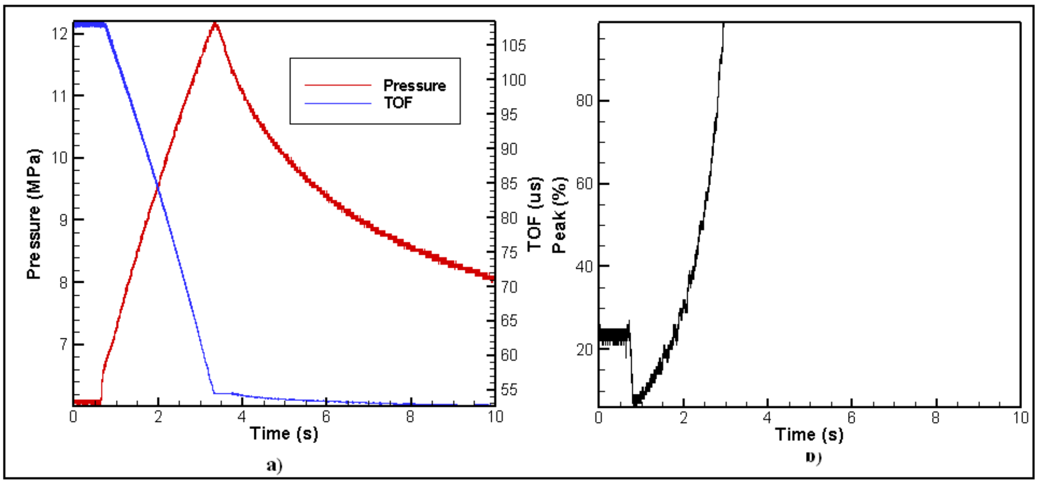

Figure 49 a) Measured pressure and time of flight versus time for Test 5 b) Peak data versus time for Test 5

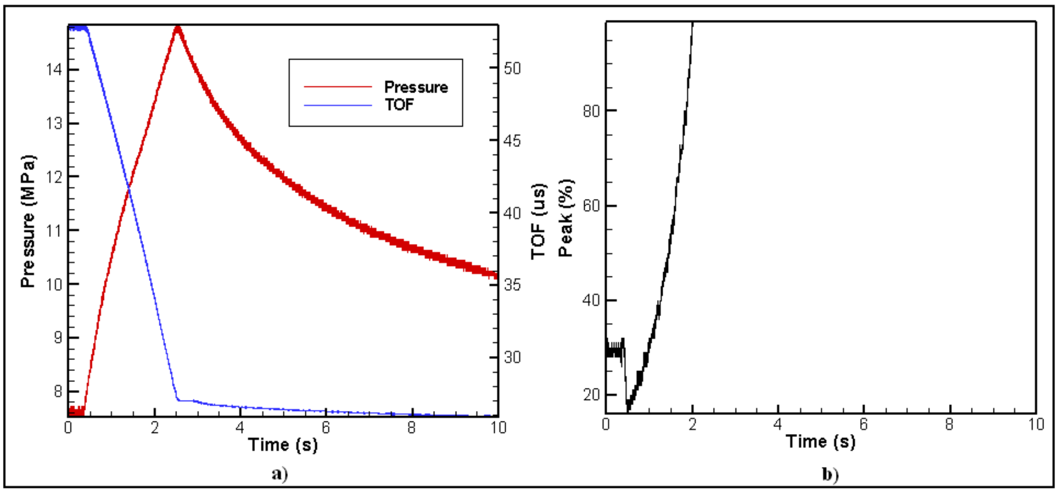

Figure 50 a) Measured pressure and time of flight versus time for Test 6 b) Peak data versus time for Test 6

These tests were performed by a new propellant batch and propellant type. If the measured data of tests that belong to HSTYPE1 propellant are considered, it seems convenient except end time of burning process. Automatic gain control was not active while these tests were being performed. For this reason, all of the measured peak data which show the amplitude of the signal 100% value at the end of the test. Also the combustion data of tests that belong to HSTYPE1 propellant is summarized in Table 7.

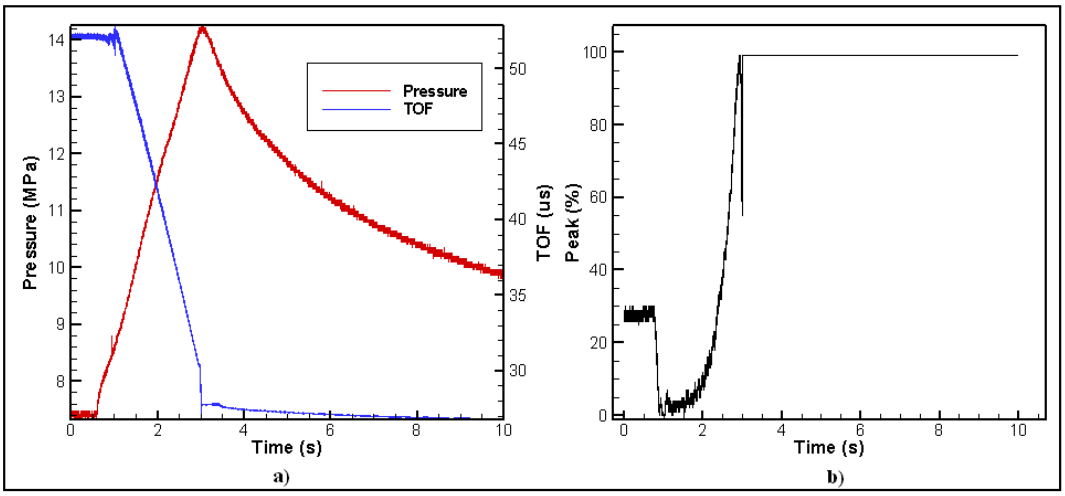

Figure 51 a) Measured pressure and time of flight versus time for Test 7 b) Peak data versus time for Test 7

Time of flight, pressure and peak values is shown in Figure 51 for test 7. As seen from the Figure 51, at the beginning of the test time of flight is fluctuated. It is thought that this is due to signal that were collected during the test. During the test, the gate that captures the signal reflected from the burning surface of propellant could have captured wrong signal.

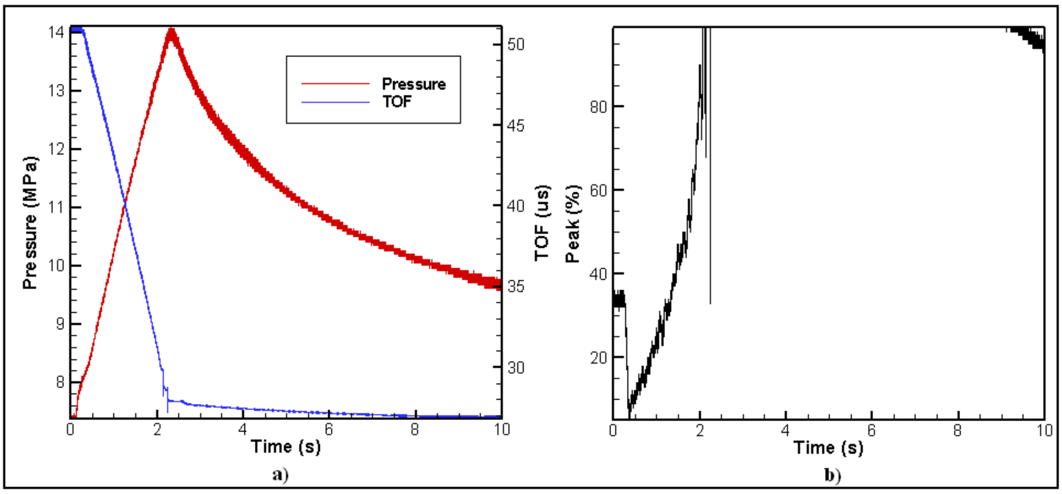

Figure 52 a) Measured pressure and time of flight versus time for Test 8 b) Peak data versus time for Test 8

If Figure 52 is considered, peak value belongs to signal exceeds the maximum value at the end of the test. At the end of the burning of propellant, the amplitude of the signal reflected from the burning surface gets bigger and unites with the signal reflected from the coupling material.

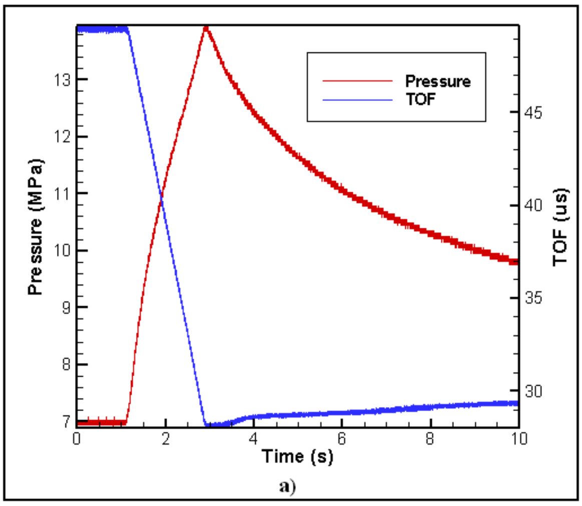

Figure 53 a) Measured pressure and time of flight versus time for Test 9

Table 7 Combustion Data of Tests

Test Number	First Pressure (MPa)	Maximum Pressure (MPa)	Start Time of Burning Process (s)	Finish Time of Burning Process (s)	Burning Time (s)
5	6.05	12.21	0.7	3.34	2.64
6	7.62	14.84	0.373	2.53	2.157
7	7.37	14.26	-	3.03	-
8	7.40	14.11	0.24	2.31	2.07
9	6.98	13.96	1.14	2.92	1.78

For test 7, the time that comes across the start of combustion is indefinite because of fluctuating at the beginning of the test. For this reason, the beginning time of burning process was not determined.

In Figure 54, the burning rate versus pressure of batch is shown. If the figure is examined, closed bomb test result that belongs to test 9 is different from other closed bomb test results and static firing test results.

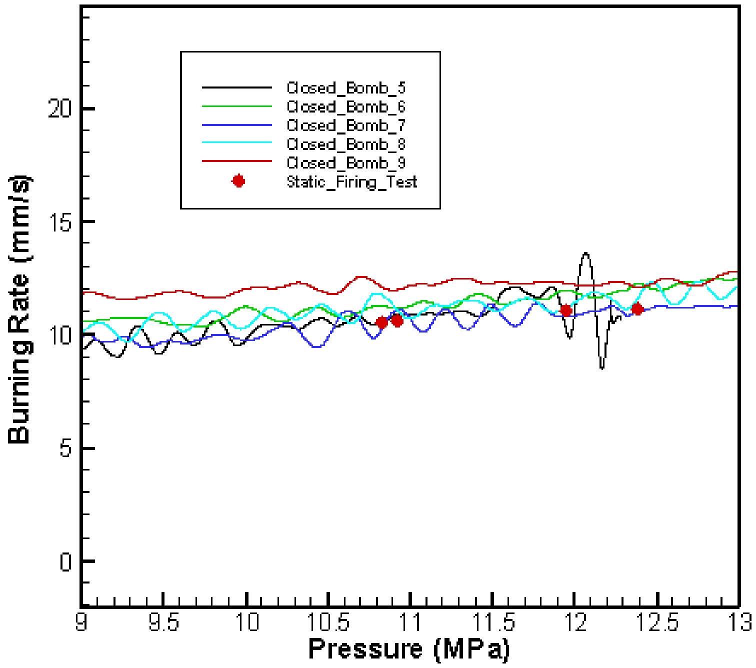

Figure 54 Burning Rate Value for HSTYPE1 propellant versus pressure

Burning rate values that obtained with closed bomb results are compared with static firing test results and seen that there are differences between the results. These differences can come from various causes such as uncertainty of the test setup, quality of the echoes and nature of the methods.

Table 8 Burning Rates of HSTYPE1

Pressure (MPa)	Burning Rates Determined from Static Firing Tests (mm/s)	Burning Rate Determined from Closed Bomb Tests (mm/s)	Stdev of Closed Bomb Tests (mm/s)	Average of Closed Bomb Tests (mm/s)
10.83	10.58	10.85	0.423	11.22
		11.14		
		11.04		
		11.12		
		11.95		
10.92	10.64	10.48	0.836	11.14
		11.23		
		10.12		
		11.74		
		12.11		
11.95	11.10	10.39	0.778	11.29
		11.93		
		10.76		
		11.13		
		12.23		
12.38	11.17	12.23	0.550	11.58
		10.96		
		11.51		
		12.06		

5.5 Results of HSTYPE2

Three closed bomb tests were performed with propellant HSTYPE2. The measured data and the obtained results are discussed below.

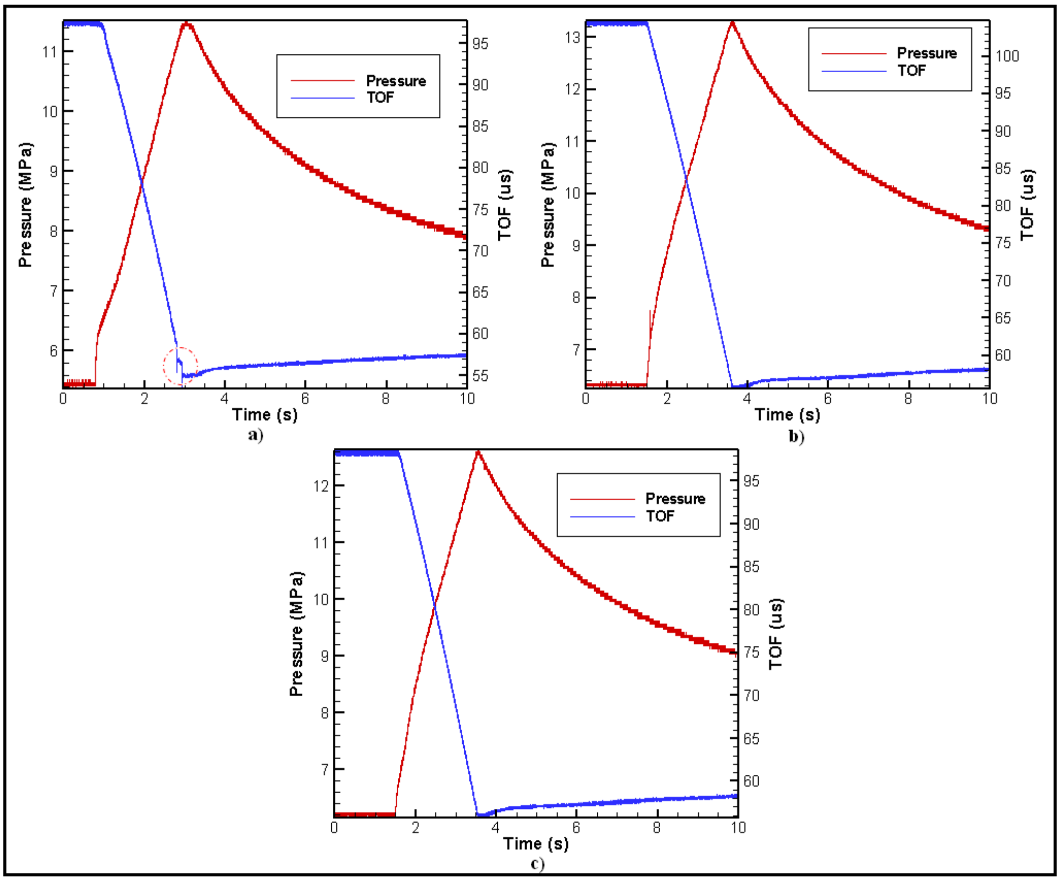

Figure 55 Measured pressure and time of flight versus time for a) Test 10 b) Test 11 c) Test12

The first eight closed bomb tests were performed without using automatic gain control. After that, automatic gain control is always used.

Table 9 Combustion Data's of Test 10,11,12

Test No.	First Pressure (MPa)	Maximum Pressure (MPa)	Start time of Burning Process (s)	Finish time of Burning Process (s)	Burning Time (s)
10	6.34	13.33	1.49	3.62	2.13
11	6.3	13.28	1.46	3.60	2.14
12	6.25	12.65	1.5	3.52	2.02

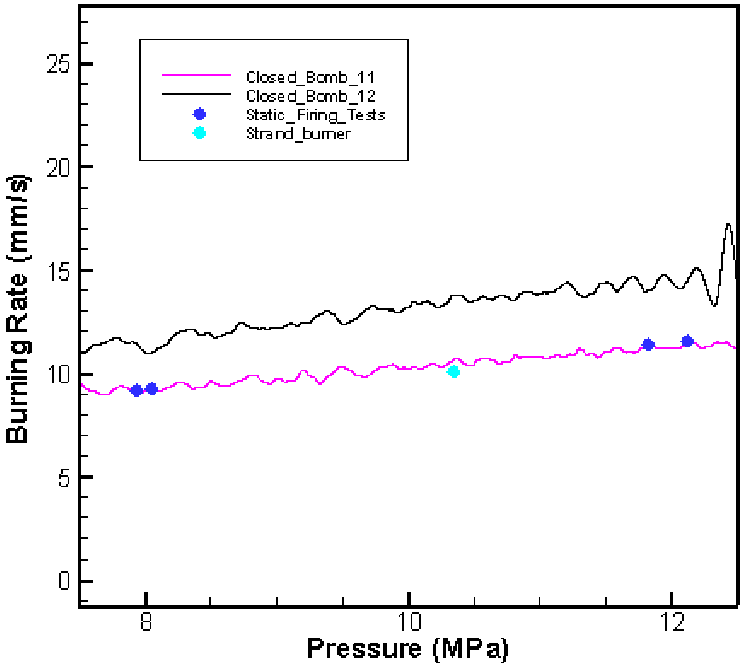

Figure 56 Burning Rate Value versus pressure for Test 11 and Test 12

According to Figure 56, test 12 is a little different from test 11 and the results that belong to test 12 are far from the strand burner test results and static firing test results. Strand burner test results and static firing test results seem same so the results prove each other. For this reason the accuracy of the results of test 12 should be examined. Burning rate line versus time is not calculated for test 10 due to undefined time that belongs to end of burning process.

5.6 Results of HSTYPE3

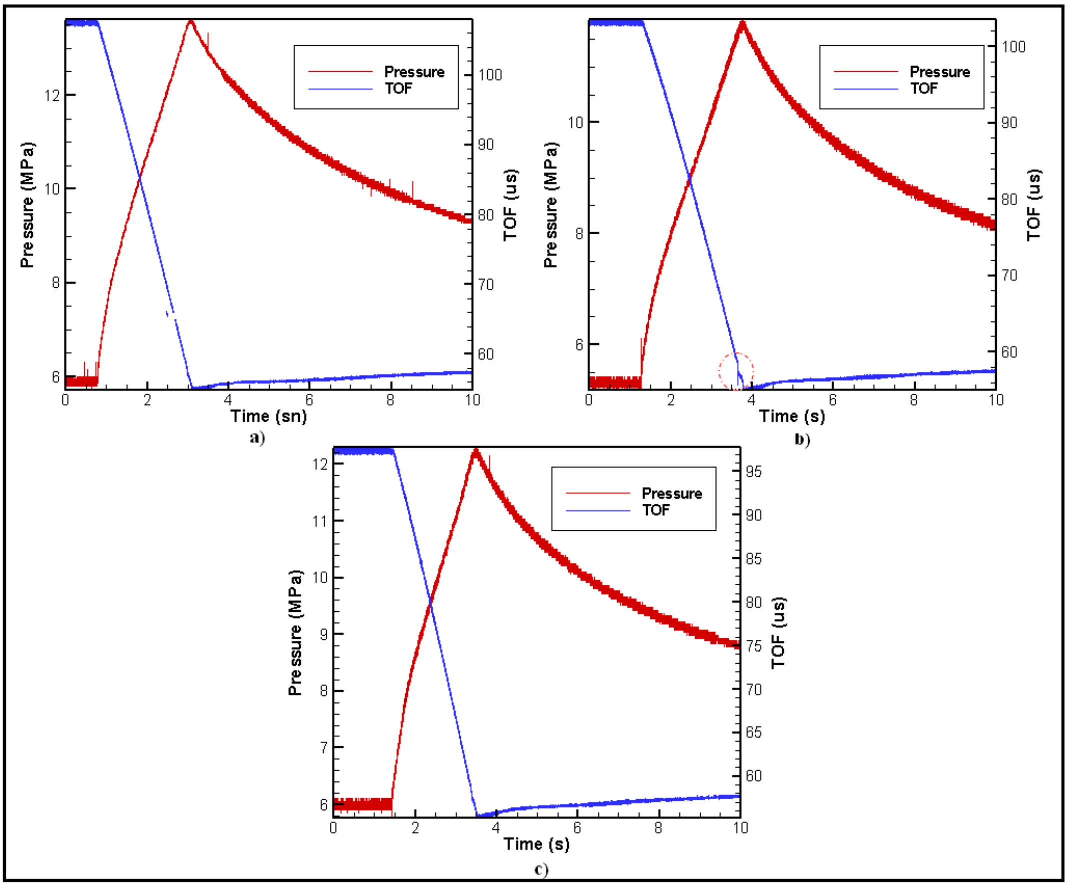

Figure 57 Measured pressure and time of flight versus time for a) test 13 b) test14 and c) test 15

By using the same propellant composition, propellant samples that belong to test 13, test 14 and test 15 were prepared. If the results are considered, it can easily be seen that time of flight data of test 14 has a fluctuation at the end of burning process. As known, closed bomb is pressurized with an inert gas which in that study is nitrogen before the ignition of the propellant. If Table 10 which summarizes the data of burning process belong to tests is searched, one can easily see that test 13 and test 15 have same first pressure but maximum pressures of them are different from each other. In other words, the propellants compositions related to propellant samples are same but release different levels of energy hence have different burning rates.

As a result, test 14 and test 15 results are compatible with the static firing test results. But the trend of burning rates that belong to test 13 is quite different from other tests and static firing test results.

Table 10 Combustion Data's of Test HSTYPE3

Test No.	First Pressure (MPa)	Maximum Pressure (MPa)	Start time of Burning Process (s)	Finish time of Burning Process (s)	Burning Time (s)
13	6.0	13.57	0.77	3.08	2.31
14	5.37	11.77	1.27	3.77	2.5
15	6.1	12.30	1.40	3.49	2.09

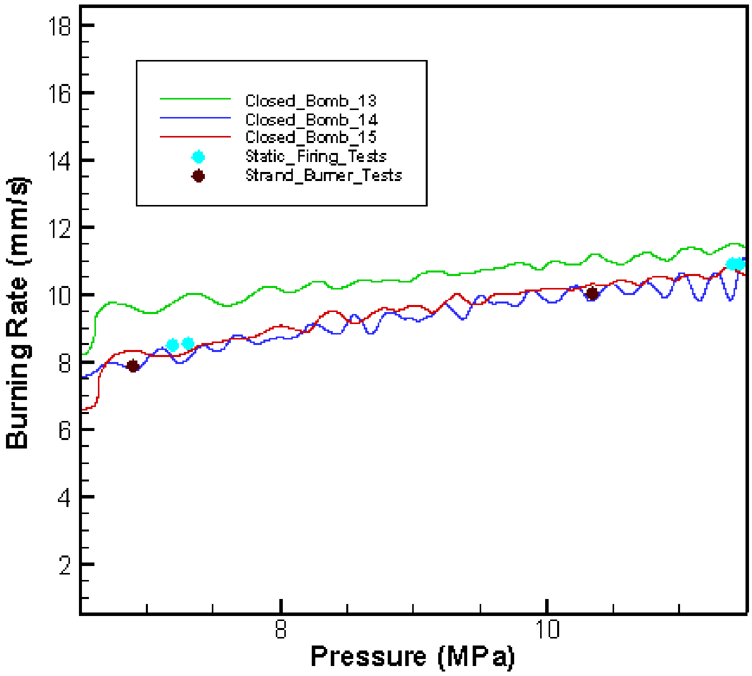

Figure 58 Burning Rate Value versus pressure that belongs to HSTYPE3

5.7 Results of HSTYPE4

During the test that was done by using propellant batch named HSTYPE4, the data is not collected properly. The TOF which was measured at the time of peak pressure was not rational. Time of flight data with respect to time and pressure data are shown in Figure 59. Time of flight data that belongs to test 17 is raised to high values during the test. The reason of that could not be fully determined.

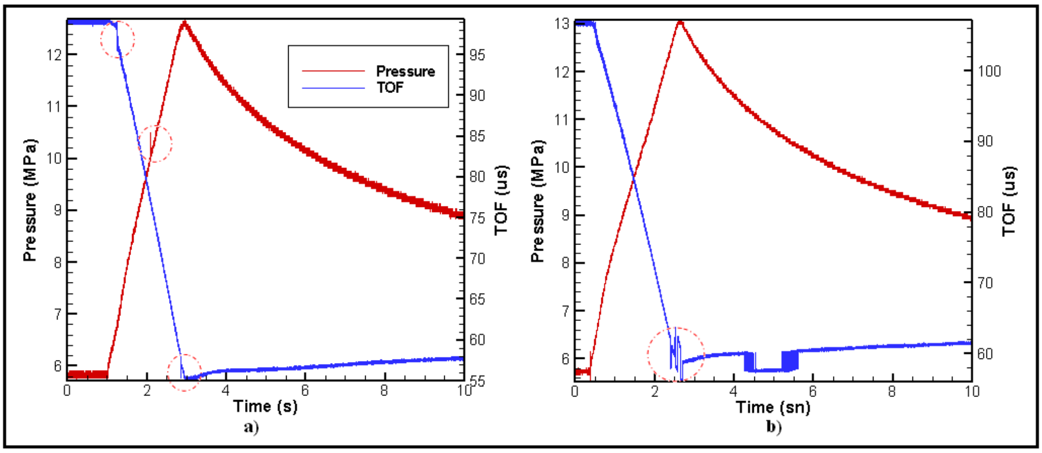

Figure 59 Measured pressure and time of flight versus time for

a) Test 16 b) Test 17

The time of flight data belong to test 17 is investigated and inaccurate times of flight data are eliminated. Burning rate values of test 16 and 17 with respect to pressure are given in Figure 60.

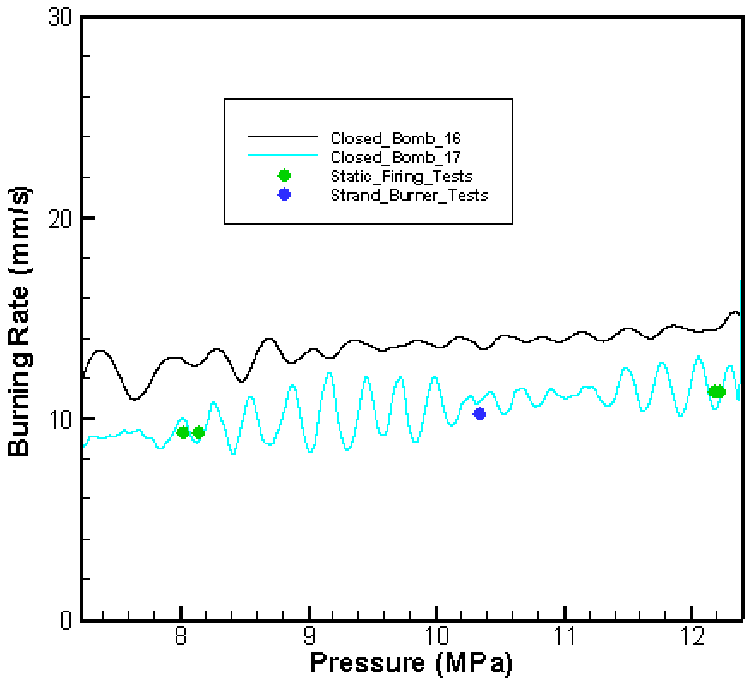

Figure 60 Burning Rate Value versus pressure belong to HSTYPE4

The burning rates that belong to test 16 are different from the static firing test results.

Table 11 Combustion Data belong to HSTYPE4

Test No.	First Pressure (MPa)	Maximum Pressure (MPa)	Start time of Burning Process (s)	Finish time of Burning Process (s)	Burning Time (s)
16	5.91	12.65	1.00	2.95	1.95
17	6.0	13.09	0.426	2.64	2.21

5.8 Results of BTYPE1

This test group was performed with aluminized propellant. Outputs of tests are represented in Figure 61. The data seem smooth and continuous. The burning rates obtained from these test is plotted in Figure 62. The results seem compatible with each other but the trend of closed bombs is quite different from the trend of static firings.

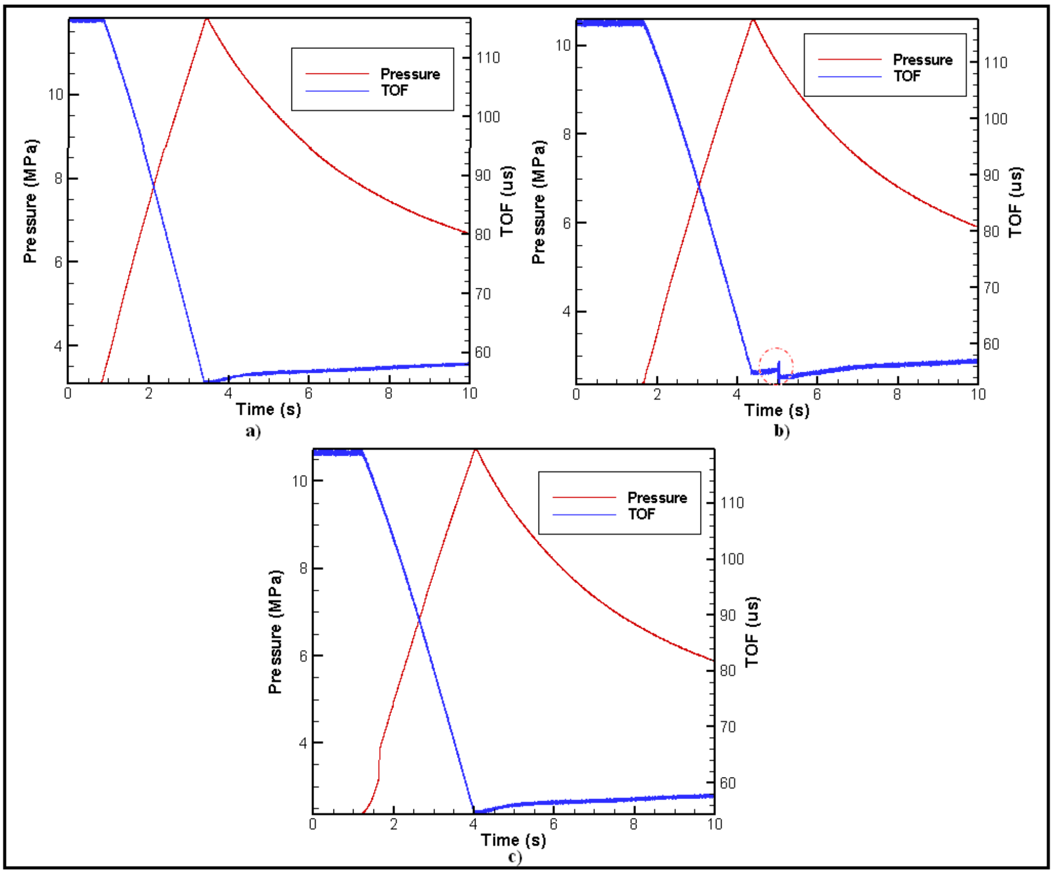

Figure 61 Measured pressure and time of flight versus time for a) Test 31 b) Test 32 c) Test 33

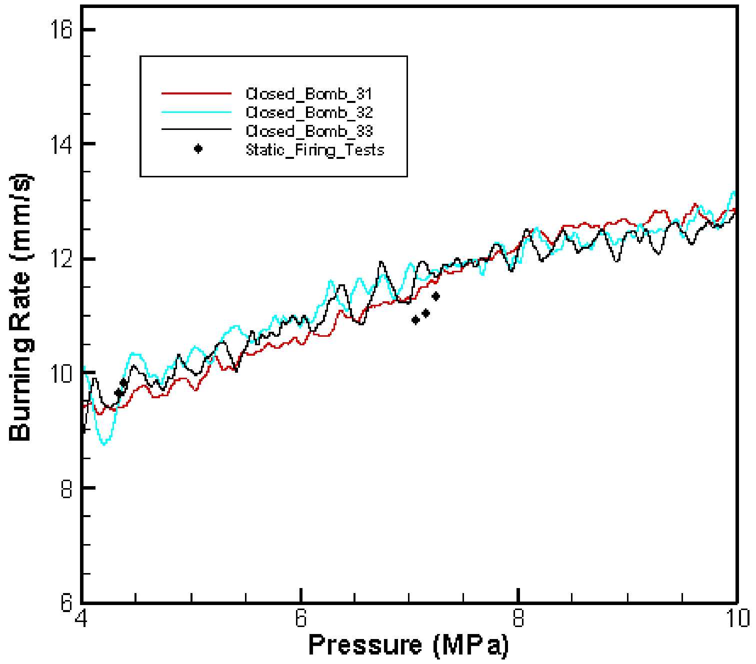

Figure 62 Burning rate versus pressure that belongs to BTYPE1

Table 12 Combustion Data belong to BTYPE1

Test No.	First Pressure (MPa)	Maximum Pressure (MPa)	Start time of Burning Process (s)	Finish time of Burning Process (s)	Burning Time (s)
31	3.12	11.84	0.836	3.414	2.58
32	2.37	10.58	1.66	4.387	2.73
33	2.38	10.74	1.195	4.038	2.84

5.9 Results of HSTYPE5

Error factors that affect the measurement of burning rates are investigated and are reviewed in Appendix A. After some revisions of measurement method 12 tests are performed with the same batch of propellant (%82 AP %9.5 HTPB) which has same composition.

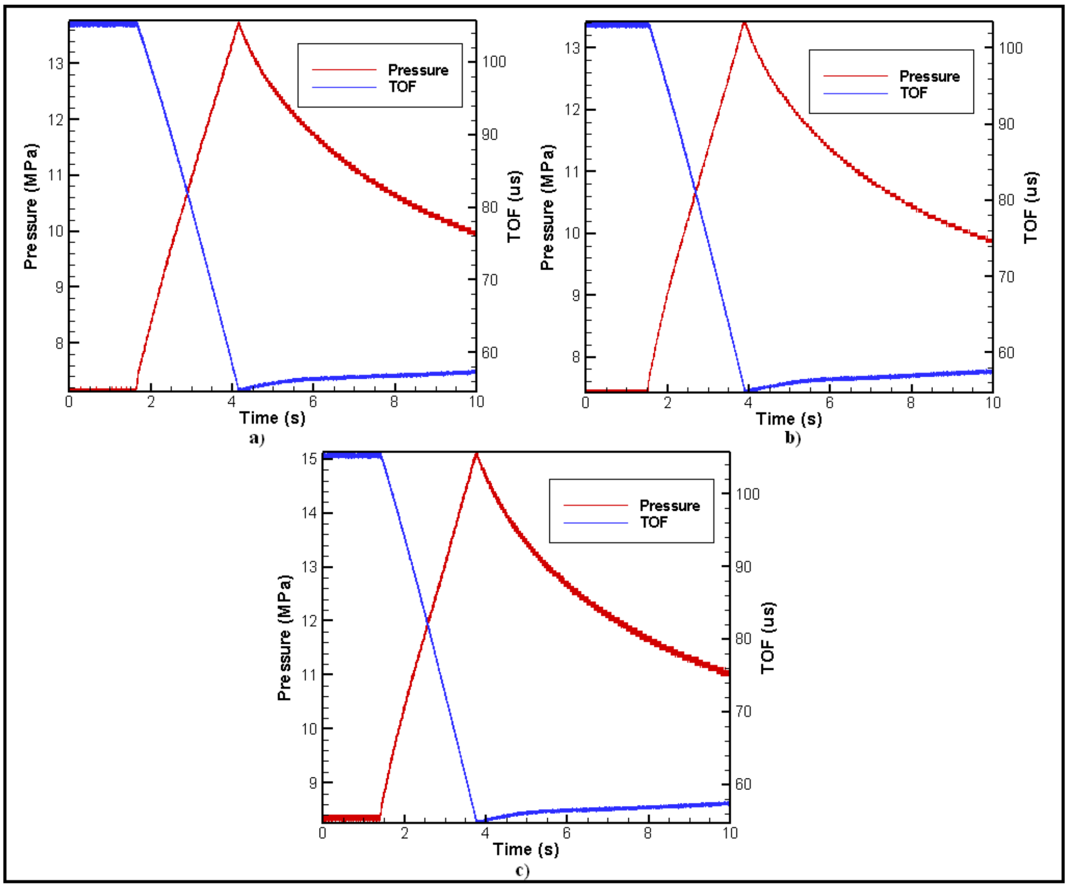

Figure 63 Measured pressure and time of flight versus time for
a) Test 19 b) Test 20 c) Test 21

The measured pressure and time of flight data are investigated after every test due to search for signal quality. The test environment and test setup affect the signal quality.

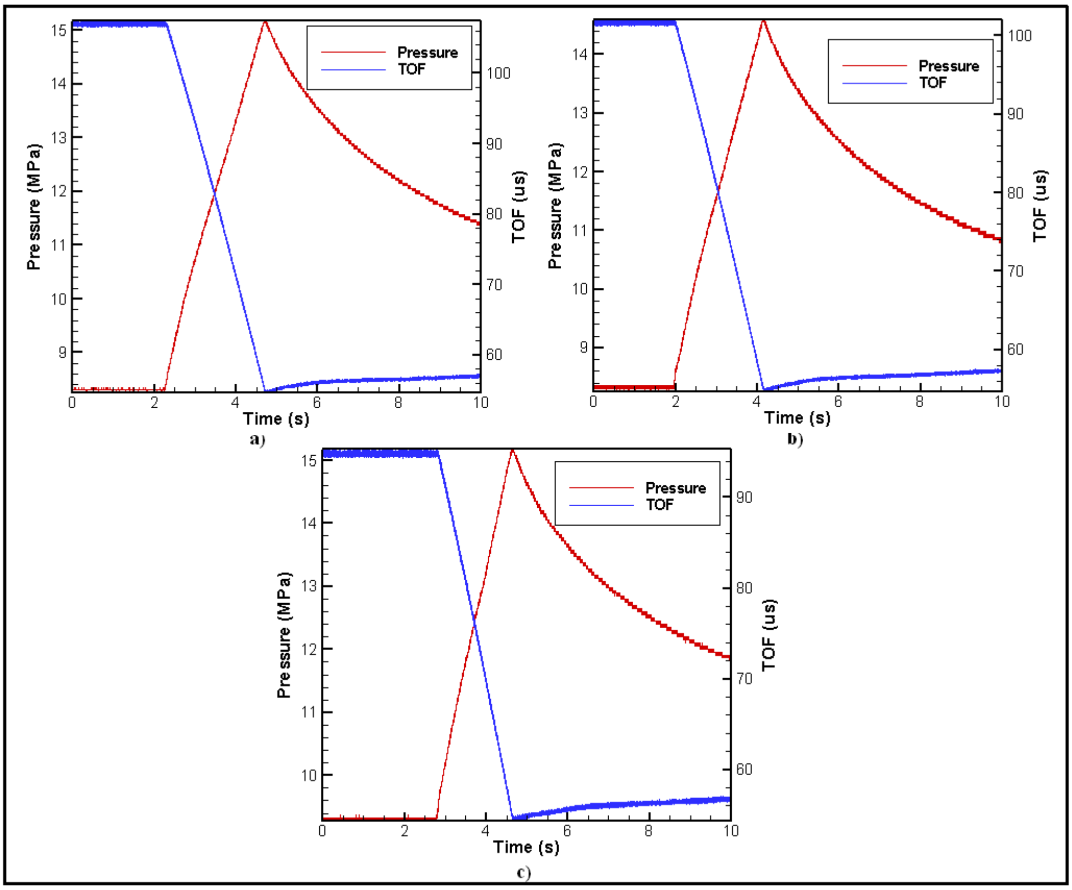

Figure 64 Measured pressure and time of flight for

a) Test 22 b) Test 23 c) Test 24

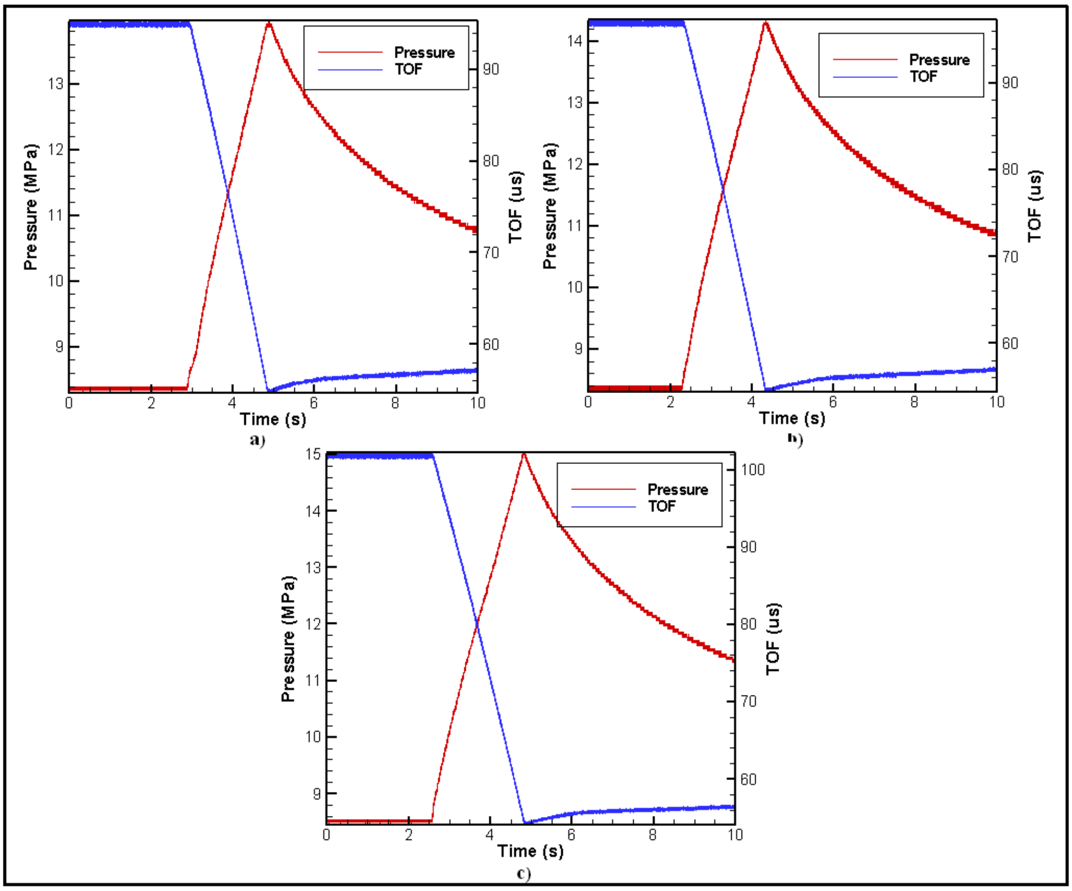

Figure 65 Measured pressure and time of flight versus time for

a) Test 25 b) Test 26 c) Test 27

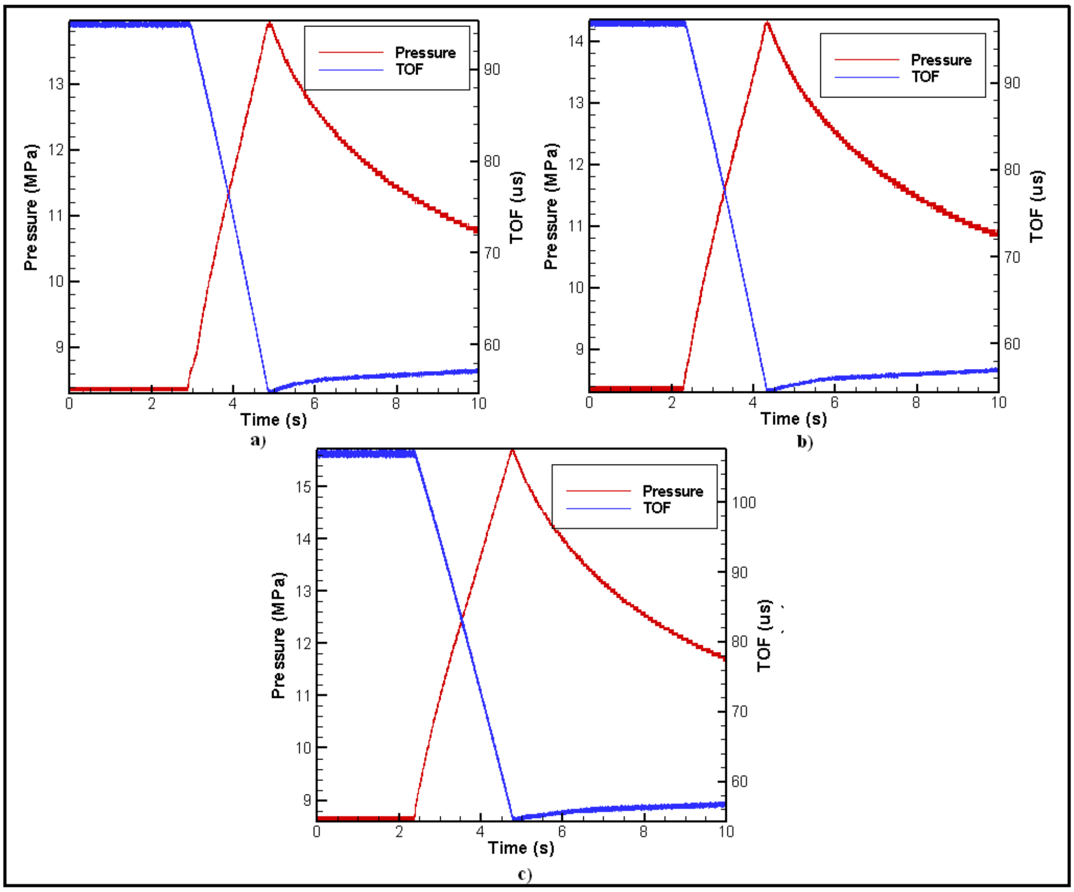

Figure 66 Measured pressure and time of flight versus time for a) Test 28 b) Test 29 c) Test 30

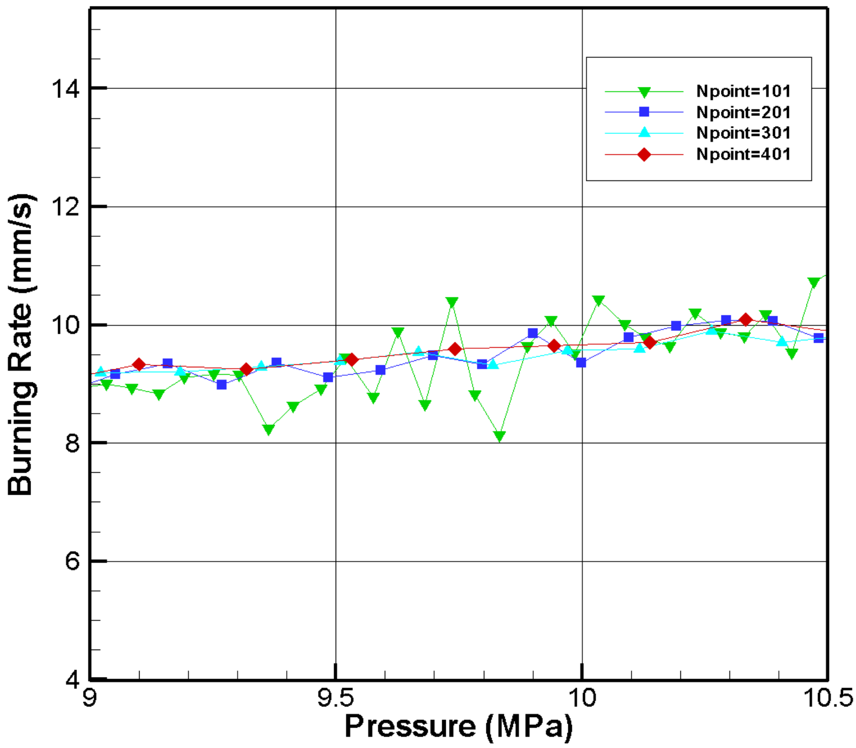

Figure 67 Effect of Npoint on burning rate evaluation

In Figure 67 the effect of number of points (Npoints) which is used for regression of measured data is seen. This evaluation is performed for test 19.

The burning rate is computed from the measured data such as TOF determined by the echo processing. The closed bomb tests were performed at a repetition rate of 5000 Hz. By applying the equation (1) between 9 to 10.5 MPa, dimensionless temperature coefficient a is found as 0.9186 [Npoint=101] , 1.041 [Npoint=401] and pressure exponent n is found as 0.585 [Npoint=101], 0.535 [Npoint=401]. The correlation coefficient of them are respectively 0.833 and 0.916.

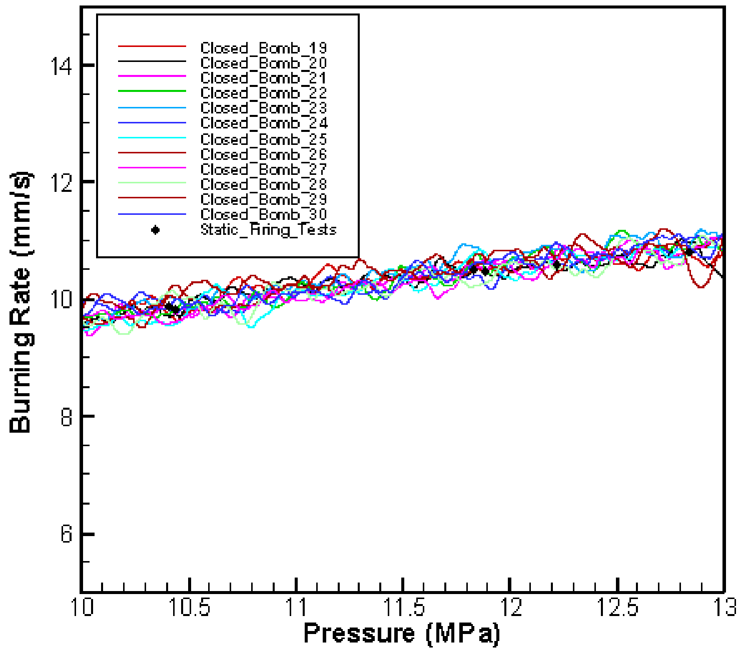

Figure 68 Burning Rate versus pressure of HSTYPE5

For the same batch of the propellant, 12 closed bomb tests were performed in order to check the repeatability and accuracy of the ultrasonic system. Table 13 and Table 14 show the burning rates of each method at different pressure levels.

Table 13 Burning Rates at 10.34 MPa

Pressure (MPa)	Burning Rates Determined From Closed Bombs (mm/s)	Burning Rates Determined From Static Firing Tests (mm/s)	% Difference
10.34	10.033	9.828	2
	9.836	9.854	0.18
	9.743	9.884	1.42
	9.673	9.916	2.45
	9.904	9.872	0.32
	9.998	9.912	0.86
	9.600	9.836	2.4
	9.780	9.896	1.18
	9.693	9.792	1.02
	9.905	9.851	0.54
	9.889	-	-
	9.836	-	-
Mean	9.8240	9.864	-
Standard Deviation	0.1313	0.0395	-

Table 14 Burning Rates at 13.79 MPa

Pressure (MPa)	Burning Rates Determined From Closed Bombs (mm/s)	Burning Rates Determined From Static Firing Tests (mm/s)	% Difference
13.79	10.649	10.668	0.18
	10.555	10.645	0.85
	10.346	10.766	3.90
	10.547	10.713	1.55
	10.380	10.568	1.78
	10.266	10.642	3.53
	10.312	10.695	3.58
	10.477	10.736	2.41
	10.233	-	-
	10.649	-	-
	10.555	-	-
	10.346	-	-
Mean	10.406	10.679	-
Standard Deviation	0.128	0.0623	-

Maximum % 3.9 difference in burning rates between two methods is obtained at 13.79MPa. This difference comes from various effects such as casting process of the propellant, distribution of the AP particles in samples, nature of the methods and uncertainties of measurement devices. Although burning rates of static firing tests are comparable with the closed bomb test results, the pressure exponents determined from two methods are different from each other as shown in Table 15. Determining of pressure exponent from static firing tests is based on calculating the slope from a few firing tests but pressure exponents determined from closed bombs are based on calculating the slope from a continuous line in a pressure range that is why results are different from each other .Two methods were compared by means of accuracy. The standard deviation of the closed bomb tests of this batch is 0.1313 (from twelve measurements) for HSTYPE5 propellant whereas standard deviation of the static firing test method is 0.0395 (from ten measurements) at 10.34 MPa reference pressure.

Table 15 Pressure Exponents of HSTYPE5

Range of Pressure (MPa)	Pressure Exponent Determined from Static Firing Tests	Pressure Exponent Determined from Closed Bomb Tests
10.34-12.41	0.485	0.542

5.10 Assessment of Burning Rate Measurement Methods Performed in Roketsan

One of the main objectives of this thesis is to substitute a burning rate evaluation method instead of static firing tests which are highly cost and more time consuming. For this reason, burning rate evaluation methods carried out in Roketsan are compared with each other by means of cost, time and amount of wasted propellant.

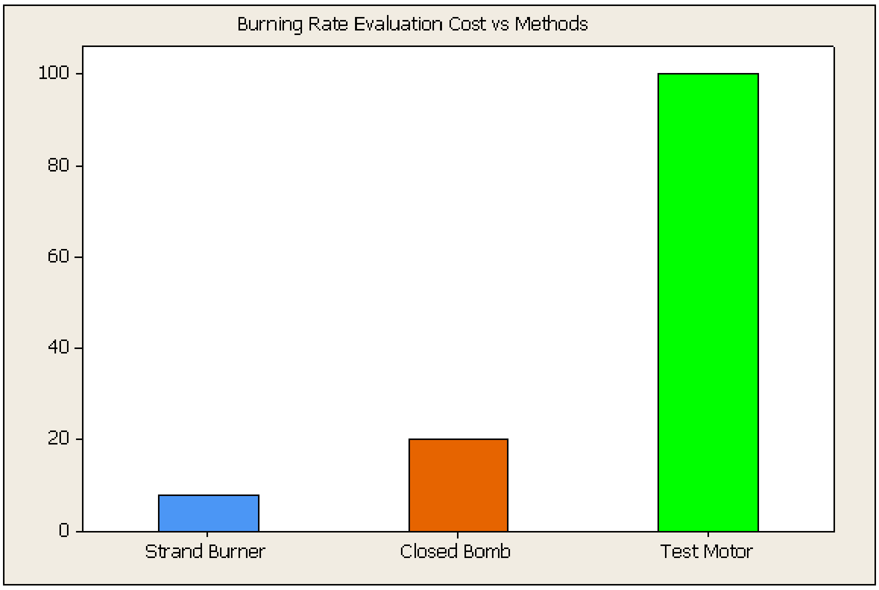

Figure 69 Burning Rate Evaluation Cost versus Methods

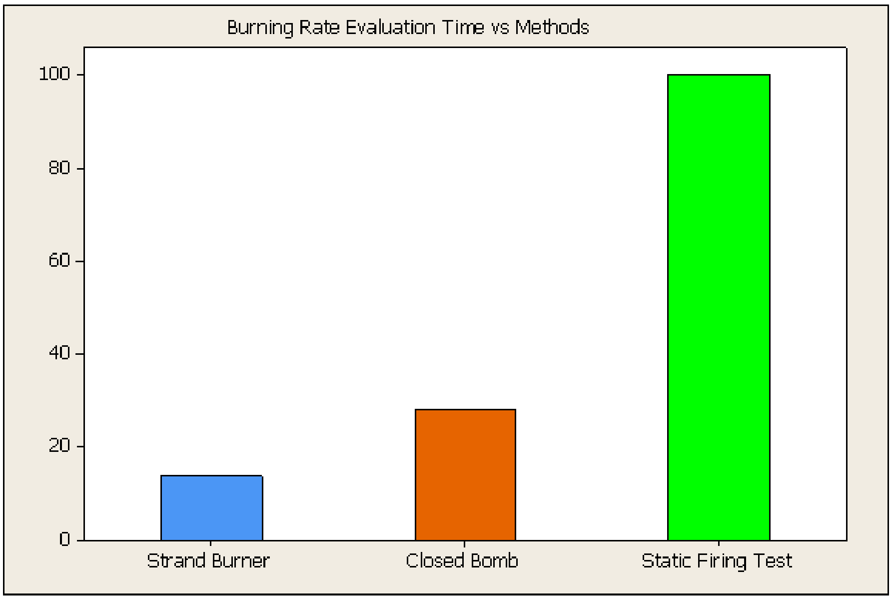

Figure 70 Burning Rate Evaluation Time versus Methods

Static firing tests are the most money and time comsuming method among other burning rate evaluation methods. Strand burner method is the cheapest way but this method results are not accurate as others.

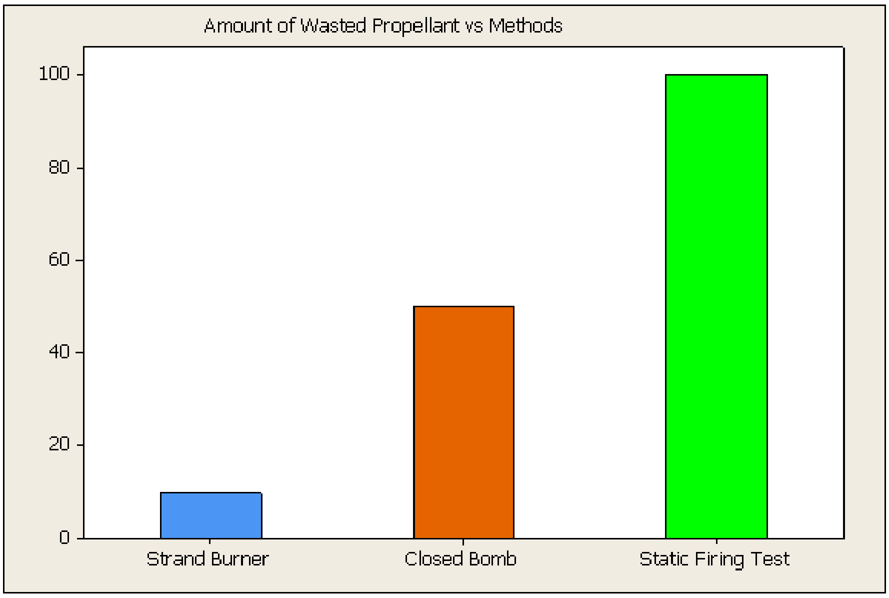

Figure 71 Amount of Wasted Propellant versus Methods

5.11 Conclusion

In this section, results obtained from closed bomb tests are examined and compared with the static firing tests. First eight tests were performed without using automatic gain control. For this reason it showed drastic variation of the return echo amplitude during the combustion. When the amplitude reached the saturation level, deformation of the echo was occurred and the determination of the "top of the hill" position leading to the propogation time determination included an error which should be seen in the burning rate variation as function of time.

As a result of these tests, it was seen that especially igniter type and coupling material acoustic empedance affected the quality of signal. First eighteen tests were performed with bag type igniter. Especially at the beginning of the tests during the ignition phase of the propellant return echo amplitude was decreased before the regression started. This was due to an ignition delay. For that reason ignition type was changed.

Comparison between conventional methods such as strand burner and static firing test and closed bomb tests equipped with ultrasonic measurement method for burning rate evaluation are performed by means of accuracy, time, cost and consumed amount of propellant. Strand burner method has some advantages among other methods but the test results are not enough accurate for using batch check control of propellant.

CHAPTER 6

ULTRASONIC MEASUREMENT ON TEST MOTORS

6.1 Introduction

In the scope of this thesis, ultrasonic measurement method is performed on tests motors. After the qualification of ultrasonic measurement method on closed bombs, test motor studies are performed. Three types of solid composite propellant type are surveyed with the scope of ballistic performance evaluation. The test results are compared with the static firing test results at same pressure levels.

Table 16 Test Motors Used in Application

Test Number	Propellant Name	Conditioning Temperature (^{0}C)	Composition of Propellant
1	ANTYPE1	21	(%86 AP, %10 HTPB)
2	CRTYPE1	21	(%86 AP, %10 HTPB)
3	BTYPE2	21	(%72 AP, %9 HTPB, %19 Al)

6.2 Experimental

The ultrasonic measurement method and software used are explained in Chapter 3. This non-destructive method was applied on test motors and three successful tests were performed. In this section manufacturing of the test motors and details of the test setup are illustrated. The main parts of the test motor are shown in Figure 72. The pressure measurement is carried out by fixing the pressure transducers at front flap. At the same time, ultrasonic transducers are placed on main body.

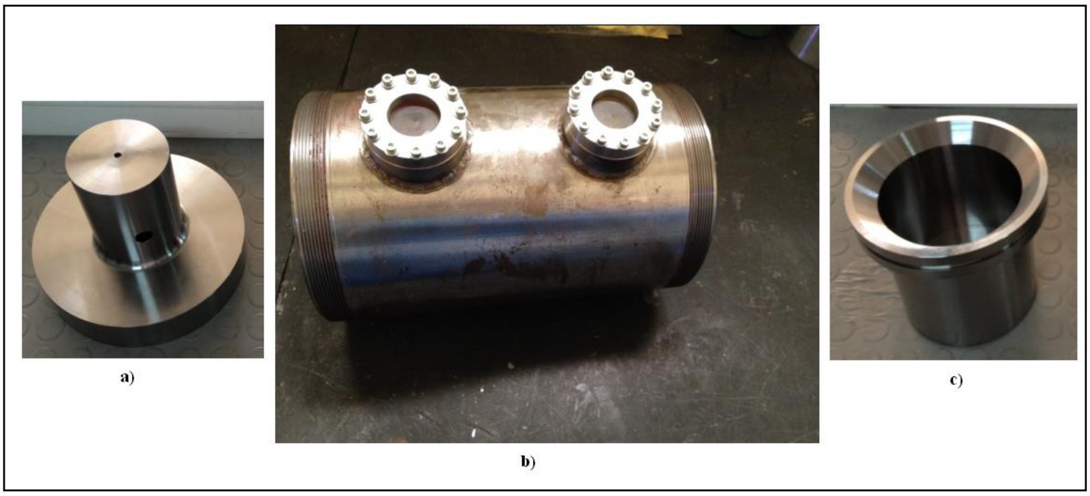

Figure 72 Components of the test motor a) front flap b) main body c) back flap

Technical drawing of the test motor is shown in Figure 73. The echoes reflect from burning surface are collected with ultrasonic channels by ultrasonic transducers. Pressure data are collected with two pressure transducers which have two types, strain gage and piezoelectric.

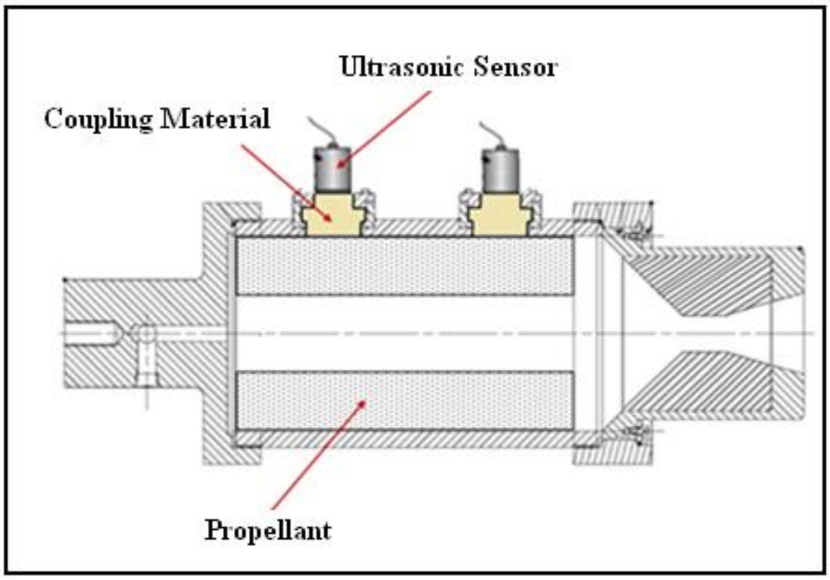

Figure 73 Technical Drawing of Test Motor

6.3 Test Preparation

Before the firing test, coupling material is casted and manufactured by turning in a stall as shown in Figure 74. The casting process of the coupling material is explained in Chapter 5.

Figure 74 Coupling Material used in test motor firing tests

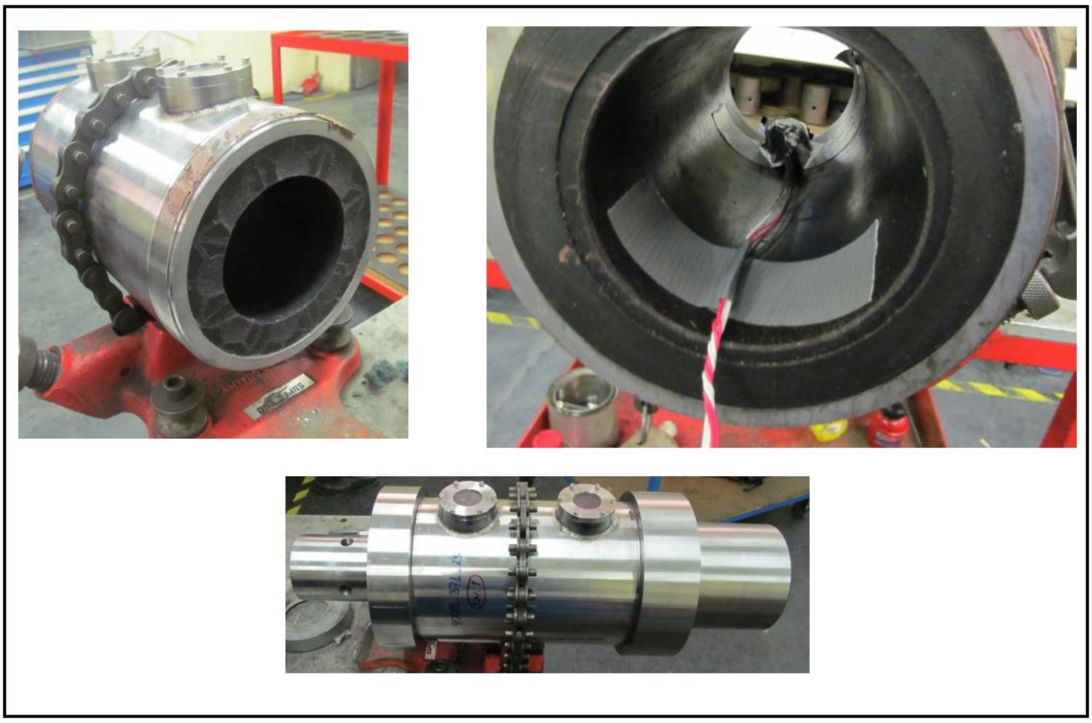

Figure 75 Assembly process of the test motor

The steps of the assembly process of the test motor is shown in Figure 75. The propellant is poured in the motor and igniter is sticked to the propellant surface.

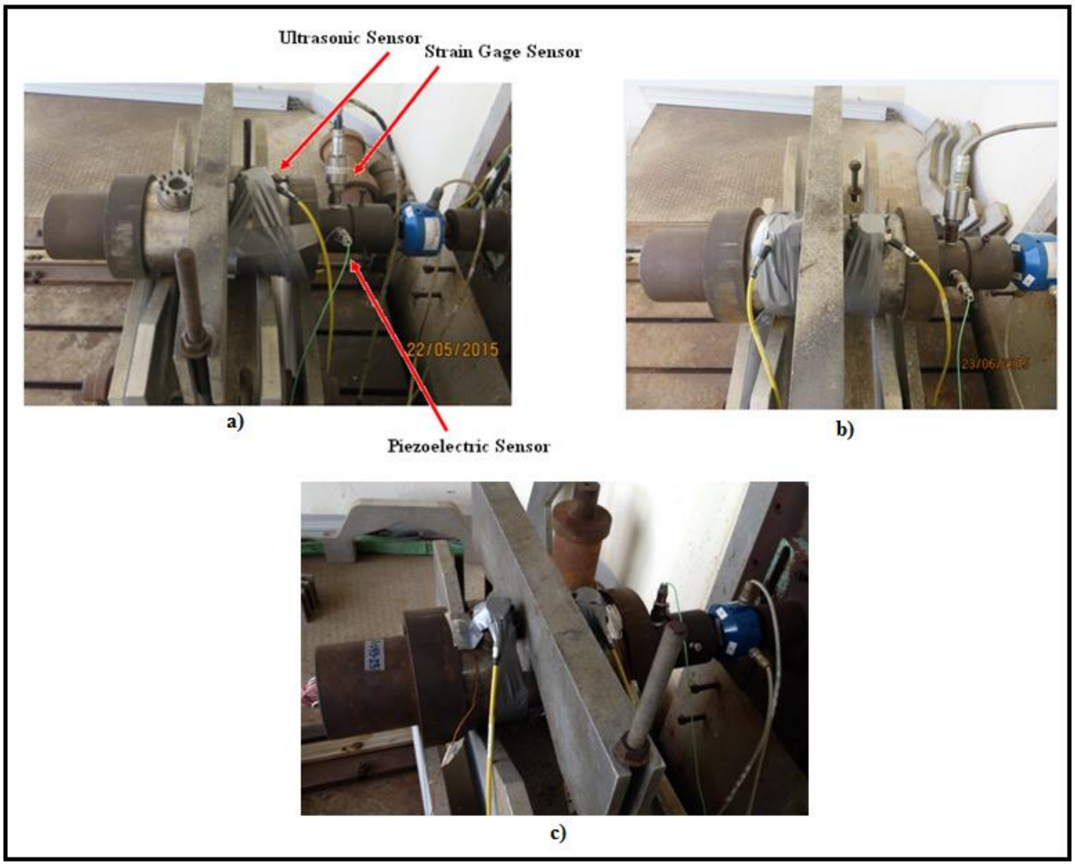

Figure 76 Test Motor Firings that belong to a) Test 1 b) Test 2 c) Test 3 placed at ground test platform

The test motors before the firing test are shown in Figure 76. Tests motor are placed at ground test platform and are fired.

6.4 Results and Discussions

6.4.1 Test 1

A composite solid propellant (%86 AP, % 10 HTPB) is tested by static firing test motor. Time of flight and pressure data is collected with respect to time. Burning process is started when the time of flight is started to decrease. End of burning time is the tail of the pressure data as shown in Figure 77. During the test, two types of sensor were conducted to measure the pressure in the chamber of the test motor. Piezoelectric sensor measures the pressure lower than the strain gage sensor does. It was thought that this discrepancy comes from calibration of the piezoelectric sensor. It is seen that came true by conducting the second test.

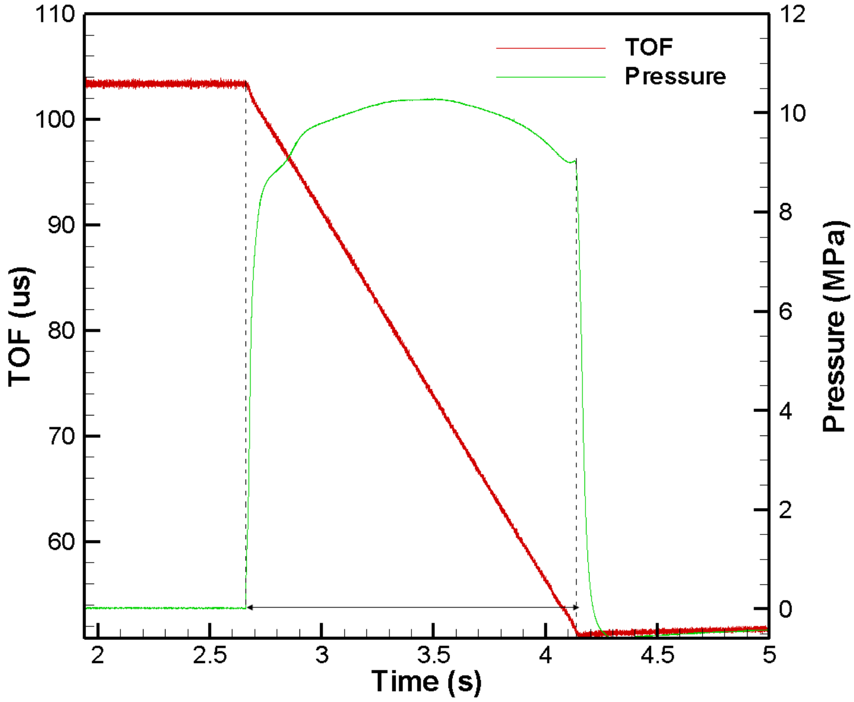

Figure 77 Pressure and Time of Flight data with respect to time for test 1

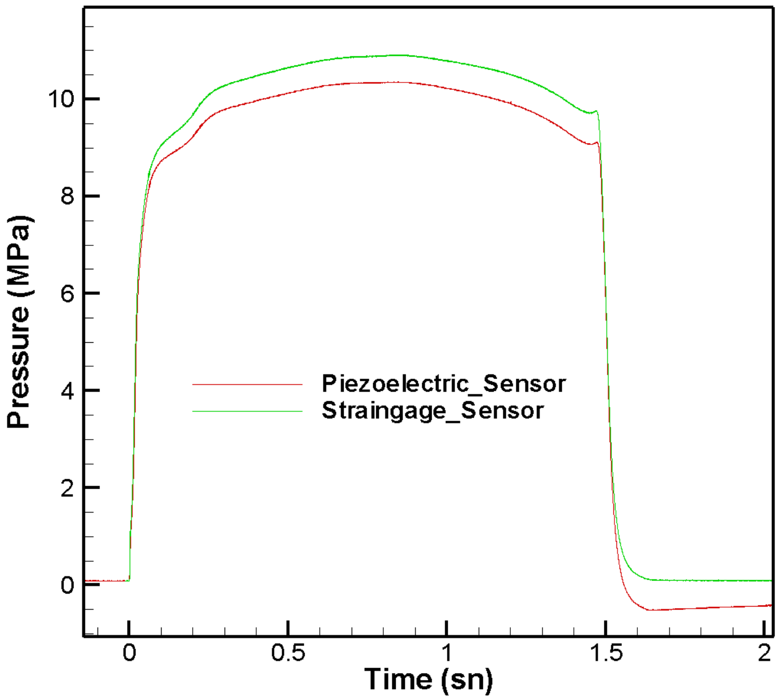

Figure 78 Pressure data collected by two types of sensor for test 1

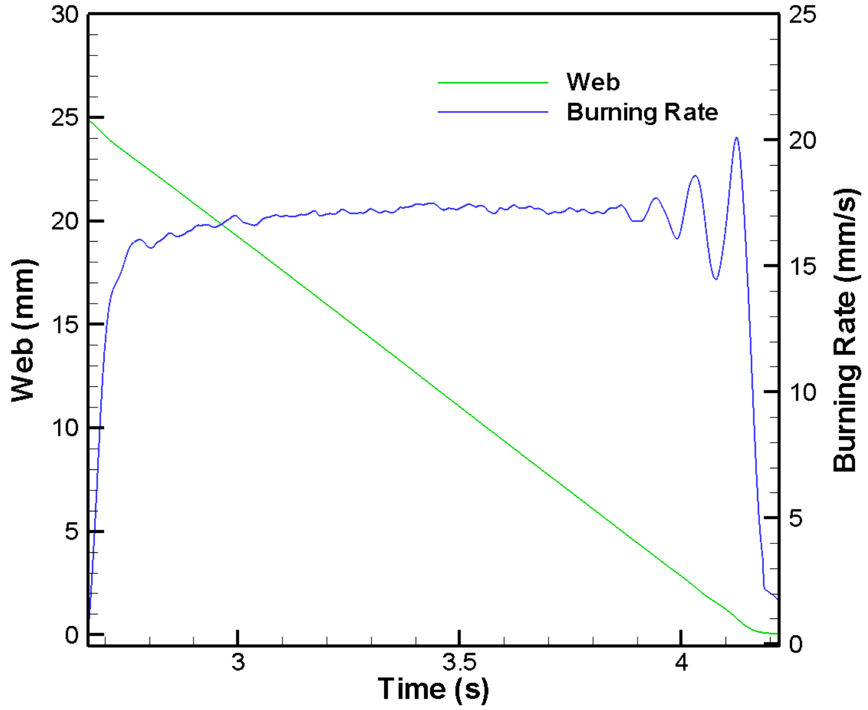

Figure 79 Burning rate and web thickness with respect to time for test 1

Burning rate and web thickness of the burned propellant with respect to time are calculated via the burning rate formula given in Equation (8). All of the propellant grain in the motor is burned during the test.

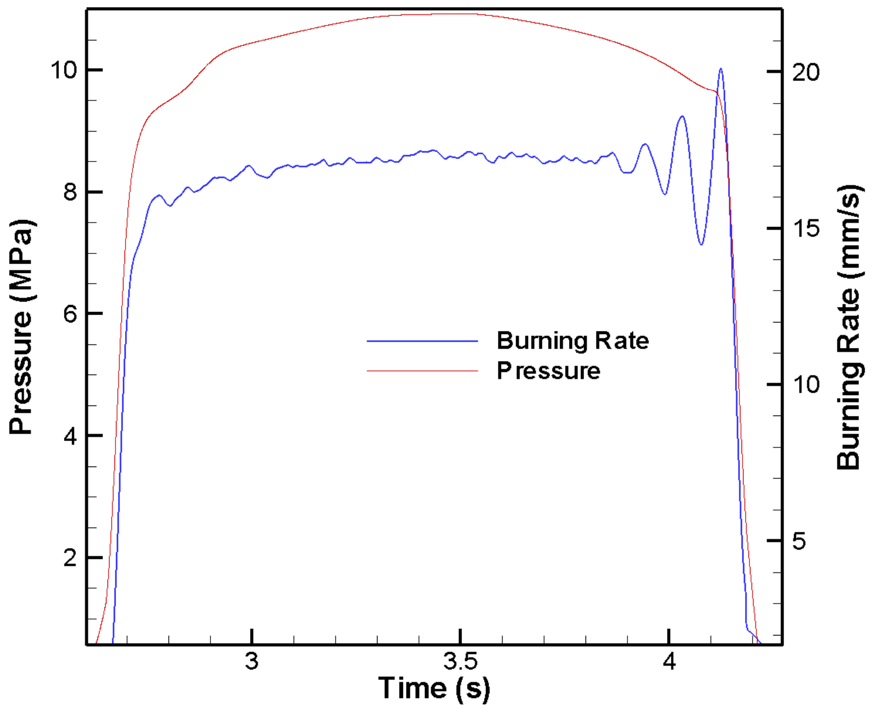

Figure 80 Burning rate and pressure with respect to time for test 1

The burning rate and pressure are plotted as a function of time. Trend of the burning rate seems same as the pressure trend. Large fluctuations are observed at the end of the burning process. These fluctuations are overlapped of the propellant echo with secondary echoes.

For this propellant batch, also static firing tests are performed with other type of subscale test motors. Apart from the ultrasonic test motor, seven tests were performed with the aim of evaluation of burning rate of this propellant batch. These results are compared with each other. For ultrasonic test motor, burning rate is averaged between the 2 and 4 MPa and compared with the burning rates determined using a standard measurement technique (web/time method) as shown in Table 17. The average burning rate data obtained from ultrasonic test motor is approximately 0.75 % lower than the 6C4 test motor results and 1.9% higher than the 127 mm test motor results. These results show that, test motor's results which is fired for burning rate determination with ultrasonic measurement method are convenient with other subscale test motor's results. It is concluded that, implementation of ultrasonic measurement method on test motor is successful.

Table 17 Results of the Methods

Method	**Pressure (Mpa)**	**Burning Rate (mm/s)**
127 mm Test Motors	10.34	16.8
6C4 Test Motors	10.34	17.25
Ultrasonic Test Motor	10.34	17.12

6.4.2 Test 2

In test 2, another non aluminized propellant type called CRTYPE1 is used. Time of flight data are collected with two channels that belong to ultrasonic sensors during the test. In test 1, pressure data collected by two independent sensors were different from each other. For this reason before test 2, piezoelectric sensor was calibrated by dead weight and the calibration curve can be found in Appendix G. After the calibration, test 2 was performed and the measured pressure is plotted as a function of time in Figure 81. The blue line which is not seen because it overlaps with the green one is illustrated the pressure measured by piezoelectric sensor. The green line is illustrated the pressure measured with the strain gage. As mentioned before, time of flight data is measured with two different ultrasonic sensors. The blue line in Figure 81 is illustrated the time of flight measured with channel one and the red line is illustrated the time of flight measured with channel two. Two sensors are placed on the ultrasonic test motor very closely. For this reason the time of flight data are very close to each other.

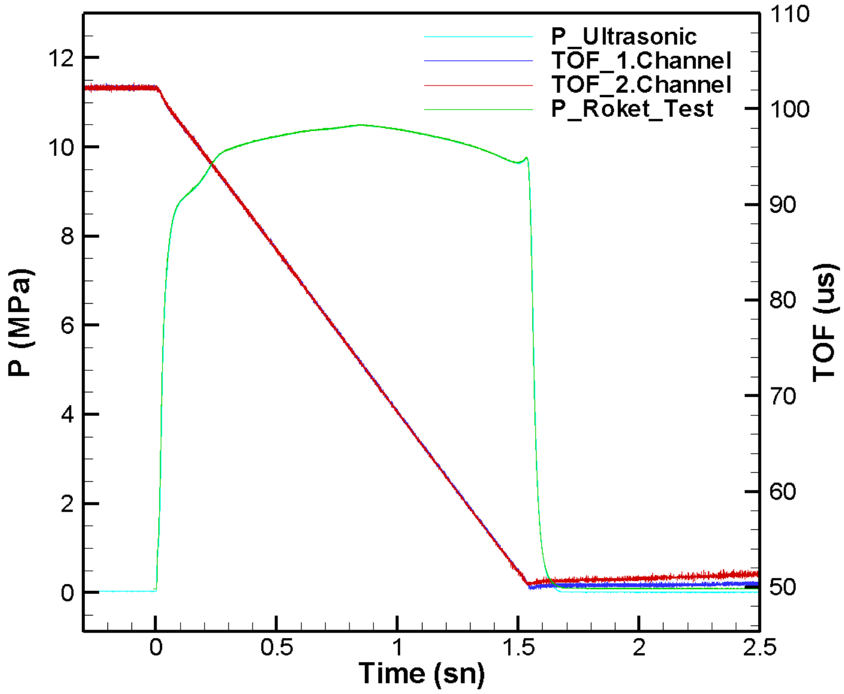

Figure 81 Pressure and Time of Flight data with respect to time for test 2

The burning rate and the web thickness that was burned is plotted with respect to time is shown in Figure 82. As test 1, at the end of the burning process, fluctuations are observed. The grain geometry in the test motor is chosen for neutral burning. For this reason burning rate trend seems neutral as the motor pressure.

Comparison of the buring rates determined from conventional method and ultrasonic measurement method is shown in Table 18. The relative error to the conventional method is 1.25 % at the pressure of 10.34 MPa.

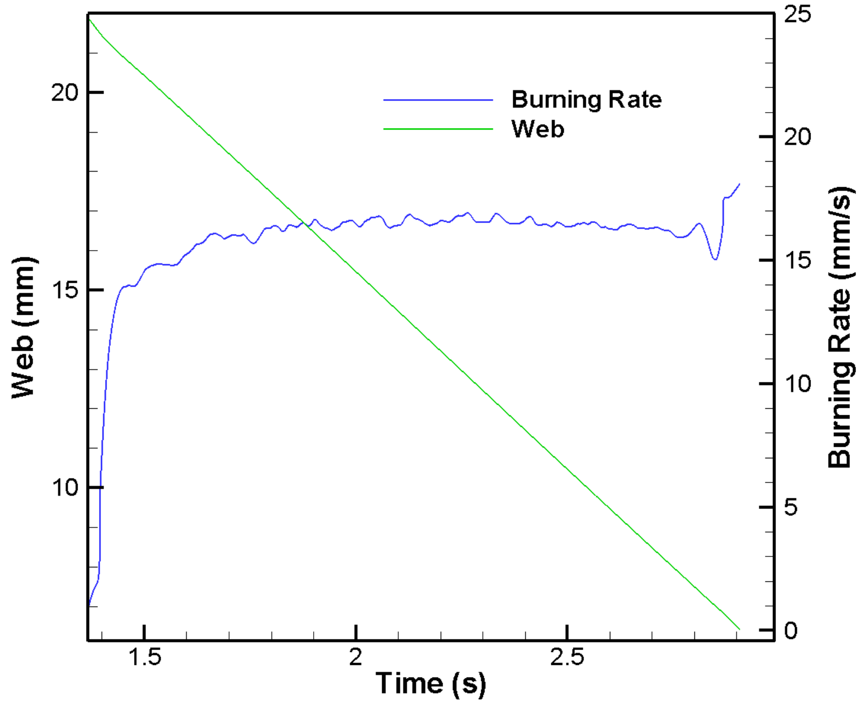

Figure 82 Burning rate and web thickness with respect to time for test 2

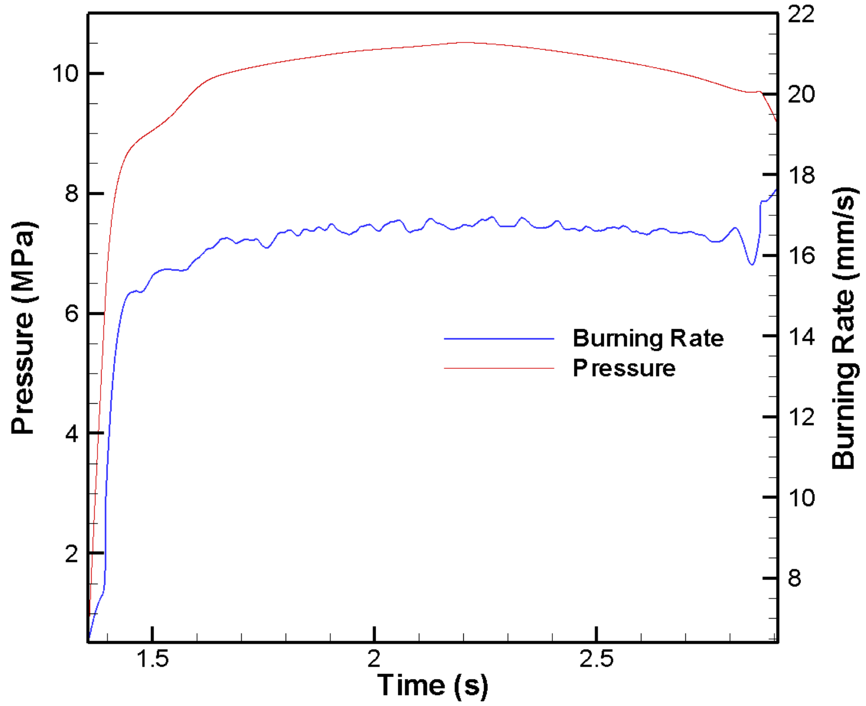

Figure 83 Burning rate and pressure with respect to time for test 2

Table 18 Results of the Methods

Method	Pressure (MPa)	Burning Rate (mm/s)
6C4 Test Motors	10.34	16.82
Ultrasonic Test Motor	10.34	16.61

6.4.3 Test 3

An aluminized composite propellant is used to obtain burning rate in this test. Also two ultrasonic transducers were used but one of them did not measure the time of flight data which reflect from the burning surface. That is why one channel data was used for the computations.

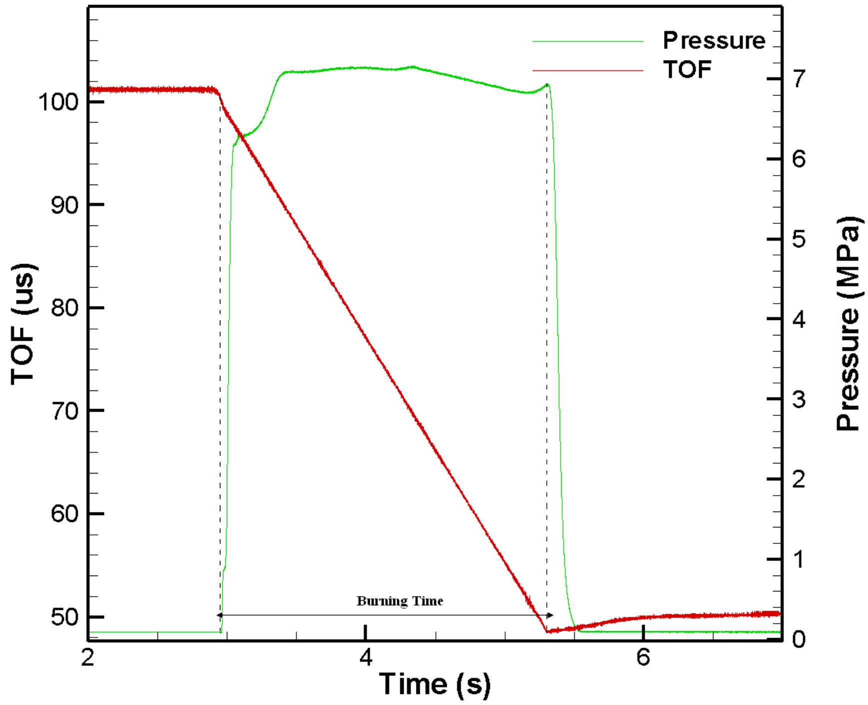

Figure 84 Pressure and Time of Flight data with respect to time for test 3

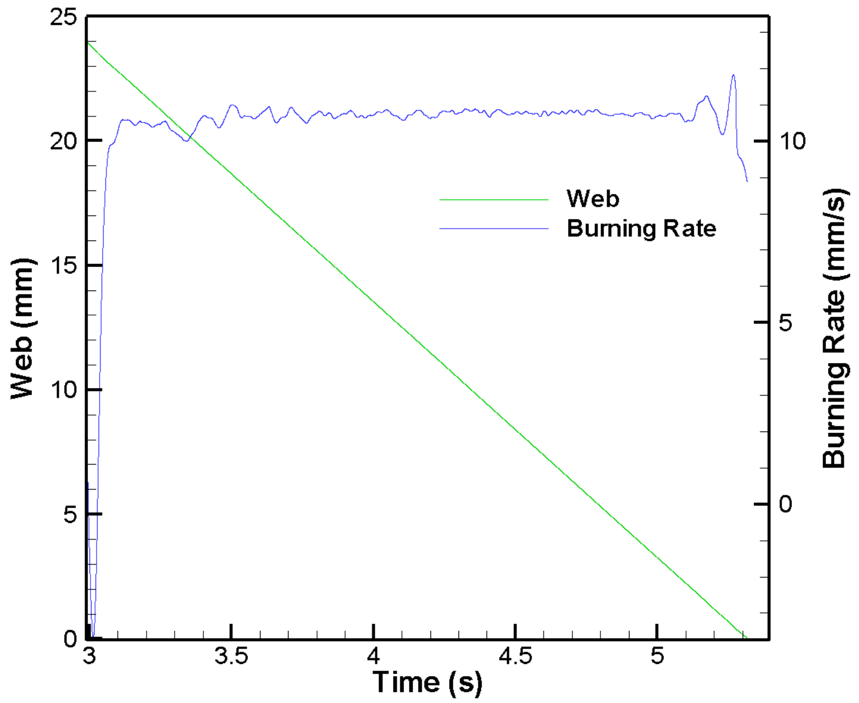

Figure 85 Burning rate and web thickness with respect to time for test 3

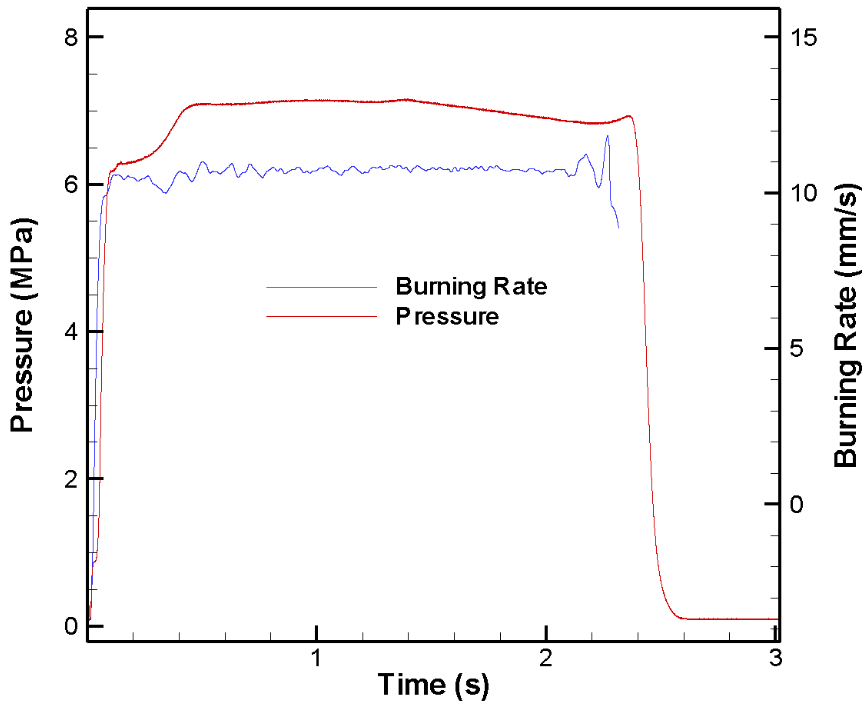

Figure 86 Burning rate and pressure with respect to time for test 3

If Figure 86 is considered, it can easily seen that 10% pressure rise does not affect the burning rate between 0.14 and 0.4 seconds. Pressure effect on burning rate is represented by pressure exponent in the equation (1) mentioned in Chapter 2. Hence this can be explained by low pressure exponent.

Table 19 Results of the Methods

Method	Pressure (MPa)	Burning Rate (mm/s)
127 mm Test Motors	6.9	10.91
Ultrasonic Test Motor	6.9	10.73

In Table 19, results obtained from conventional test motors and ultrasonic test motor are compared. According to results, burning rate calculated from ultrasonic test motor is 1.65% lower than the conventional test motor.

6.5 Conclusion

Ultrasonic measurement method is applied on test motors with the main target of burning rate evaluation and achieving to gain ability of non-destructive method. Three tests were performed with composite propellants, one is with aluminized propellant. The results were compared with static firing test results which were performed with the same batch of propellants. Burning rates determined from static firing tests are the average values which settle over the average pressure. For this reason comparison was done with the burning rates that belong to these average pressures for ultrasonic motors.

CHAPTER 7

NUMERICAL STUDIES

7.1 Introduction

In this part, a numerical study is performed with the aim of estimating the temperatures occurred at the motor case during the static firing of test 3. The preparation of subscale motor firing tests and results are submitted in Chapter 6. Before the thermal analysis of test 3, a test case was chosen in order to determine turbulence model.

7.1.1 Test Case

The test case is belonged to Traineau et al [36]. In their study simulation of a solid rocket motor without nozzle is performed with a two dimensional porous-walled duct. The aim of this study is to determine two dimensional flow effects on solid rocket motor without nozzle.

7.1.2 Determining Turbulence Model

With the aim of selecting turbulence model, the experimental results obtained from [36] are used. The study performed by Godon et al. [37] also uses the experimental results for verification of turbulence model. In this study, erosive burning phenomenon is studied and obtained an erosive burning rate model. Experimental setup that belongs to study [36] is shown in Figure 87. For determining the turbulence model that will be used for thermal analysis, simulation of this setup is used. In test case study, experimental conditions shown in Table 21 are used for boundary conditions of numerical study.

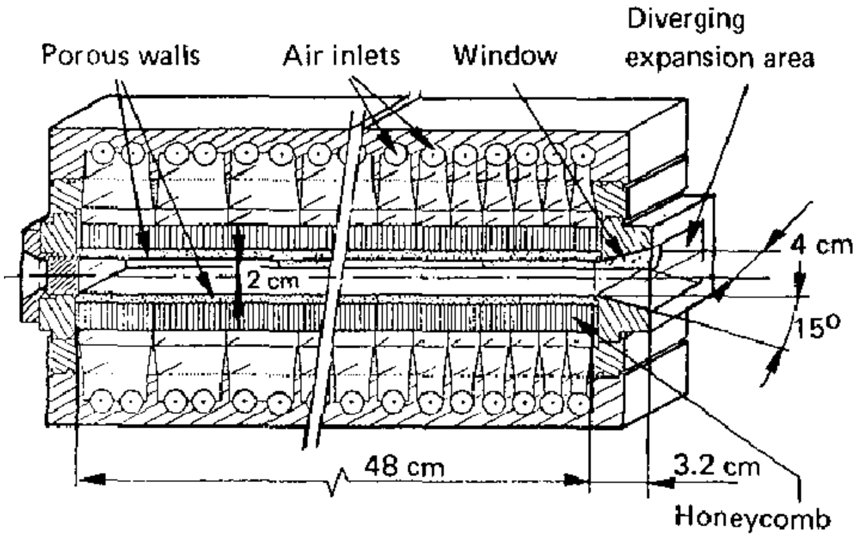

Figure 87 Experimental setup used for test case [36]

Table 20 Geometry of Duct [36]

Length	48 cm
Width	4 cm
Height	2 cm

Table 21 Experimental Conditions [36]

Uniform Specific Mass Flow Rate of Air (kg/m^2s)	13
Injection Temperature (K)	260
Specific Heat Ratio	1.4
Molecular Weight (kg/mole)	29×10^{-3}
Dynamic viscosity at the injection temperature (M.K.S)	1.66×10^{-5}
Porous Wall Porosity (μm)	50

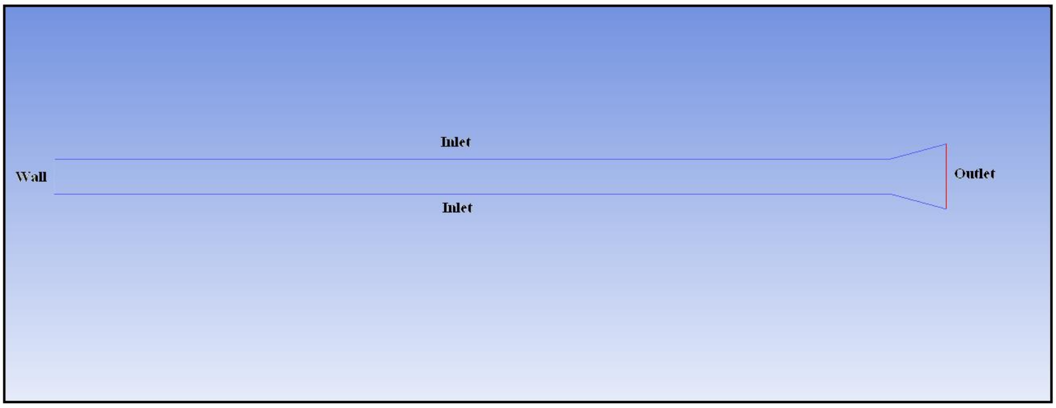

Figure 88 Geometry of the test case

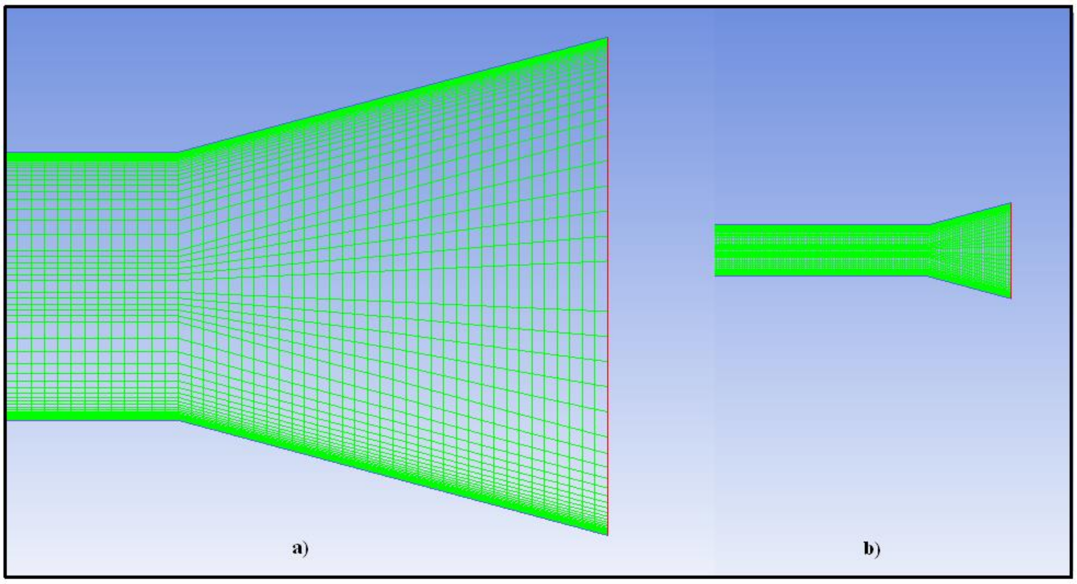

Figure 89 a) Detailed view of Mesh b) View of Mesh

In order to determine turbulence method that will be used for thermal analysis, a commercial code called ANSYS 16.0. is used for numerical studies. In Figure 88 geometry that is prepared for numerical study and boundary conditions are shown. Mesh used for numerical studies is represented in Figure 89. Number of hexagonal cells used is 23644.

7.1.3 Results

In order to determine turbulence model, a comparison between the experimental and numerical study is performed for pressure drop along the length and velocity profiles.

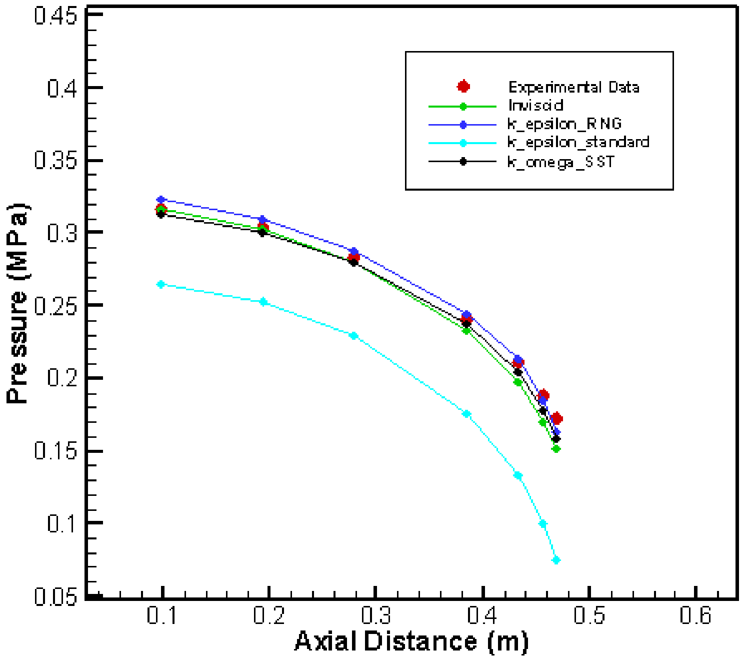

Figure 90 Axial pressure distribution

Turbulence models that were used for comparison are k-epsilon standard, k-epsilon RNG, and k-omega SST. Also inviscid case is searched. As shown in Figure 90, except k-epsilon standard, rest of them are comparable with the experimental results. Inviscid case is also comparable with experimental results for determinig pressure distribution. This is the result of effect on shear stresses along the duct on pressure. Shear stresses does not have huge effect on pressure distribution.

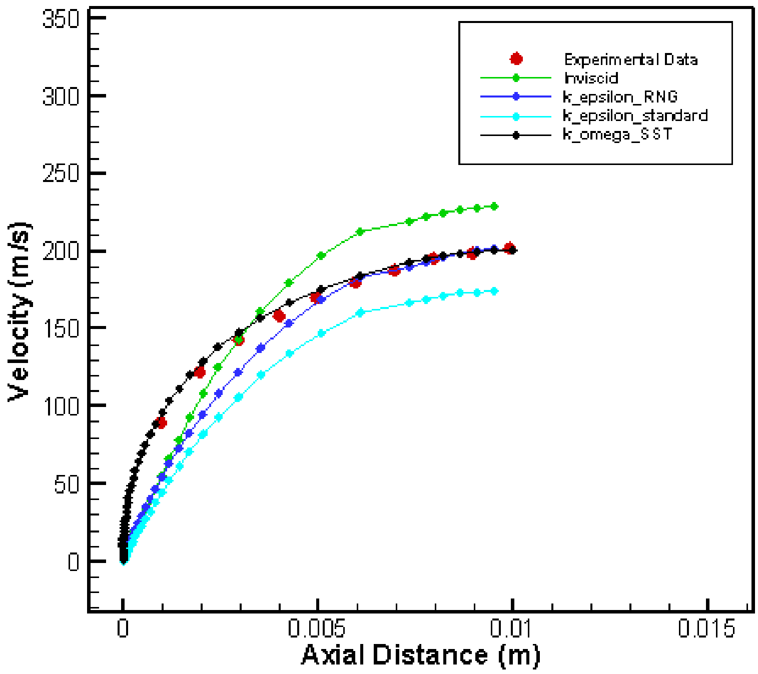

Figure 91 Velocity profile at location 0.401 m

The velocity profile at location 0.401 m measured from experimental study and determined from numerical studies is shown in Figure 91. As expected inviscid case does not predict velocity profile because of shear stresses. K-omega SST and k-epsilon RNG turbulence models seem closest to experimental result.

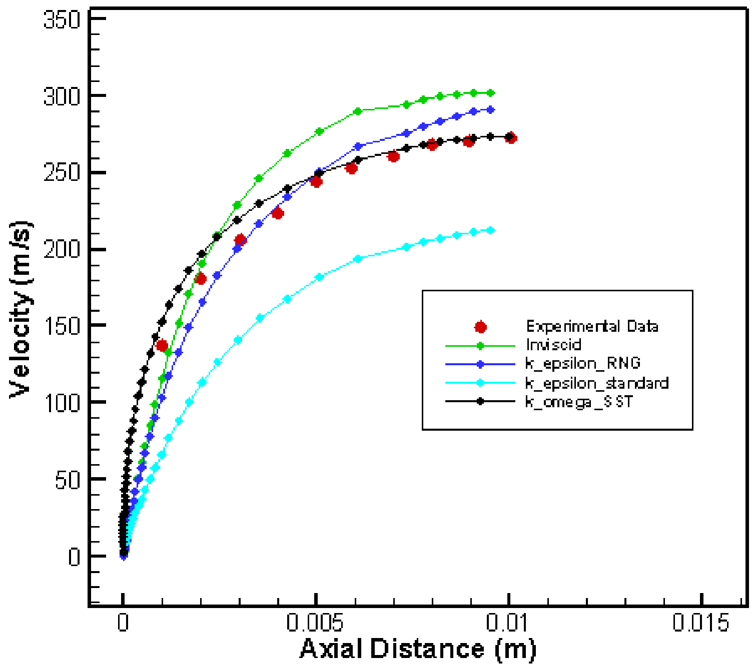

Figure 92 Velocity profile at location 0.461 m

The velocity profile at location 0.461 m measured from experimental study and determined from numerical studies is shown in Figure 92. For this velocity profile determination, k-omega SST turbulence model predicts closer to experimental result.

7.1.4 Conclusion

For performing thermal analysis of test motor, a test case was chosen from the open literature. Wide range of turbulence flow characteristics are occurred in this test case. That is the answer of reason of selecting this type of test case for verification of turbulence model.

According to comparisons of pressure distribution and velocity profiles, k-omega SST turbulence method is used for further numerical study.

7.2 Thermal Analysis of Subscale Test Motor

During the firing of Test 3 presented at Chapter 3, thermocouples were used for measuring the temperatures at determined locations. The propellant composition used in this test is %72 AP, 9% HTPB, 19% Al. Purpose of this study is determining the thermal profile at motor case. Turbulence model k-omega SST was chosen for numerical study. In Figure 94, the mesh that was used for thermal and flow analyses is seen. Quadrilateral mesh was used.

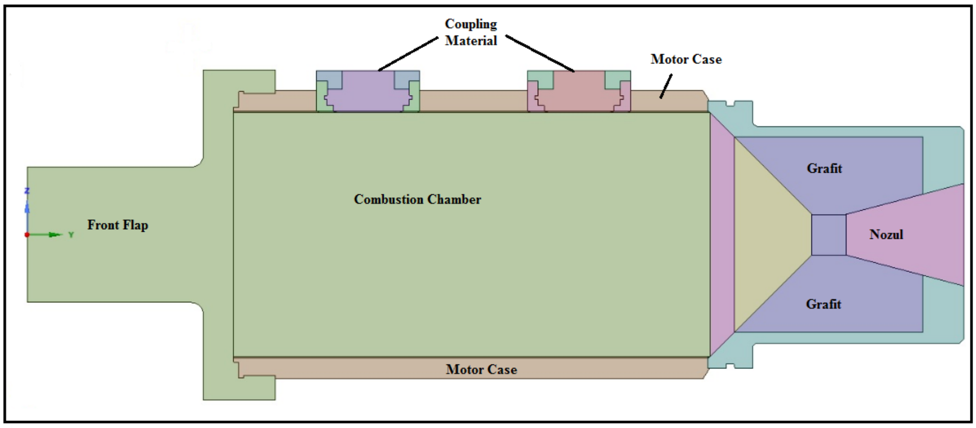

Figure 93 Subscale Test Motor

Table 22 Mesh Structure and Number

Mesh Type	Cell Number
Quadrilateral	922116

Table 23 Boundary Conditions

Inlet1	Mass flow inlet of gas	0.85 kg/s
Inlet 2	Mass flow inlet of alumina particles	0.4565 kg/s
Outlet	Outlet	-
Temperature	Total temperature	3600 K

In this study propellant that includes aluminum particles was used. After burning of the aluminum particles (19%), alumina particles (%34) are occurred. For this reason, mass flow rates of gas and alumina particles are inserted separately in program.

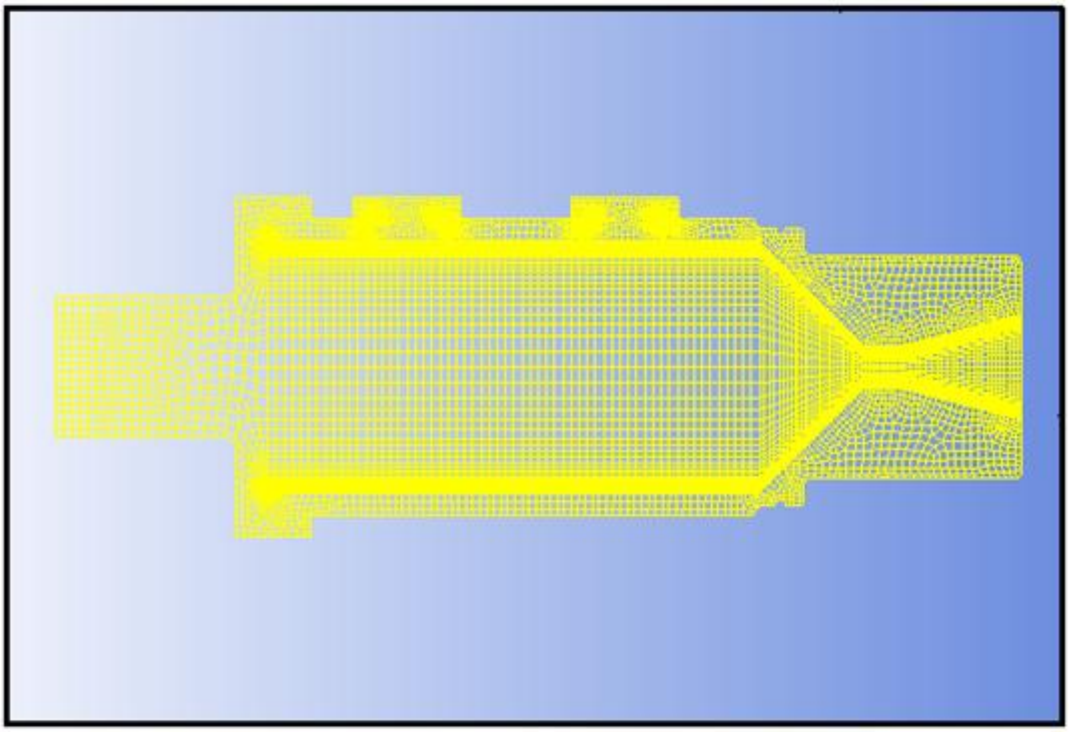

Figure 94 Mesh view of subscale test motor

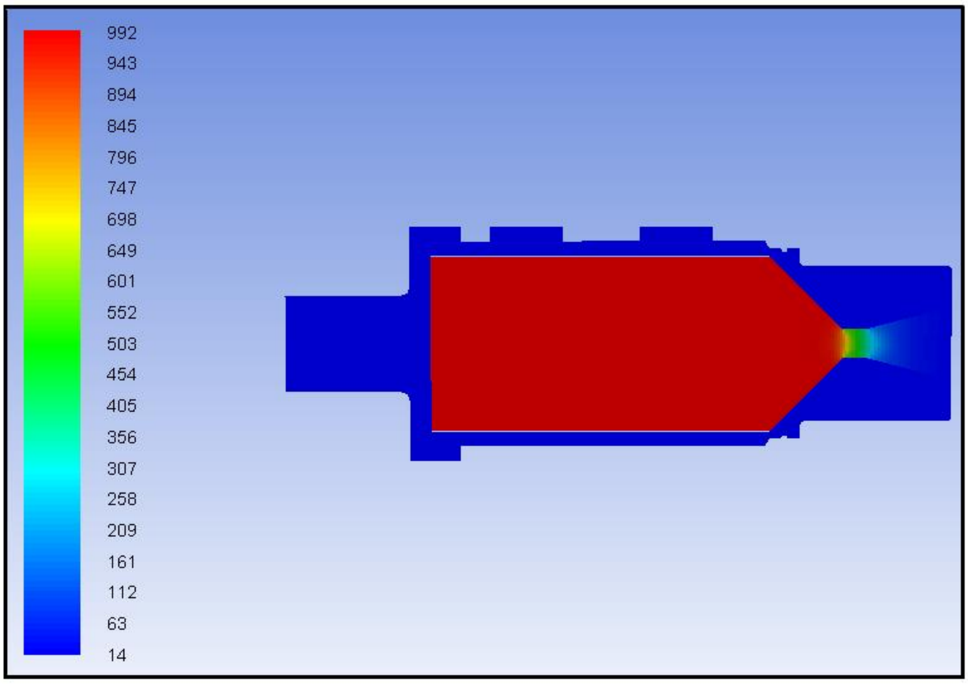

Figure 95 Static pressure distribution in test motor

In Figure 95, static pressure distribution in the test motor is seen. In numerical study, the steady case which the web thickness remains 1 mm is solved. According to test 3, the experimental shows that when the web thickness of the propellant is 1 mm, the pressure which is measured by pressure transducer is 1000.3 Psi (6.92 MPa). It is observed that 1% difference is occurred between the calculated and measured pressure. So numerical study is converged by applying "mass flow rates" boundary conditions.

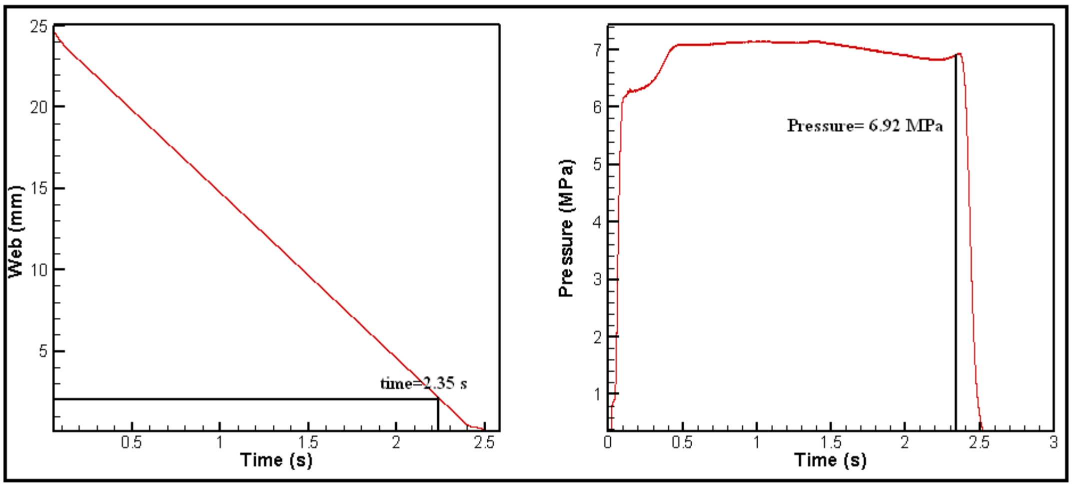

Figure 96 Test results obtained from test 3

Figure 97 represents the places that thermocouples are inserted during the firing test motor 3.

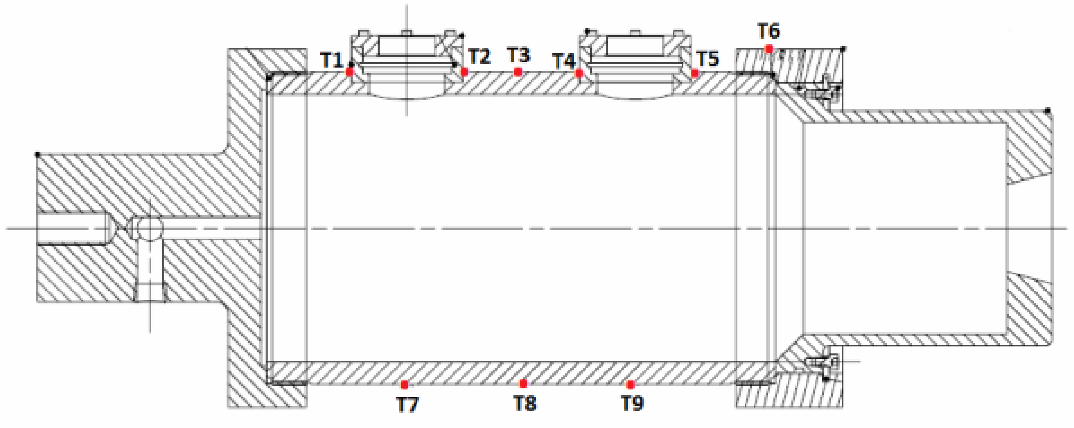

Figure 97 Termocouples places belong to test 3

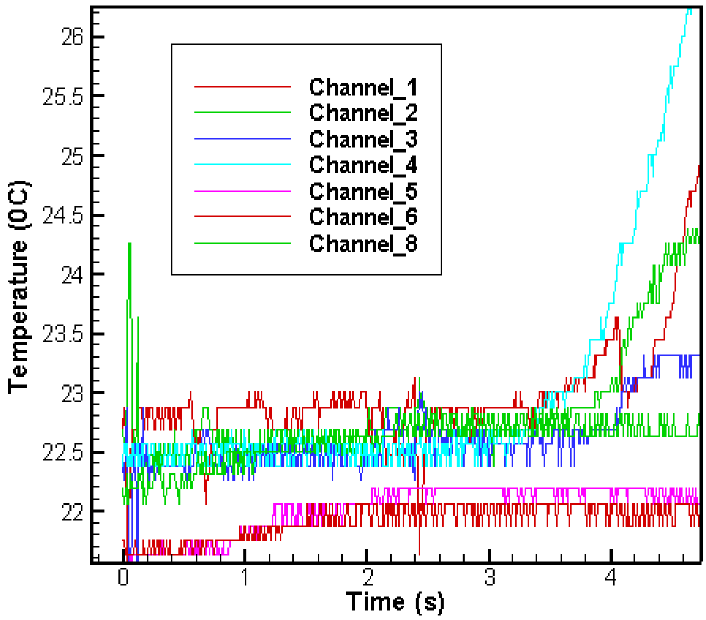

Figure 98 Temperature distibution on test motor obtained by thermocouples

Temperature measurement of test motor 3 was performed with the main target of determining critical points that threat the structure of the motor. The results are shown in Figure 98. The results show that maximum temperature is not exceed 28 ^{0}C.

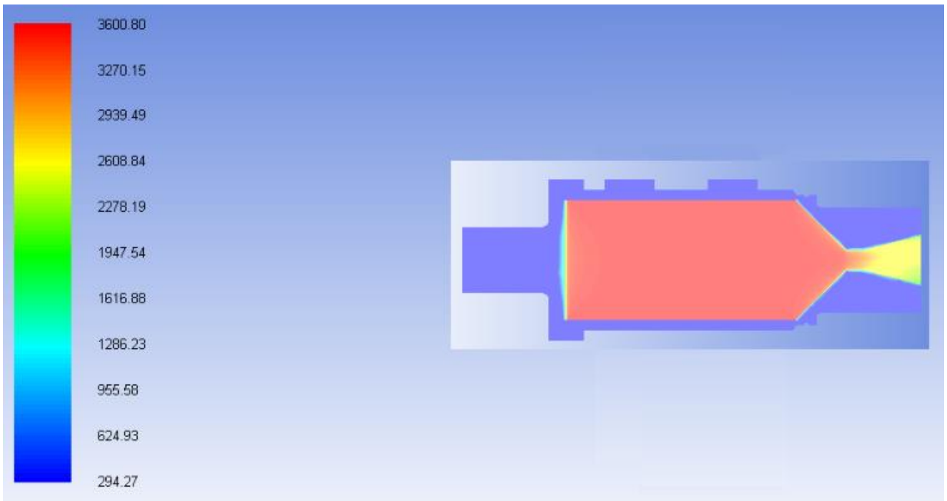

Figure 99 Temperature (Kelvin) distibution on test motor obtained from numerical analysis

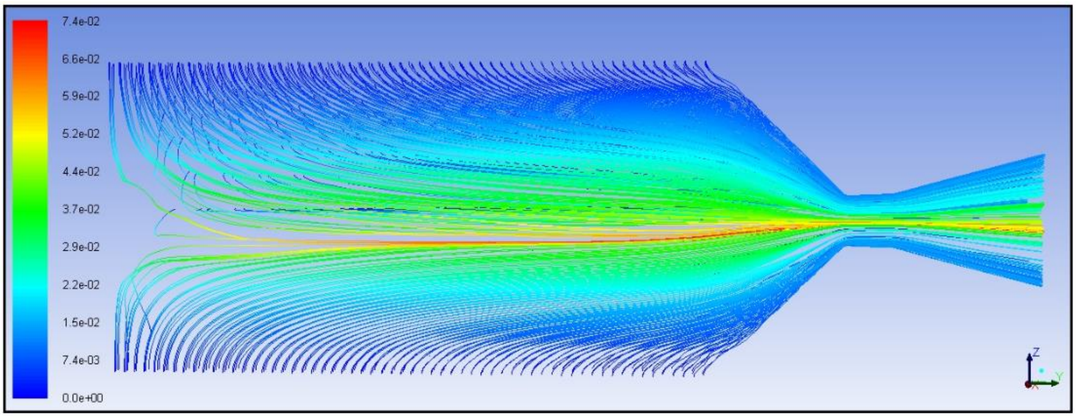

Figure 100 Alumina particles distribution in test motor

In Figure 100 residence time (s) of alumina particles in combustion chamber is seen. The propelant compostion used in the test includes aluminium particles. After ignition aluminium react with oxygen and alumina particles are occurred.

CHAPTER 8

UNCERTAINTY ANALYSIS

8.1 Introduction

The burning rates of propellants are determined by various experimental methods. For these experimental methods there is always an implied uncertainty, U, this should be determined to discuss the results and settle a band for these results. Uncertainty defines an interval which the true value should be searched between these intervals. True value of the test will lay 95% of the time, X±U [12]. The uncertainty is usually includes two main errors, systematic errors and random errors. Systematic errors usually called bias as a constant component and random errors called precision as a variable component. Both of them made up the elemental errors [12]. So one can define uncertainty as,

$$\mathrm{U} = \sqrt{\mathrm{B}^2 + \mathrm{P}^2} \tag{7}$$

In a calculation that requires measured variables, X, each of the variables will have an associated uncertainty,$\mathrm{U_X}$, and must be accounted for. The result of the calculation, r, is called the data reduction equation [12]

$$\mathrm{r} = \mathrm{r}(\mathrm{X_1}, \mathrm{X_2}, \ldots\ldots.., \mathrm{X_i}) \tag{8}$$

The total uncertainty of the data reduction equation is

$$\mathrm{U_r^2} = \left(\frac{\partial \mathrm{r}}{\partial \mathrm{X_1}}\right)^2 \mathrm{U_{X_1}^2} + \left(\frac{\partial \mathrm{r}}{\partial \mathrm{X_2}}\right)^2 \mathrm{U_{X_2}^2} + \cdots + \left(\frac{\partial \mathrm{r}}{\partial \mathrm{X_i}}\right)^2 \mathrm{U_{X_i}^2} \tag{9}$$

Another method that is called direct Monte Carlo simulation is used instead of traditional uncertainty analysis to avoid calculating thousands of partial derivatives [32]. In this method, errors for measurement X_i are randomly drawn from a Gaussian distribution with a mean equal to zero and a standard deviation equal to one half its associated uncertainties. The errors are then added to the X_is and the result, r, is calculated with the X_is . This process is repeated 10000 times to get 10000 values of r. The standard deviation, σ, of the r values is calculated and then multiplied by two in order to get the uncertainty, U_r [12]

$$U_r = 2\sigma \tag{10}$$

The 2σ interval will contain the true value r 95% of the time.

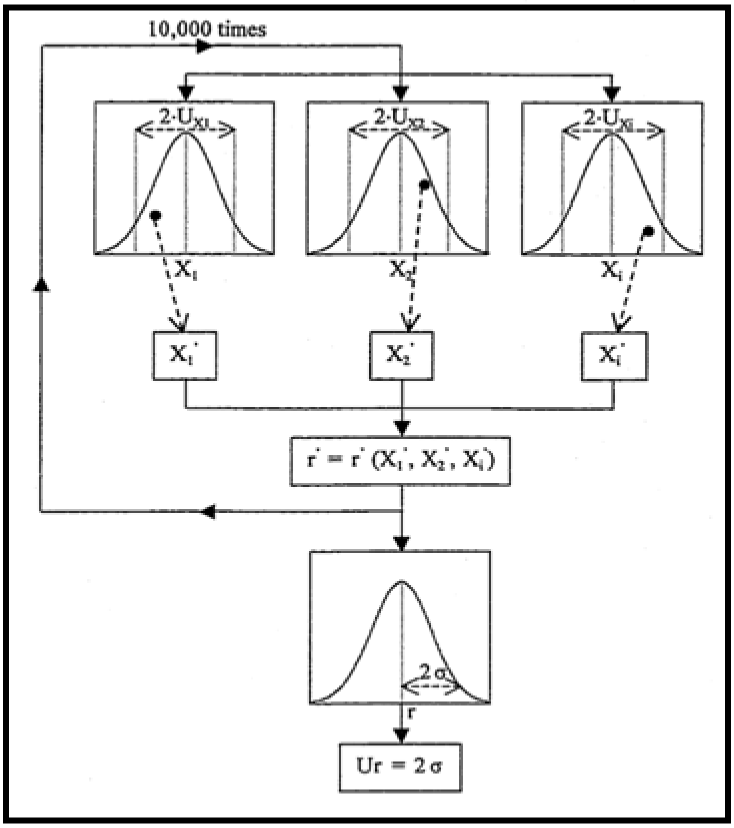

Figure 101 Direct Monte Carlo Simulation Diagram used in uncertainty Measurement [33]

8.2 Related Literature Survey

Uncertainty analysis of the ultrasonic measurement method is performed first by Dauch [33]. Three propellant types were investigated by using closed bombs. Propagation time is the most influential component which is a measured quantity. As expected pressure does not a high effect on burning rate uncertainty. Initial thickness of the propellant also influences the burning rate evaluation. It was found that using a thicker propellant sample for tests induces a low relative uncertainty which ranges between 3.5% and 5%.

As an extension work, [12] and [34] are studied on uncertainty determination of ultrasonic measurement method. But addition to Dauch [33] work, uncertainty of time of flight was not assumed constant. A range of 0.1-0.5 μs in 0.025 μs increments was used for propagation time uncertainty along with EDUM method, new digital Zero Crossing and Cross Correlation methods. In this study closed bomb test setup was used with six propellant samples. Eventually, the results determined from three methods are nearly same and propagation time uncertainty does not have a large effect on burning rate uncertainty.

According to Kang et al [35], uncertainty values determined from two different methods for measuring time of flight of the reflected signals are closer to each other. In this study three types of propellants were used. Uncertainties came from initial thickness of the propellant, pressure and time of flights are taken into account for determining uncertainty of initial thickness. In this study for uncertainty measurement conventional uncertainty analysis is performed instead of Monte Carlo Method. Relative uncertainty of initial propellant thickness is increasing with the decreasing of initial length of propellant.

In this study, uncertainty of closed bombs is investigated. It is seen from Figure 102 that, uncertainty of the tests shows downward trend as pressure increases. Also number of regression point affects the uncertainty. As expected, while the number of regression points is increasing, uncertainty decreases. The reason is standard deviation of linear regression process. All of the other uncertainties came from pressure and initial thickness, are same except uncertainty came from linear regression.

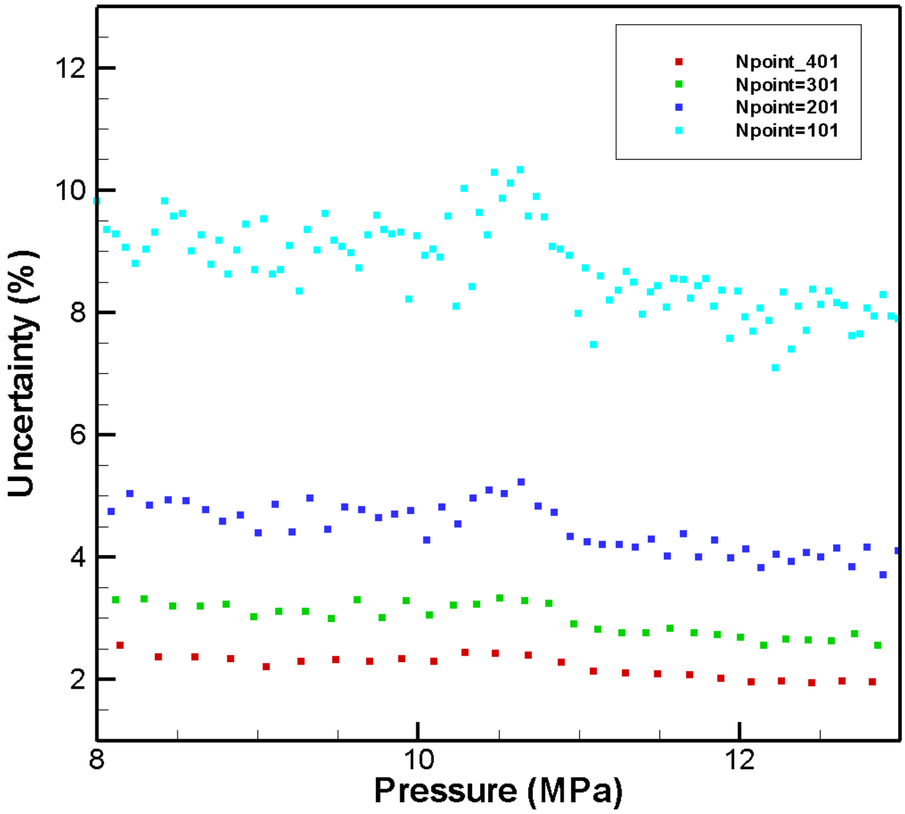

Figure 102 Uncertainty of Closed Bomb Tests versus Pressure

CHAPTER 9

CONCLUSIONS AND RECOMMENDATIONS

9.1 Conclusions

In this thesis study, burning rate evaluation of various aluminized and non-aluminized propellants was considered by means of burning rate with ultrasonic measurement method. To achieve this goal, a closed test setup was installed and 33 closed bomb tests were performed with 8 different propellant batches. The results of these tests were compared with the firings of subscale test motors which were performed with same propellant compositions. With the aim of qualification of ultrasonic measurement method, 12 closed bomb tests that belong to HSTYPE5 were performed. According to results obtained from these tests, at 10.34 MPa reference pressure maximum 2.45% difference between static firing tests and closed bomb tests was obtained. In order to consider the repeatability of tests, standard deviation of the tests was considered. Standard deviation of static firing tests was 0.0385 mm/s whereas 0.1313 mm/s standard deviation was measured for closed bomb tests. This result shows that repeatability of static firing tests is better than closed bomb tests. However this evaluation is performed for only one batch. Evaluation of repeatability of two burning rate evaluation method should be done for various propellant batches.

Regarding to test motor study, a test motor which was designed and manufactured for ultrasonic applications was fired three times with ultrasonic measurement method. All of the tests were quite successful by means of determining burning rate. Evaluation of burning rate in real time was first achieved by these tests. Up to these tests, only average burning rates over the average pressures were obtained. Test motor firings which were performed with ultrasonic measurement method were compared with conventional static firing tests. Comparison was performed with only average burning rates at specific average pressures because average burning rates can be obtained from conventional static firing tests. The results were compatible with each other.

In order to determine temperature values occurred on motor case during the firing, a numerical study was performed. At the beginning, for choosing applicable turbulence model, an experimental study was determined as a test case. By comparing pressure and velocity profiles, k-omega SST turbulence model was chosen for further numerical analysis. After choosing the turbulence model, thermal analysis of ultrasonic test motor was performed with ANSYS 16.0.

An uncertainty study was performed for closed bomb tests belong to HSTYPE5 propellant batch with the main target of searching uncertainty sources of the tests. It was seen that uncertainty is changed between 2% and 10% range with respect to regression points.

9.2 Recommendations

For further studies, degradation rate of insulation materials such as EPDM should be studied with ultrasonic measurement method. In Roketsan still degradation of insulation materials is measured by conventional method such as measuring thickness of insulation before test and after test.

Another important topic is an erosive burning phenomenon which is seen especially in long rockets. For this topic, burning rates of local places on the test motor can be determined by ultrasonic measurement method.

Regarding to closed bombs, as a further study temperature effect on burning rate which is high should be considered and uncertainty of hot and cold closed bomb tests should be searched. There are not enough studies regarding to this topic in the literature.

REFERENCES

1) Traineau J.C., Kuentzmann P., *Ultrasonic Measurements of Solid Propellant Burning Rates in Nozzleless Rocket Motors.* Journal of Propulsion and Power, 1986. 2(3): p. 215-222.

2) Gupta G., Jawale L., Mehilal, Bhattacharya B., *Various Methods for the Determination of the Burning Rates of Solid Propellants - An Overview,* Central European Journal of Energetic Materials, 2015. 12(3): p. 593-620.

3) Sutton G. P., Biblarz O., *Rocket Propulsion Elements,* 7th edition, John Wiley & Sons, 2001.

4) A.V.T., *Evaluation of Methods for Solid Propellant Burning Rate Measurements.* RTO Technical Report 43, 2002.

5) Cauty, F., *Non-Intrusive Measurement Methods Applied to Energetic Material Regression Rate Determination.* 2nd International High Energy Materials Conference & Exhibit Madras, Chennai (India), 1998.

6) Cauty F., Eradès Ch., *Ultrasound Measurement Method: Errors, Noise and Sensitivity.* Combustion, Explosion, and Shock Waves, 2000. 36(1): p. 54-61.

7) Cauty F., *The Ultrasound Waves: a Measurement Tool for Energetic Material Characterization.* 40th AIAA/ASME/SAE/ASEE Joint Propulsion Conference and Exhibit, Fort Lauderdale (Florida), 2004.

8) Cauty F., Eradès Ch., *Progress in Determining the Burning Rate of a Composite Solid Propellant Using an Ultrasound Technique.* 30th International Conference of ICT, Karlsruhe (Germany), 1999.

9) Jeenu R., Pinumalla K., Deepak D., *Industrial adaptation of ultrasonic technique of propellant burning rate measurement using specimens.* Journal of Propulsion and Power, 2013. 29(1): p. 216-226.

10) Marshall M.A., *Methods of Analysis of Ultrasonic Echoes To Determine Solid Propellant Burning Rates.* M.S. Thesis, Dept. of Mechanical and Aerospace Engineering, University of Alabama in Huntsville, 2008.

11) Jones D.A., *Advanced Digital Methods for Solid Propellant Burning Rate Determination.* M.S. Thesis, Dept. of Mechanical and Aerospace Engineering, University of Alabama in Huntsville, 2015.

12) Evans A. J., *Monte Carlo Assessment of Solid Propellant Burning Rate Measurement,* M.S.. Thesis, Dept. of Mechanical and Aerospace Engineering, University of Alabama in Huntsville, 2013

13) Cauty F., Louaze G., Eradès Ch., *Ultrasound method: Towards the automation of the solid propellant burning rate determination.* International Journal of Energetic Materials and Chemical Propulsion 2009. 8(2): p. 113-132.

14) Cauty F., Demerais J.Cl., Eradès Ch., *Determination of Solid Propellant Burning Rate Sensitivity to the Initial Temperature by the Ultrasonic Method.* International Journal of Energetic Materials and Chemical Propulsion, 1994. **3**: p. 642-653.

15) Deepak D., Jeenu R., Sridharan P., Padmanabhan M.S., *Determination of Pressure Dependence of Burning Rate in Solid Motors Using Ultrasonic Technique.* Journal of Propulsion and Power, 1998. 14(3): p. 290-294.

16) Cauty F., Carmicino C., Russo-Sorge A., *The Pressure Sensitivity of the Ultrasonic Waves Velocity: A Contribution to a Better Determination of the Energetic Material Regression Rate.* International Journal of Energetic Materials and Chemical Propulsion, 2007. **6**(6): p. 749-774.

17) Marshall M. A., Evans J.A., Frederick R. A., Marlow D. M., *UAH Solid Propellant Characterization.* 43rd AIAA/ASME/SAE/ASEE Joint Propulsion Conference & Exhibit, Cincinnati (OH), 2007.

18) Mumcu B., *Application of Ultrasonic Burning Rate Measurement Method on Closed Bombs.* M.S. Thesis, Dept. of Aerospace Engineering, Middle East Technical University, 2013.

19) Linn C. A. B., Jackson D. I., Moser M.D., *Use of Cross-Correlation Waveform Analysis to Determine Burning Rate Using Ultrasonic Technique.* 42nd AIAA/ASME/SAE/ASEE Joint Propulsion Conference and Exhibit, Sacramento (California), 2006.

20) Rochford E.E., *Temperature Sensitivity Measurements of Solid Rocket Propellants.* M.S. Thesis, Dept. of Mechanical and Aerospace Engineering, University of Alabama in Huntsville, 1999.

21) R. Frederick, Traineau J.C., Popo M., *Review of Ultrasonic Technique for Steady State Burning Rate Measurements.* 36th AIAA/ASME/SAE/ASEE Joint Propulsion Conference and Exhibit, Huntsville (Alabama), 2000.

22) Oh H. T., Kim H. J., Song S. J., Ko S. F., Kim I. C., Yoo J. C. Jung J. Y., *Investigation of Ultrasonic Methods for Measuring Burning Rates of Solid Propellants.* Review of Quantitative Nondestructive Evalu, 2008. **27**: p. 1512-1519.

23) Hasegawa K., Hori K., *Novel Burning Rate Measurement Technique for Solid Propellant by Means of Ultrasonics.* Combustion, Explosion, and Shock Waves, 2010. 46(2): p. 188-195.

24) Kohga M., Frederick R. A., Moser M. D., *Ultrasonic Properties of Propellant Ingredients.* Journal of Propulsion and Power, 2004. 20(1): p. 135-141.

25) Salvo R. D., Frederick R. A., Moser M. D., *Direct Ultrasonic Measurement of Solid Propellant Combustion Transients* 35th AIAA/ASME/SAE/ASEE Joint Propulsion Conference & Exhibit, Huntsville (Alabama), 1999.

26) Song S. J., Jeon J. H., Kim H. J., Kim I. C., Yoo J. C., Jung J. Y., *Burning Rate Measurement of Solid Propellant Using Ultrasound - Approach and Initial Experiments.* Review of Quantitative Nondestructive Evaluation, 2006. 25: p. 1229-1236.

27) Song S. J., Kim H.J., Ko S. F., Oh H. T., Kim I. C., Yoo J. C., Jung J. Y., *Measurement of Solid Propellant Burning Rates by Analysis of Ultrasonic Full Waveforms.* Journal of Mechanical Science and Technology, 2009. 23: p. 1112-1117.

28) McQuade W. W., Dauch F., Moser M. D., Frederick, R. A., *Determination of the Ultrasonic Burning Rate Technique Resolution.* 34th AIAA/ASME/SAE/ASEE Joint Propulsion Conference and Exhibit, 1998.

29) Cauty F., Demarais J. C., *Ultrasonic Measurement of the Uncured Solid Propellant Burning Rate.* 21st International Congress of ICT, Karlsruhe,1990.

30) Cauty F., *Ultrasonic Method Applied to Full-Scale Solid Rocket Motors,* Journal of Propulsion and Power, 2000. 16(3): p. 523-528.

31) Halıcı Ö., Arkun U., Demirbaş M., *Ultrasonik Ölçüm Cihazı Kabulü ve Kullanıcı Eğitimi*, 22-29 Ekim 2007, Onera, Fransa

32) Dauch F., Moser M.D., Frederick R. A., and Coleman H.W., *Uncertainty Assessment of the Pulse-Echo Ultrasonic Burning Rate Measurement Technique*, 35th AIAA/ASME/SAE/ASEE Joint Propulsion Conference & Exhibit, Los Angeles (California), 1999.

33) Dauch F., *Uncertainty Analysis of the Ultrasonic Technique Applied to Solid Propellant Burning Rate Measurement*, Ms. Thesis, Dept. of Mechanical and Aerospace Engineering, University of Alabama in Huntsville, 1999

34) Evans J. A., Penton A., Frederick R. A., *Uncertainty of Solid Propellant Burning Rates*, 45th AIAA/ASME/SAE/ASEE Joint Propulsion Conference & Exhibit, Denver (Colorado), 2009.

35) Kang T., Kim H. J., Song S. J., Ko S. F., Kim I. C., Yoo J. C., Jung J. Y., *Uncertainty Analysis of Ultrasonic Methods for Measuring Burning Rate of Solid Propellant*, Review of Quantitative Nondestructive Evaluation, 28, 1894-1901, 2009

36) Traineau J. C., Hervat P., Kuentzmann P., *Cold Flow Simulation of a Two-Dimensional Nozzleless Solid Rocket Motor*, 22nd AIAA/ASME/SAE/ASEE Joint Propulsion Conference & Exhibit, Huntsville (Alabama), 1986

37) Godon J. C., Duterque J., Lengelle G., *Solid Propellant Erosive Burning*, Journal of Propulsion and Power, 1992. 8(4): p. 741-747.

APPENDIX A

STUDIES FOR RESEARCH OF ERROR SOURCES

Some results obtained from closed bomb tests that were done with ultrasonic measurement method are far away from the static firing test results. For this reason some studies were performed for research of error sources. In this part, the sources of error are discussed and some conclusions are resolved.

A.1 The Research of Error Source Calculating of Burning Rate

For the purpose of calculating the burning rate of propellants a Matlab (R2012) code was written. The ultrasonic measurement method which is used in this thesis was bought from the research center called ONERA in 2007. During the training session that was done in ONERA, seven tests were performed. The Binary files of the test results were given to the stuff of Roketsan. Also the burning rates that were calculated for these tests were given. In this part, the results that were calculated in ONERA are compared with the results that were calculated by me. In Table 24 the details of the tests that were performed in ONERA are given.

Table 24 The Details of Tests

No	Propel lant	Couplin g Material	Thickne ss of Propella nt	Thickness of Coupling Material	Weight of Propella nt	C_p	C_c	k_p	l_p
1	Butala ne	CY230+ %18 SiO2	30.30	37.44	56.55	1915	2630	2.50E-04	5.0E-05
2	Butalit e	CY230	40.47	34.70	54.40	1920	2300	2.30E-04	5.0E-05
3	Butala ne	CY230+ %18 SiO2	30.38	33.10	64.30	1915	2630	2.50E-04	5.0E-05
4	Butalit e	CY230	20.20	48.30	-	1920	2300	2.30E-04	5.0E-05

A.1.1 Test Case 1

The burning rate that calculated from test case 1 is compared with the results calculated by burning rate calculation code. Comparison of burning rates is shown in Figure 103.

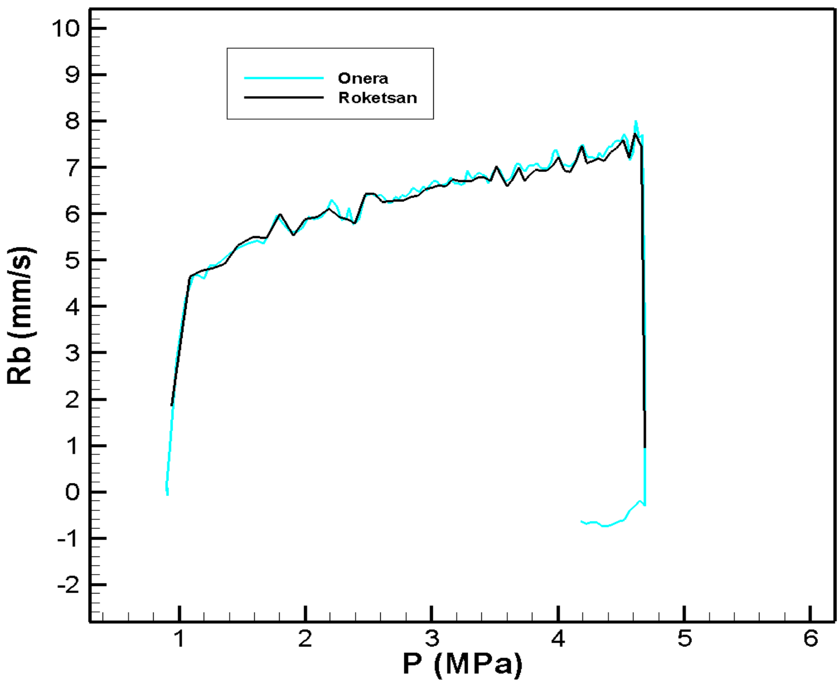

Figure 103 Burning rate results of test case 1

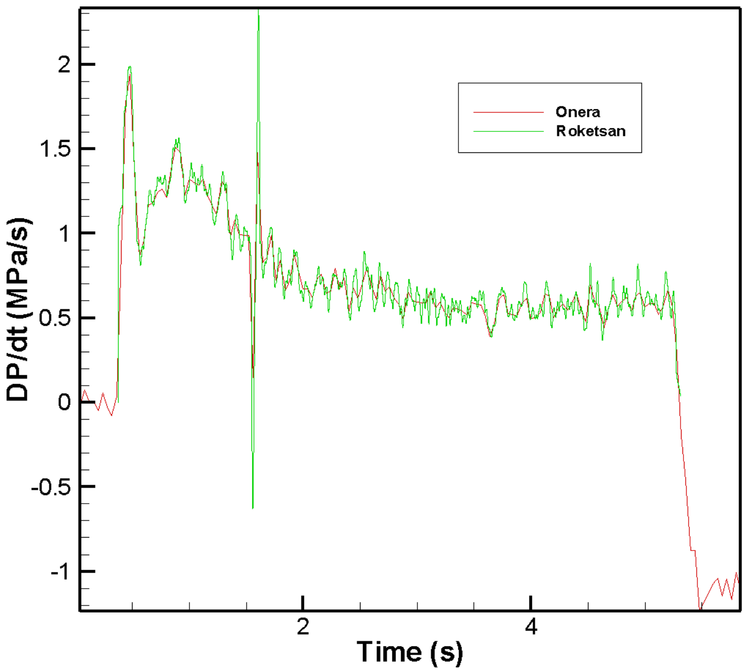

Figure 104 Derivative of Pressure with Respect to Time

Derivative of pressure with respect to time is shown in Figure 104. The data that calculated in research center are compared with the results that calculated by the burning rate code. As it is seen from Figure 103, there is no such a big difference between the results. The derivative of pressure with respect to time shows oscillations.

A.1.2 Test Case 2

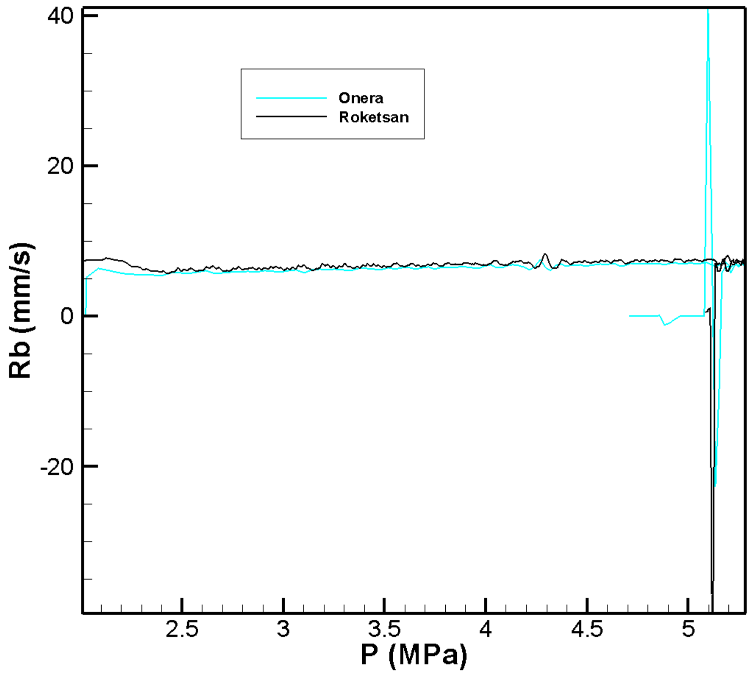

Figure 105 Burning rate results of test case 2

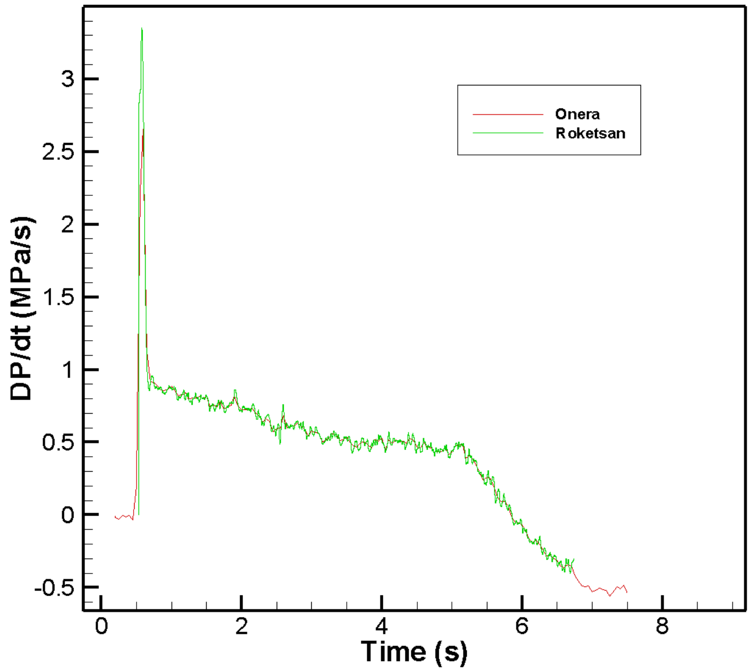

Figure 106 Derivative of Pressure with Respect to Time

The results that belong to test case 2 are shown in Figure 105 and Figure 106. As seen from the figures the results that calculated are almost same.

A.1.3 Test Case 3

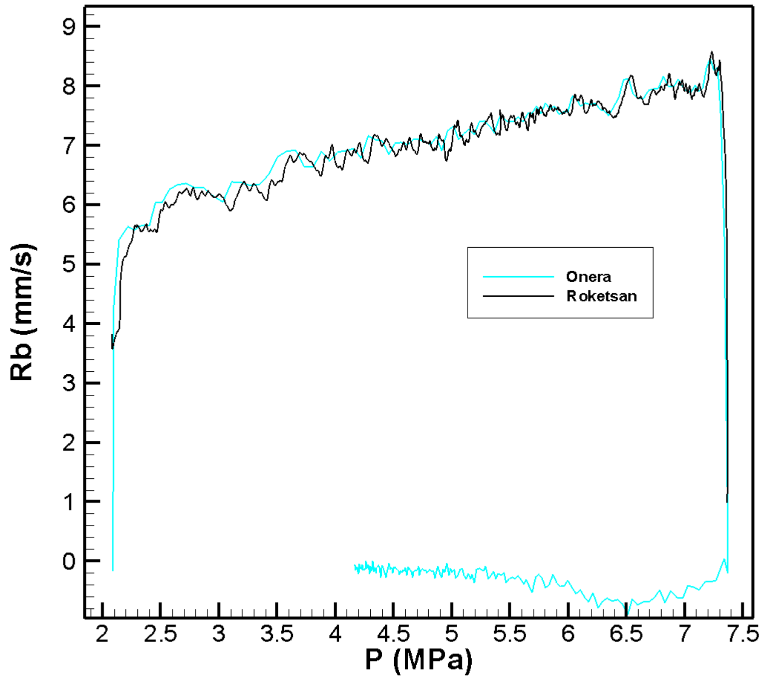

Figure 107 Burning rate results of test case 3

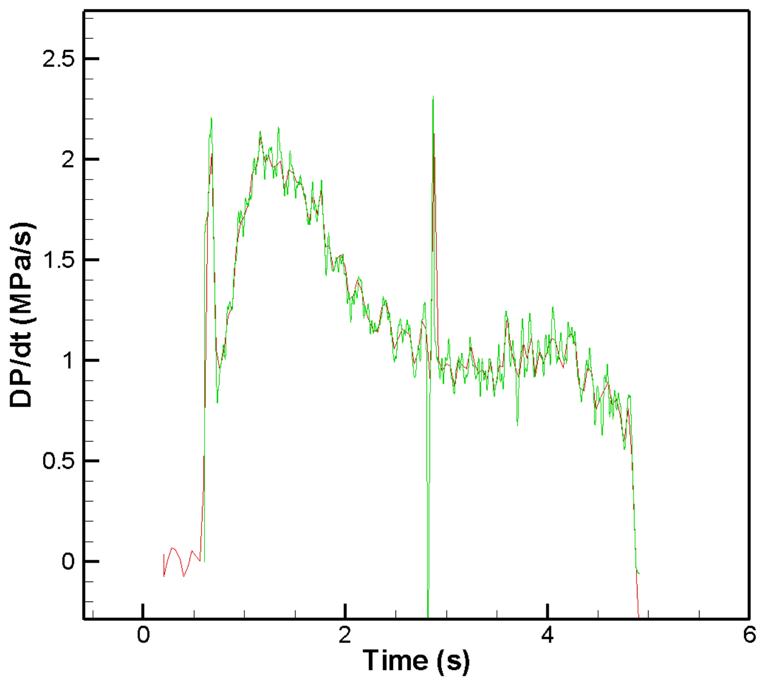

Figure 108 Derivative of Pressure with Respect to Time

Also the results obtained from test case 3 are compared and showed in Figure 107 and Figure 108. Result of the comparison of these test results shows us that the trend of the test results is almost same.

A.1.4 Test Case 4

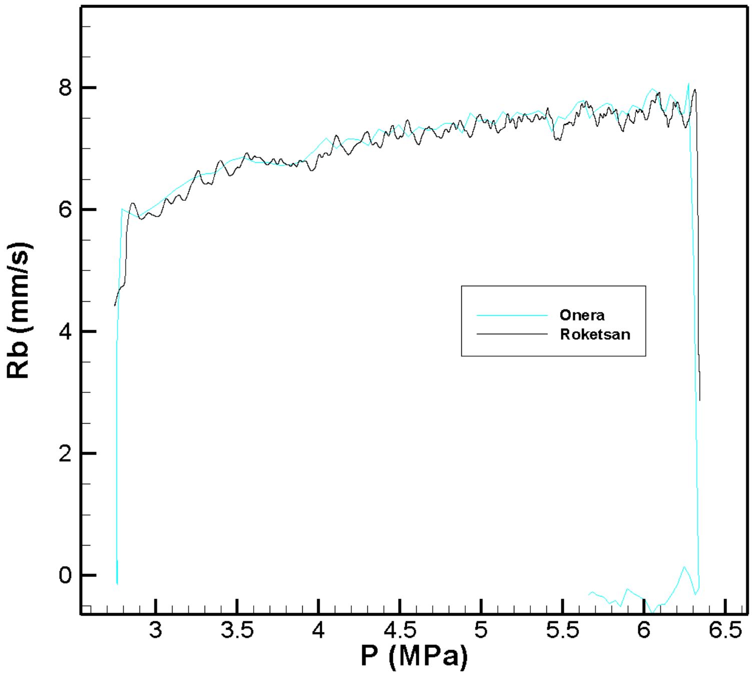

Figure 109 Burning rate results of test case 4

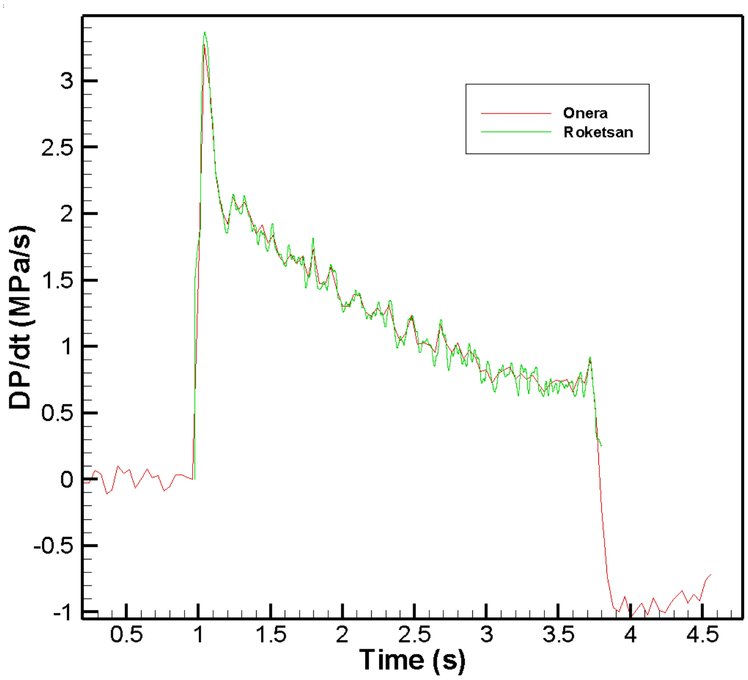

Figure 110 Derivative of Pressure with Respect to Time

The results obtained from the tests that were done in ONERA were compared with the results calculated in Roketsan. The figures above were considered and concluded some results. The results are almost same. So burning rate calculation code is verified with the burning rates calculated in ONERA.

APPENDIX B

PRESSURE EFFECT ON WAVE PROPOGATION

Sound waves propagate through the medium such as solids, liquids and gases. There are two common wave propagation types, one is longitudinal and the other one is shear (transverse) waves. Longitudinal waves propagate as direction of wave propagation whereas shear waves propagate as perpendicular to the direction of wave propagation.

Wave propagation is influenced by temperature and pressure. In this study temperature effect on wave propagation is neglected. An example of calculation of kp belong to OMTYPE1 is shown in Figure 111. Kp value of this test is taken 0.0018 with a correlation coefficient R^2 is very close to 1 (0.9876).

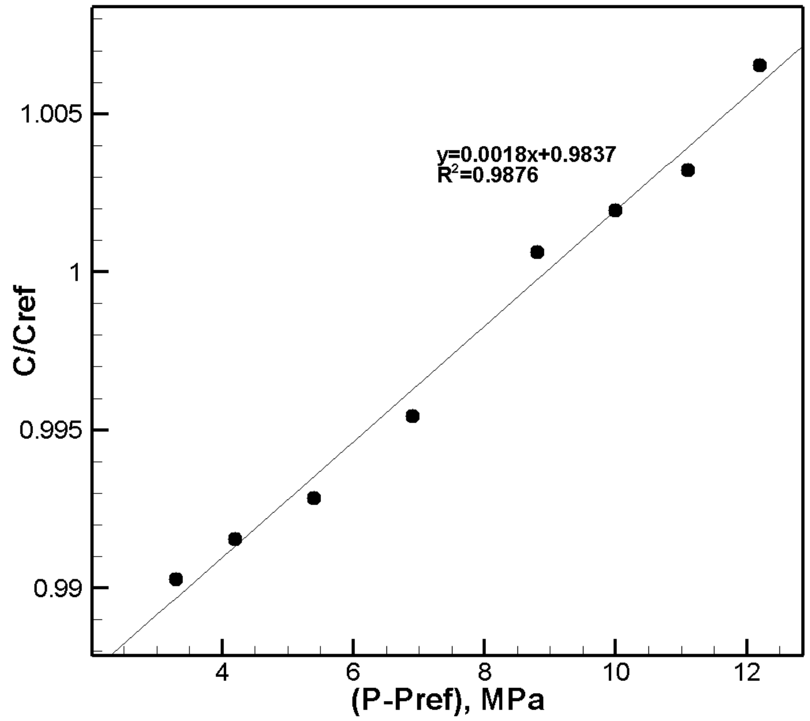

Figure 111 Wave velocity variation with pressure for propellant

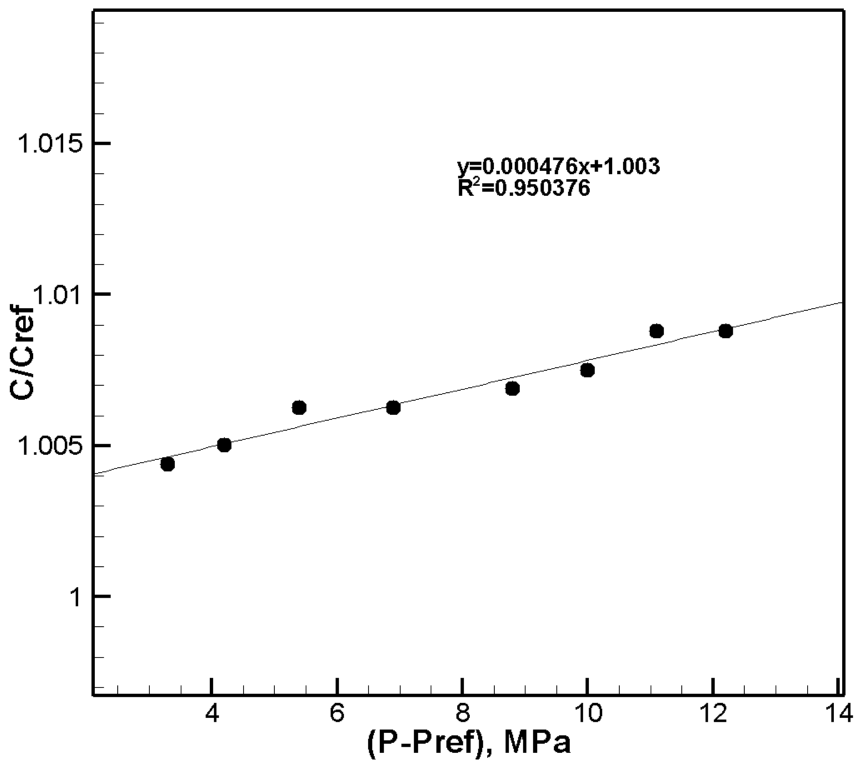

Figure 112 Wave velocity variation with pressure for coupling material

Figure 112 represents the lp (sensitivity coefficient of coupling material) value belong to OMTYPE1 test. Lp value of this test is taken 0.000476 with a correlation coefficient R^2 (0.950376).

APPENDIX C

STANDARD OPERATING PROCEDURE

This part will summarize the steps after finishing the entegration of closed bomb test setup. These steps are belonged to Software that was used with ultrasonic measurement method.

C.1 Configuration of ACL-8112 DG/HG

- Run 8112UTIL.exe on the screen of computer
- The configuration of the data collecting card is performed at this screen. This card configuration has to checked before every test.

Figure 113 Card configuration screen

➢ After configuration of the card, check the measurement of pressure inside the closed bomb by "Function Testing".

C.2 Settings of Screen

The main screen of the software is shown in Figure 114.

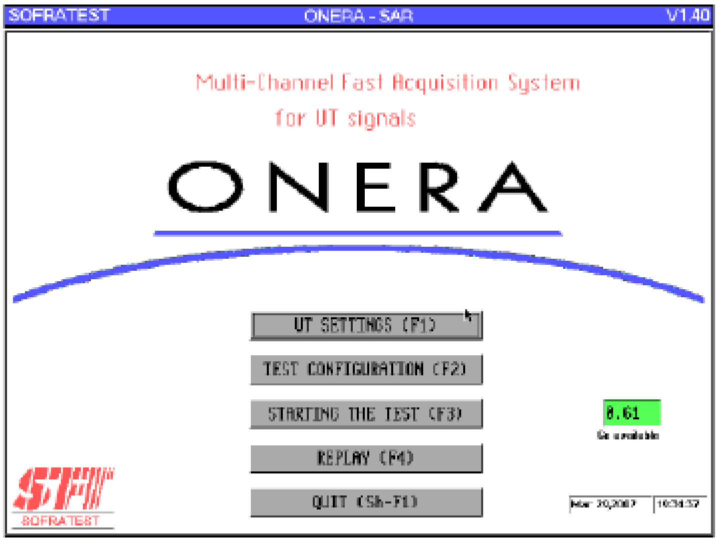

Figure 114 Welcome screen of the software

C.3 Ut Settings

Press UT setting on opened page. At this point, ultrasonic sensor is placed on propellant sample holder surface and the echo which reflects from the propellant surface is checked. If the amplitude of the signal is not enough, gain of the signal is increased. But it should be not forgotten, if the gain of the signal is increased also this increase noise. After checking the echoes reflecting from propellant surface and interface ultrasonic transducer is fixed on the propellant sample holder.

➢ For opening setting of the old test, push the button Files→Open a File→130213t and the settings of the new test can be done by modifying old setting.

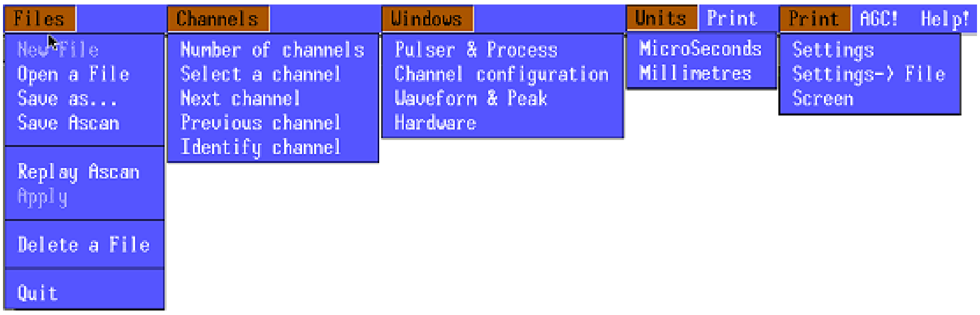

Figure 115 UT setting

- By pushing Channels→Number of channels, the ultrasonic channel that used during the test is entered.

- On the top of the screen, by pressing the button "Windows" “Channel Configuration” can be selected and enter 1 microsecond for “Post Trigger Delay”

On the screen of UT settings, enter **Pulse Amplitude**, **Pulse Width** and acoustic velocity (**UT velocity**) values. The echo reflects from the burning surface of propellant is tracked by "Automatic Gain Control"

Gate G1 Start: This represents start of the gate which control the continuity of the signal.

Gate G1 Width: This represents the width of the gate

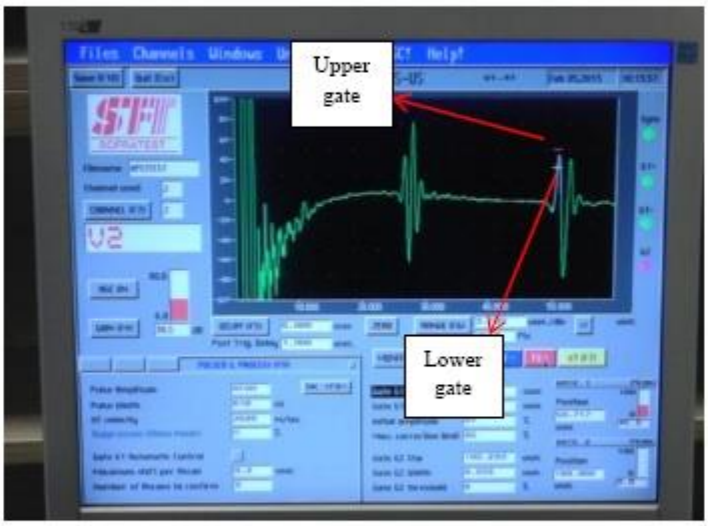

Figure 116 The place of G1

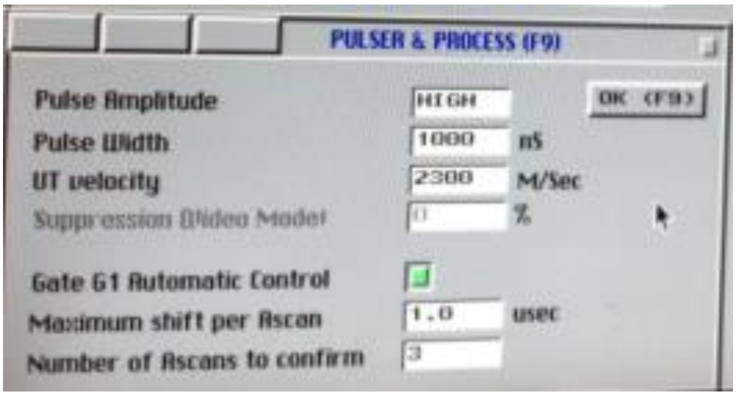

Figure 117 Pulser& Process

For obtaining a visible signal, **Pulse Width** can be changed for every test.

Gate G2 Start: The echo that is emitted from the ultrasonic transducer is shown in Figure 118.

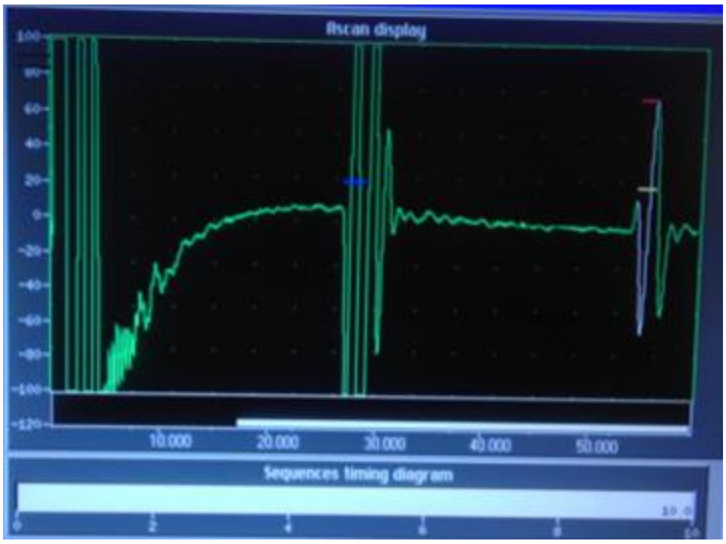

Figure 118 Test configuration

Gate G2 Width: This represents the width of the gate

The ultrasonic settings are done by the screen **Windows→Waveform&Peak**

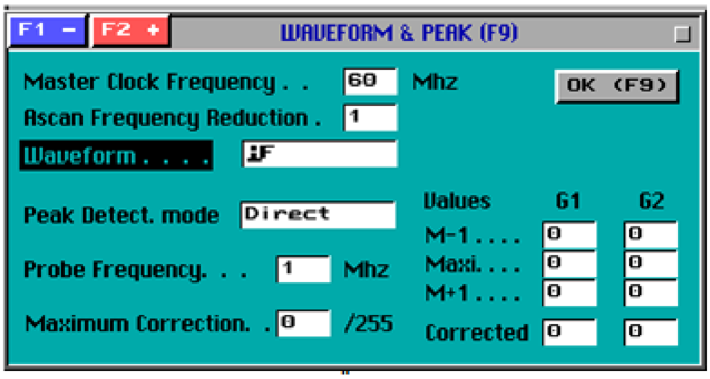

Figure 119 WaveForm&Peak

- On the top of the screen, "Units"→"Milimeters" is picked and the screen of echo is changed to length. Check the "UT velocity" by comparing the coupling material length and the measured length of coupling material.

- Save the settings and closed the screen

- The test setting can be saved as Files→Save as→ Filename

C.4 Starting the Test

- For beginning the test, push the "STARTING THE TEST" on the main screen of the software. At this part, name of test, file name and number of analog channels are entered. The configuration file for test is picked and name of the recorded file is written on "Recording data Filename". And push the button "RUN" for starting the test. At the same time, the current is sent to igniter for starting the test.

- When ready for test, count from three and push run to record the data.

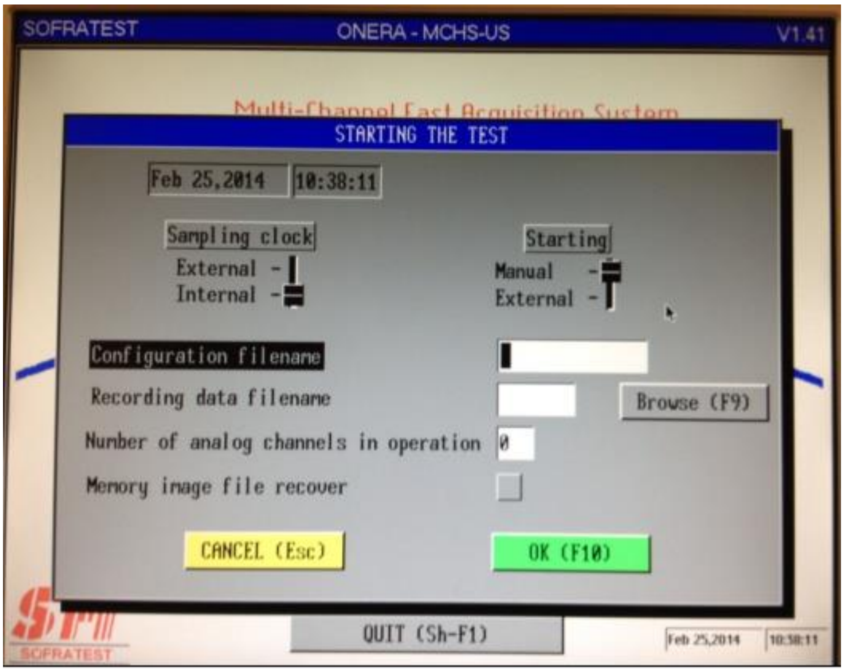

Figure 120 Starting the test screen

C.5 Replay

- The results of the test can be seen again by “REPLAY”. So, the success of the test and the signals motion can be seen from this screen. If everything is ok, write the test data on CD.

Table 25 The Steps for Running a Test

	Definition of Steps
1	Leakage test for closed bombs has to be performed
2	Piezoelectric sensor has to be checked
3	Configuration of ACL-8112 DG/HG card has to be performed
4	Ultrasonic sensor is placed top of the propellant sample holder and the signal which is reflected from the propellant surface is checked if it is seen at the monitor of the program
5	If the amplitude of the obtained signal is enough, ultrasonic sensor is placed after now.
6	Enter the number of channel from the button of Channels→Number of channels
7	Enter the post trigger delay of ultrasonic sensor from the button of Windows→ChannelConfiguration→PostTriggerDelay→ 1
8	Pulse Amplitude, Pulse Width and UT velocity (sound of speed) are entered on the monitor of UT settings
9	Enter the“G1 Start”and“Gate G1 Width”.
10	Enter “Pulse Width ”, “Pulse Amplitude”, “Maximum Shift per Ascan” and “Number of Ascans to Confirm” on the monitor of Pulser and Process
11	Compare the coupling material length with the signals that you see on the monitor
12	If you use automatic gain control, active “AGC in operation”
13	Fill the Test Configuration form
14	Enter the values of “Starting the test” part
15	Push Run for test startup
16	Data are written in a CD.

APPENDIX D

ASCAN FILE OF CLOSED TEST BOMB

Type of card :2
Sequence no :1
Ascan count :50000
PRF :5000
Digitizer Frequency :30000 Kz
Window start :18.07 us
Window width :51.20 us
Ascan size :1536 pts

Time(s)	Ana 1 (v)	Ana 2 (v)	Channel	TOF (us)	Peak (%)	Gain (dB)
0.00020	0.62012	0.00000	1	098.333	028	036.8
0.00040	0.62012	0.00000	1	098.200	030	036.8
0.00060	0.62012	0.00000	1	098.533	031	036.2
0.00080	0.62012	0.00000	1	098.067	027	036.2
0.00100	0.62012	0.00000	1	098.300	027	036.5
0.00120	0.62012	0.00000	1	098.400	028	036.8
0.00140	0.62012	0.00000	1	098.333	029	036.8
0.00160	0.62500	0.00000	1	098.333	029	036.5
0.00180	0.62012	0.00000	1	098.333	029	036.5
0.00200	0.62012	0.00000	1	098.333	029	036.5
0.00220	0.62012	0.00000	1	098.200	028	036.5
0.00240	0.62012	0.00000	1	098.467	029	036.5
0.00260	0.62012	0.00000	1	098.233	029	036.5
0.00280	0.62500	0.00000	1	098.367	029	036.5
0.00300	0.62012	0.00000	1	098.333	028	036.5
0.00320	0.62500	0.00000	1	098.333	028	036.5
0.00340	0.62012	0.00000	1	098.200	027	036.8
0.00360	0.62012	0.00000	1	098.467	029	036.8
0.00380	0.62012	0.00000	1	098.233	029	036.8
0.00400	0.62012	0.00000	1	098.367	029	036.5
0.00420	0.62012	0.00000	1	098.333	029	036.5
0.00440	0.62500	0.00000	1	098.467	029	036.5
0.00460	0.62012	0.00000	1	098.067	029	036.5
0.00480	0.62012	0.00000	1	098.433	029	036.5
0.00500	0.62012	0.00000	1	098.333	029	036.5
0.00520	0.62012	0.00000	1	098.400	029	036.5
0.00540	0.62012	0.00000	1	098.233	028	036.5

0.00560	0.62500	0.00000	1	098.500	029	036.5
0.00580	0.62012	0.00000	1	098.333	029	036.5

………………………………………………………………………………..
………………………………………………………………………………..
………………………………………………………………………………..
………………………………………………………………………………..

9.99940	0.90332	0.00000	1	058.300	029	019.9
9.99960	0.90820	0.00000	1	058.400	029	019.9
9.99980	0.90332	0.00000	1	058.200	029	019.9
10.00000	0.90332	0.00000	1	058.267	029	019.6

APPENDIX E

BURNING RATE CALCULATION CODE

```
%%%%%%%%%%%%//Reading the Measured Data//%%%%%%%%%%%%%%

clc
clear all;
load INPUT.dat
time = INPUT(:,1); %test time
ana1 = INPUT(:,3); %Analog Channel 1 (V)
ana2 = INPUT(:,2); %Analog Channel 2 (V)
TOF =  INPUT(:,5);  %Time of Flight (microseconds)
peak = INPUT(:,6); %peak of the signal (%)
gain = INPUT(:,7); %(dB)

%%%%%%%%%%%%%%%//Material Properties//%%%%%%%%%%%%%%

Cpref = 1886;%acoustic velocity of propellant (m/s)
Ccref = 2620;%acoustic velocity of couplant (m/s)
kp  = 0.0018;   %pressure dependency of propellant (1/MPa)
lp  = 0.00047;  %pressure dependency of couplant (1/MPa)
Epi = 25.33;    %initial propellant thickness (mm)
Ec  = 35.03;    %couplant thickness (mm)

%%%%%%%%%%%%%%//Reference Values//%%%%%%%%%%%%%%%%%%%%%%%%%%%%%

Pref = 0.1;     %reference pressure (MPa)

plot(time,TOF,'r-+');


%Beginning of the Test

Test_baslama=input('test baslama zamanini giriniz ');
Test_bitis=input('test bitis zamanini giriniz ');

begin=find(INPUT(:,1)==Test_baslama);
min_index_p=find(INPUT(:,1)==Test_bitis);
datat = min_index_p-begin;
timet = ones (datat,1);
ana1t = ones (datat,1);
ana2t = ones (datat,1);
TOFt = ones (datat,1);
peakt = ones (datat,1);
gaint = ones (datat,1);

i=1;
```

```
for j=begin:min_index_p
    timet(i,1) = time (j);%time during combustion (s)
    ana1t(i,1) = ana1 (j);%analog channel 1 during combustion (V)
    ana2t(i,1) = ana2 (j);%analog channel 2 during combustion (V)
    TOFt(i,1)  = TOF (j)/2;%TOF during combustion (microseconds)
    peakt(i,1) = peak (j); %peak during combustion (%)
    gaint(i,1) = gain (j); %gain during combustion (dB)
    i=i+1;
end

TOFts = smooth(TOFt,401,'lowess'); %Robust local regression using
weighted linear least squares and a 2nd degree polynomial model with
10% span
figure
plot(TOFt,'ro-');
legend('Data','Smoothed Data')
hold on
plot(TOFts,'o-');
title('Smooth TOFts');

ana2ts = smooth(ana2t,401,'lowess'); %Robust local regression using
weighted linear least squares and a 2nd degree polynomial model with
10% span
figure
plot(ana2t,'ro');
legend('Data','Smoothed Data')
hold on
plot(ana2ts,'o-');
title('Smooth ana2ts');
end

coef1 = 10;%ana2ts to pressure (V to MPa)
Pg = ana2ts*coef1; %pressure (MPa)
P=Pg+0.1;

TOF_ilkveriler = TOFt(1:1000)/2;
TOF_ilkortalama = sum(TOF_ilkveriler)/1000;

for i=1:datat+1
    deltaP(i,1) = P(i,1)-Pref;  %P-Pref (MPa)
end

for i=1:datat+1
    deltaTOF(i,1) = TOF_ilkortalama-TOFts(i,1);  %wave propagation
variation (microseconds)
end

%%%%%%%%%%%//Time Derivatives//%%%%%%%%%%%%%%%

DdeltaTOF(1,1) = 0;%derivative of deltaTOF w.r.t. time for the first
data
DP(1,1) =0;%derivative of pressure w.r.t. time for the first data

for i=2:datat
    DdeltaTOF(i,1) = (deltaTOF(i+1,1)-deltaTOF(i-
1,1))/(timet(i+1,1)-timet(i-1,1));  %derivative of deltaTOF w.r.t.
time (microseconds/seconds)
    DP(i,1) = (P(i+1,1)-P(i-1,1))/(timet(i+1,1)-timet(i-
1,1));%derivative of pressure w.r.t. time (MPa/seconds)
end
```

```
DdeltaTOF(1,1)=DdeltaTOF(2,1);
DdeltaTOF(datat+1,1) = DdeltaTOF(datat,1); %derivative of deltaTOF
w.r.t. time for the last data
DP(datat+1,1) = DP(datat,1);               %derivative of pressure
w.r.t. time for the last data


clc;
iter=1;
Cpref(iter)=Cpref;
error(iter)=10;
es=0.0001;
maxit=100000;
if nargin<2||isempty(es),es=0.0001;end
if nargin<3||isempty(maxit),maxit=100000;end
 while error(iter)>=0.0001
     for i=1:datat
         Wb(i,1)=((Cpref(iter)/(2*(1-kp*(deltaP(i,1)))))*(-
deltaTOF(i,1)*1e-6 + (2*Epi*1e-3/Cpref(iter)) + (2*Ec*1e-
3*lp*deltaP(i,1)/Ccref)))*1000;
         rb (i,1) = (DdeltaTOF(i,1)*1e-6 - (((2*Epi*1e-
3/Cpref(iter)-deltaTOF(i,1)*1e-6+2*Ec*1e-3*lp*deltaP(i,1)/Ccref)/(1-
kp*deltaP(i,1)))*kp+2*Ec*1e-3*lp/Ccref)*DP(i,1)) *
(Cpref(iter)/(2*(1-(kp*deltaP(i,1))))))*1000;
     end
z=trapz(rb);
Z(iter,1)=Wb(1,1)-Wb(i,1);
error(iter+1)=abs(Epi-Z(iter,1))/abs(Epi)*100;
iter=iter+1;
if Z>=Epi
Cpref(iter)=Cpref(iter-1)-abs(Z(iter-1,1)-Epi)/10;
else
Cpref(iter)=Cpref(iter-1)+abs(Z(iter-1,1)-Epi)/10;
end
if iter>=maxit,break,end
 end
 end
Cpref=Cpref(iter);

for i=1:datat+1
    rb (i,1) = (DdeltaTOF(i,1)*1e-6 - (((2*Epi*1e-3/Cpref-
deltaTOF(i,1)*1e-6+2*Ec*1e-3*lp*deltaP(i,1)/Ccref)/(1-
kp*deltaP(i,1)))*kp+2*Ec*1e-3*lp/Ccref)*DP(i,1)) * (Cpref/(2*(1-
(kp*deltaP(i,1))))))*1000;
    Wb(i,1)=(Cpref/2*(1-kp*deltaP(i,1)))*((2*Epi*1e-3/Cpref)-
deltaTOF(i,1)*1e-6+2*Ec*1e-3*lp*deltaP(i,1)/Ccref)*1000;
end
z=trapz(rb);
Z=z*0.0002;


filename = 'P_rb.dat';
fid = fopen(filename, 'w');

for row=1:nrows
     fprintf(fid,'%6.4f %6.4f\n',P(row),rb(row));
end

fclose all
```

APPENDIX F

UNCERTAINTY DETERMINATION OF CLOSED BOMBS

Measured quantities of closed bomb tests are pressure, propagation time and propellant initial thickness. In this uncertainty analysis, the major uncertainties belong these measured quantities will account to uncertainty in burning rate.

F.1 Uncertainty in Initial Thickness of the Propellant

Initial thickness of the propellant (Wp,ini) is directly measured parameter. First eighteen propellant samples that were used during the closed test bombs were casted to teflon molds and the remained propellant samples were lathed from the whole propellant sample.

There are two error sources of initial thickness of the propellant which are non-perpendicularity of the propellant surface and random thickness measurement error. Non-perpendicularity of the propellant surface must be less than 1 degree [33]. 1 degree non-perpendicularity means 0.698 mm difference in length for the 40 mm propellant diameter. So the bias error of the initial propellant thickness is,

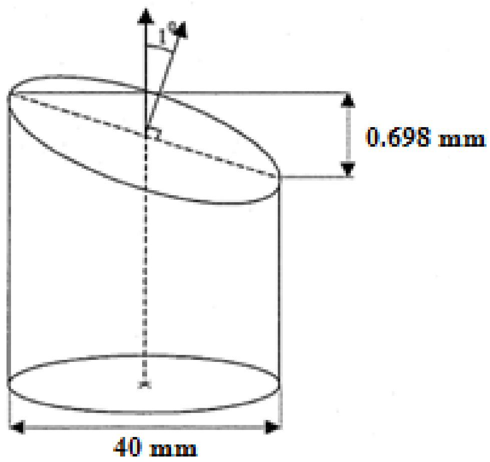

Figure 121 Non-perpendicularity of the propellant sample

$$\mathrm{B}_{\mathrm{Propellant}} = 0.698\ \mathrm{mm} \tag{10}$$

Random error of the initial propellant thickness is determined by repeated measurement of the samples by different persons. The initial propellant thickness of a propellant sample was measured twelve times and precision of this measurement is,

$$P_{Propellant} = 0.0196\ mm \tag{11}$$

So the total uncertainty is,

$$U_{Propellant} = \sqrt{B_{Propellant}^2 + P_{Propellant}^2} \tag{12}$$

$$U_{Propellant} = \sqrt{B_{Propellant}^2 + P_{Propellant}^2} = \sqrt{(0.698^2) + (0.0196^2)} = 0.698\ mm \tag{13}$$

F.2 Uncertainty in Pressure

The total uncertainty coming from measurement of pressure is made of three sources. First source is the pressure transducer itself. The second source of the uncertainty is digitization of the data acquisition system. The third component of the uncertainty is random error that comes from pressure measurement.

The first component of the uncertainty comes from pressure transducer itself (Kistler 701A). According to calibration certificate, the reading is accurate at 0.21% of full scale. Transducer can measure up to 35 MPa so the error comes from transducer is,

$$B1_{pressure} = 0.0525\ MPa \tag{14}$$

The second component of the uncertainty comes from digitization of the data acquisition system. In this setup, 12 bit Analog to Digital board is used for a range of 5800 Psi. This means an error of 0.00977 MPa.

$$B2_{pressure} = 0.00977\ MPa \tag{15}$$

The third component of the uncertainty comes from dead weight.

$$P_{pressure} = 0.00620\ MPa \tag{16}$$

The total uncertainty;

$$U_{pressure} = \sqrt{B1_{pressure}^2 + B2_{pressure}^2 + P_{pressure}^2} = \sqrt{(0.0525^2) + (0.00977^2) + (0.006} = 0.0029\ MPa \tag{17}$$

F.3 Uncertainty in Propagation Time

Error in the measurement of the propagation time includes systematic error and random error. The systematic error is due to the digitization in the data acquisition system and is estimated to be around 0.02 μs [33]. The second error source comes from measurement of propagation time, random error.

The systematic component of the uncertainty comes from digitization in the data acquisition system:

$$B_{propagationtime} = 0.02\ \mu s \quad (19)$$

The second component of the uncertainty comes from measurement of propagation:

$$P_{propagationtime} = 0.1439\ \mu s \quad (20)$$

So the total uncertainty is;

$$U_{propagationtime} \quad (21)$$

$$= \sqrt{B^2_{propagationtime} + P^2_{propagationtime}} = \sqrt{(0.02^2) + (0.1439^2)}$$

$$= 0.145\ \mu s$$

APPENDIX G

CALIBRATION of PRESSURE SENSOR

Table 26 Calibration Table

Pressure (Mpa)	Pressure (Psi)	Amplifier	Computer 1(V)	Computer 2(V)
1	145	0.99	0.498	0.503
2	290	1.97	0.991	0.996
3	435	2.96	1.479	1.484
4	580	3.95	1.978	1.982
5	725	4.95	2.476	2.48
6	870	5.94	2.974	2.979
7	1015	6.94	3.472	3.482
8	1160	7.94	3.965	3.97
9	1305	8.94	4.468	4.473
10	1450	9.94	4.966	4.971
11	1595	10.93	5.459	5.459
12	1740	11.93	5.957	5.957
13	1885	12.93	6.46	6.465
14	2030	13.93	6.958	6.963
15	2175	14.92	7.451	7.456
16	2320	15.91	7.949	7.954

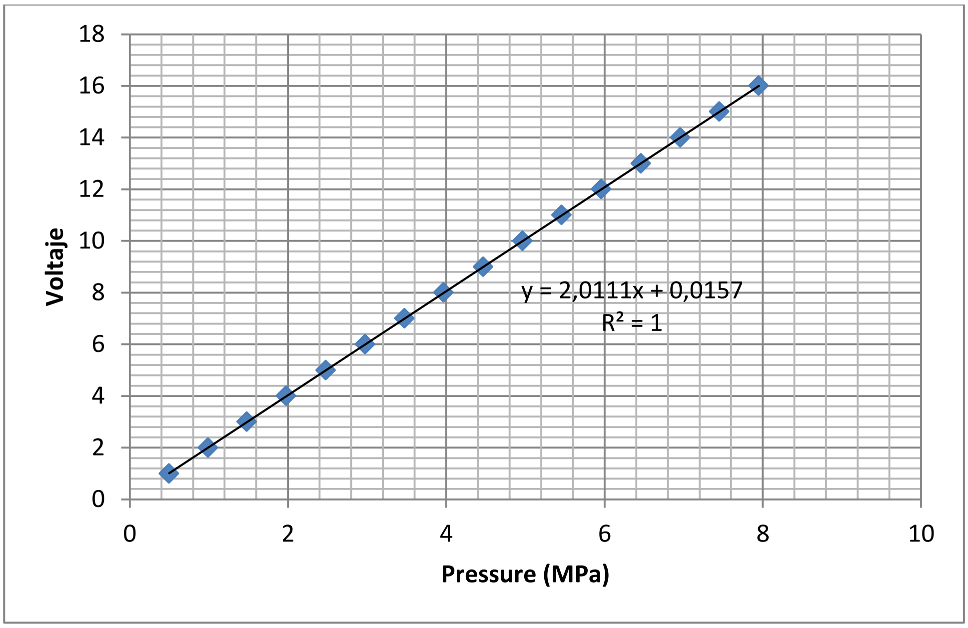

Figure 122 Calibration curve of pressure sensor

CURRICULUM VITAE

PERSONAL INFORMATION

Surname, Name **:** Atak (Kurtul), Özen
Nationality **:** Turkish (TC)
Date and Place of Birth **:** 18-04-1983, Ankara
Marital Status **:** Married
Phone **:** +90 506 488 33 74

EDUCATION

Degree	**Institution**	**Year of Graduation**
M.S.	Gazi University Mechanical Engineering	2008
B.S.	Osmangazi University Mechanical Engineering	2005
High School	Mamak Anadolu High School	2001

FOREIGN LANGUAGE

Advanced English

WORK EXPERIENCE

Year	**Place**	**Enrollment**
2016- Present	ROKETSAN A.Ş	Lead Engineer
2008- 2016	ROKETSAN A.Ş	Expert Engineer
2005-2008	Gazi University Mechanical Engineering	Research Assistant

PUBLICATIONS

ALTAÇ Z., **KURTUL Ö.**, "Natural Convection in Tilted Rectangular Enclosures with a Vertically Situated Hot Plate Inside", ULIBTK'05 15.Ulusal Isı BilimiveTekniğiKongresi 7-9 Eylül 2005, TRABZON

ONUR N., TURGUT O., ARSLAN K., **KURTUL Ö.**, An experimental and three-dimensional numerical study on the convective heat transfer inside a trapezoidal duct under constant wall temperature, Heat and Mass Transfer, vol 45, page 263-274, 2009

MUMCU B., KALKAN O., **ATAK Ö.**, KURTULUŞ F.D., ARKUN Ö.U., Ultrasonik Yanma Hızı Ölçüm Yönteminin Kapalı Bomba Uygulamaları", IV. Ulusal Havacılık ve Uzay Konferansı, Hava Harp Okulu, 12-14 Eylül 2012